NBS REPORT

8879

GPO PRICE $ _____

CFSTI PRICE(S) $ _____

Hard copy (HC) 6.00

Microfiche (MF) 1.25

ff 853 July 65

SLUSH HYDROGEN INSTRUMENTATION STUDY

by

W. J. Alspach, T. M. Flynn and R. J. Richards

NBS

U. S. DEPARTMENT OF COMMERCE
NATIONAL BUREAU OF STANDARDS
BOULDER LABORATORIES
Boulder, Colorado

THE NATIONAL BUREAU OF STANDARDS

The National Bureau of Standards is a principal focal point in the Federal Government for assuring maximum application of the physical and engineering sciences to the advancement of technology in industry and commerce. Its responsibilities include development and maintenance of the national standards of measurement, and the provisions of means for making measurements consistent with those standards; determination of physical constants and properties of materials; development of methods for testing materials, mechanisms, and structures, and making such tests as may be necessary, particularly for government agencies; cooperation in the establishment of standard practices for incorporation in codes and specifications; advisory service to government agencies on scientific and technical problems; invention and development of devices to serve special needs of the Government; assistance to industry, business, and consumers in the development and acceptance of commercial standards and simplified trade practice recommendations; administration of programs in cooperation with United States business groups and standards organizations for the development of international standards of practice; and maintenance of a clearinghouse for the collection and dissemination of scientific, technical, and engineering information. The scope of the Bureau's activities is suggested in the following listing of its four Institutes and their organizational units.

Institute for Basic Standards. Applied Mathematics. Electricity. Metrology. Mechanics. Heat. Atomic Physics. Physical Chemistry. Laboratory Astrophysics.* Radiation Physics. Radio Standards Laboratory:* Radio Standards Physics; Radio Standards Engineering. Office of Standard Reference Data.

Institute for Materials Research. Analytical Chemistry. Polymers. Metallurgy. Inorganic Materials. Reactor Radiations. Cryogenics.* Materials Evaluation Laboratory. Office of Standard Reference Materials.

Institute for Applied Technology. Building Research. Information Technology. Performance Test Development. Electronic Instrumentation. Textile and Apparel Technology Center. Technical Analysis. Office of Weights and Measures. Office of Engineering Standards. Office of Invention and Innovation. Office of Technical Resources. Clearinghouse for Federal Scientific and Technical Information.**

Central Radio Propagation Laboratory.* Ionospheric Telecommunications. Tropospheric Telecommunications. Space Environment Forecasting. Aeronomy.

---

* Located at Boulder, Colorado 80301.

** Located at 5285 Port Royal Road, Springfield, Virginia 22171.

NATIONAL BUREAU OF STANDARDS REPORT

NBS PROJECT		NBS REPORT
31506-12-3150461	March 1, 1966	8879

FINAL REPORT TO THE SPONSOR ON

SLUSH HYDROGEN INSTRUMENTATION STUDY

by

W. J. Alspach, T. M. Flynn and R. J. Richards

Cryogenics Division
NBS Institute for Materials Research
Boulder, Colorado

Prepared for the John F. Kennedy Space Center, NASA, under NASA Request Number CC-14032 for the period March 1, 1964 to March 1, 1966.

U.S. DEPARTMENT OF COMMERCE
NATIONAL BUREAU OF STANDARDS

TABLE OF CONTENTS

Table of Contents (continued) Page

Table of Contents (continued) Page

Table of Contents (continued) Page

Table of Contents (continued) Page

LIST OF FIGURES

List of Figures (continued) Page

List of Figures (continued) Page

List of Figures (continued) Page

LIST OF TABLES

ABSTRACT

27039

Means of determining the fraction solids (quality) of a mixture of solid and liquid hydrogen at the triple point were investigated. Attention was also given to the feasibility of a slush hydrogen mass flowmeter development program, and the application of conventional liquid level sensors to this system. It was determined that: (1) solid-liquid quality meters are available for some applications having a precision of approximately ± 2 percent, (2) several mass flowmeter principles could be developed for this system provided that adequate flow stands existed for the testing, proving, and developing of these meters, and (3) several conventional liquid level sensors are available which can detect one or more of the interfaces present in this solid-liquid-vapor hydrogen system.

Key Words: Cryogenic, flowmeter, hydrogen liquid-solid mixtures, instrumentation, Liquid level, quality, solid hydrogen, slush hydrogen.

1. Introduction

The Cryogenics Division of the NBS Institute for Materials Research conducted an analytical and experimental program to devise means for determining the solid phase mass fraction in a stagnant slush hydrogen mixture. The program was entitled "Slush Hydrogen Production and Instrumentation Study" and was sponsored by NASA-KSC under Purchase Request CC-14032. Work under this request number was performed during the period March 1, 1964 to March 1, 1966.

The interest in mixtures of solid and liquid (slush) hydrogen arises from the fact that even though relatively high densities at low pressures are attained through the use of liquid hydrogen as a propellant fuel, there are problems associated with handling and storing this low temperature fluid before, during, and after vehicle loading. Some of these problems are (a) short holding time caused by minimal insulation, (b) temperature stratification, resulting in pump cavitation problems, (c) sloshing of the liquid in such a manner as to affect flight stability, and (d) safety problems associated with the high vent rates before and after launch.

Further refrigeration of the liquid hydrogen to form a "slush" or mixture of solid and liquid should eliminate or reduce a number of the above problems. The use of slush hydrogen will increase holding time and reduce safety problems by providing a higher heat sink capacity before venting. Sloshing and temperature stratification problems may be reduced by the low fluidity or semi-solid nature of the slush mixture.

Current efforts directed towards the production and storage of slush hydrogen require a knowledge of the fraction solid content to select the optimum production technique, and to evaluate storage techniques. Also, slush hydrogen transfer requires a knowledge of the fraction solid content and flow rate to evaluate transfer line pressure drop, to evaluate flow surges, and to determine the amount of slush transferred. Future field type facilities for slush hydrogen applications will require a know-

ledge of the fraction solid content and flow rate in production, storage, and transfer operations. When used as a propellant, a knowledge of fraction solid content and flow rate will be required to determine total fuel mass in the vehicle tanks. Thus, the fraction solid content and flow rate of slush hydrogen are important in many applications.

1.1 Objectives of Program

The program had two major instrumentation objectives: (1) devise and develop prototype field instrumentation to determine the solid phase mass fraction in a stagnant slush hydrogen mixture and (2) investigate the feasibility of a slush hydrogen mass flowmeter development program. Identify particular problem areas and study the factors leading to the development of a slush mass flowmeter. Outline a program which might be followed to develop a mass flowmeter. The selection of a measurement method, whether for quality or flow, depends upon three criteria. First, does the physical law upon which the system is based provide a sufficient measurement coefficient to permit measurement to the degree of accuracy required? Second, are extraneous coefficients sufficiently small to permit the measurement coefficient to be utilized? Third, is the system within the state-of-the-art? Can it be built? Is it practical? These criteria were applied to the several choices of measurement to determine those most likely to succeed.

1.2 Summary

The above objectives were intended to establish means and specifications for the instrumentation of flowable mixtures of solid and liquid hydrogen. The production of these mixtures is reported in NBS Report 8881. "Characteristics of Liquid-Solid Mixtures of Hydrogen at the Triple Point".

ledge of the fraction solid content and flow rate in production, storage, and transfer operations. When used as a propellant, a knowledge of fraction solid content and flow rate will be required to determine total fuel mass in the vehicle tanks. Thus, the fraction solid content and flow rate of slush hydrogen are important in many applications.

1.1 Objectives of Program

The program had two major instrumentation objectives: (1) devise and develop prototype field instrumentation to determine the solid phase mass fraction in a stagnant slush hydrogen mixture and (2) investigate the feasibility of a slush hydrogen mass flowmeter development program. Identify particular problem areas and study the factors leading to the development of a slush mass flowmeter. Outline a program which might be followed to develop a mass flowmeter. The selection of a measurement method, whether for quality or flow, depends upon three criteria. First, does the physical law upon which the system is based provide a sufficient measurement coefficient to permit measurement to the degree of accuracy required? Second, are extraneous coefficients sufficiently small to permit the measurement coefficient to be utilized? Third, is the system within the state-of-the-art? Can it be built? Is it practical? These criteria were applied to the several choices of measurement to determine those most likely to succeed.

1.2 Summary

The above objectives were intended to establish means and specifications for the instrumentation of flowable mixtures of solid and liquid hydrogen. The production of these mixtures is reported in NBS Report 8881. "Characteristics of Liquid-Solid Mixtures of Hydrogen at the Triple Point".

1.2.1 Quality Instrumentation

A measurement of the bulk density of the mixture is a measurement of its quality. Accordingly, many different density measurement principles were reviewed for a slush hydrogen application. Of the many principles, the capacitance principle was selected. Criteria in this selection were (a) a large sample size, (b) free fluid flow into the sampling section, and (c) availability, i.e., this principle was available now as opposed to one requiring extensive development. Of the several available capacitance principle measurement systems, a system employing a matrix type sampling section was selected as it offered the advantages of (1) a large air capacitance value, (2) a large total sample, (3) a large space between the capacitor "plates" to accommodate large solid particles, and (4) free fluid movement into the sampling section from the top, the bottom, and the side.

Such a device was procured and evaluated and found to be within the specification tolerance of ± 2 percent full scale, see Section 5. This device is representative of quality instrumentation that can be obtained with a short lead time. Additional development could lead to improved capacitance devices or entirely different systems, such as those employing Nuclear Radiation Attenuation (NRA) or Nuclear Magnetic Resonance (NMR) principles, for example.

A major obstacle to continued development of improved instrumentation is the lack of a quality standard against which prototypes could be tested and proved. This is true since quality is a derived, not intrinsic, property of materials. It is recommended that this gap be filled.

1.2.2 Flow Measurement

Section 7 discusses several candidate principles for flow meters and recommends a development program that will yield such a device. The turbine type volumetric meter is discussed along with several mass flow meter principles, e.g., transverse momentum, radial flow transverse

momentum, gryoscopic transverse momentum, momentum-capacitance, and electromagnetic.

All of these are candidate principles and deserve further consideration. However, none can be developed at this time because there is no standard of slush flow against which they can be compared, proven and tested. The present situation is not unlike attempting to develop a thermometer with no temperature.

It is concluded, therefore, that a slush hydrogen mass flowmeter is feasible, and that the critical problem area which precludes such a development is the lack of a slush flow standard or facility. Section 7 outlines a program which might be followed to develop a mass flowmeter and puts primary emphasis upon the indisputable need for a slush hydrogen mass flow facility.

1.2.3 Liquid Level Measurement

The need for liquid level (quantity) measurement is obvious for propellant loading, utilization, and storage requirements. There are three interfaces possible in this mixture of solid, liquid and vapor: (1) clear liquid-vapor at the triple point, (2) stirred slush (solid plus liquid mixture)-vapor and (3) settled slush-clear liquid. Three readily available point liquid level sensors were tested for their ability to define these interfaces. They were the capacitance type, optical type, and magnetostrictive type. The first two types could discriminate all three interfaces, and the latter could find the first two. Thus point liquid level sensors are available for use in slush hydrogen and require no further development, per se. It is advised, however, that these sensors be examined critically from a safety viewpoint, since they were intended to operate at normal, not reduced, pressures.

A superconducting continuous level gage was constructed and evaluated in slush hydrogen, since this was the first possible application of this principle outside of liquid helium systems. The performance was

satisfactory, but more conventional types of continuous level gages may be preferred. The results are discussed in Section 9.

2. Fraction Solids Content, or Quality

The purpose of this study was the development of instrumentation to measure percent solid (quality) in a stagnant solid-liquid mixture of hydrogen. The instrument so developed was designed for field type applications, even though the study was conducted on a laboratory basis.

The first consideration for such a development is that quality is a derived, not an intrinsic, property of a system. To proceed in an orderly and economic manner therefore, it is first necessary to consider the nature of quality, and to determine which properties of the system should be measured in order to determine quality.

It is convenient to refer to the fraction of one phase in a heterogeneous mixture of phases as the "quality" of the mixture, a term borrowed from vapor-liquid (steam) terminology. The borrowing is not without hazard, however, for steam quality is ordinarily defined on a weight basis, while in some cases the more useful form may require a volumetric basis. The following simple manipulations are intended to define two quality terms and indicate their appropriate application. The specific case considered here is that of slush hydrogen.

Consider an equilibrium system of solid and liquid hydrogen of the following characteristics:

liquid portion: V_ℓ, M_ℓ, ρ_ℓ, v_ℓ

solid portion : V_s, M_s, ρ_s, v_s

total system : V, M, ρ, v

The apparent density of the whole system is:

$$\rho = \frac{M}{V} = \frac{M_\ell + M_s}{V_\ell + V_s} = \frac{M_\ell}{V_\ell + V_s} + \frac{M_s}{V_\ell + V_s} \qquad (1)$$

It would be handy to express $\rho = \rho(x, \rho_\ell, \rho_s)$. This can be done by normalizing the first term with respect to V_ℓ, and the second with respect to V_s:

$$\rho = \frac{\frac{M_\ell}{V_\ell}}{1 + \frac{V_s}{V_\ell}} + \frac{\frac{M_s}{V_s}}{1 + \frac{V_\ell}{V_s}}$$

$$\rho = \frac{\rho_\ell}{1 + \frac{V_s}{V_\ell}} + \frac{\rho_s}{1 + \frac{V_\ell}{V_s}}$$

An appropriate definition of quality will now complete the expression, namely:

$$x_v \equiv \frac{V_s}{V_s + V_\ell} = \frac{1}{1 + \frac{V_\ell}{V_s}} \tag{2}$$

$$(1 - x_v) = 1 - \frac{V_s}{V_s + V_\ell} = \frac{V_\ell}{V_s + V_\ell} = \frac{1}{1 + \frac{V_s}{V_\ell}}$$

The identity with the denominator above is now apparent:

$$\frac{1}{x_v} = 1 + \frac{V_\ell}{V_s}$$

$$\frac{1}{1 - x_v} = 1 + \frac{V_s}{V_\ell}$$

Thus:

$$\rho = x_v \rho_s + (1 - x_v) \rho_\ell \tag{3}$$

which is of a reasonable form.

The quality term, x_v, is so subscripted to indicate its volumetric definition, namely the volume fraction solids in the total volume. It is appropriate to use this form of quality for combinations of those specific properties which have been normalized with respect to volume, e.g., density.

A similar development for those intensive properties normalized with respect to mass (e.g., specific volume), leads to the reasonable conclusion that a quality term based on mass is required in the mixing rules, namely:

$$x_m = \frac{M_s}{M_s + M_\ell} \tag{4}$$

and, for example:

$$v = x_m v_s + (1 - x_m) v_\ell \tag{5}$$

A relation between x_m and x_v may be found from their respective definitions:

$$\frac{x_m}{x_v} = \frac{\dfrac{M_s}{M_s + M_\ell}}{\dfrac{V_s}{V_s + V_\ell}}$$

$$\frac{x_m}{x_v} = \left(\frac{M_s}{M_s + M_\ell}\right)\left(\frac{V_s + V_\ell}{V_s}\right)$$

$$= \rho_s \left(\frac{V_s + V_\ell}{M_s + M_\ell}\right)$$

$$= \rho_s \left(\frac{V}{M}\right) = \rho_s / \rho$$

$$\frac{x_m}{x_v} = \frac{\rho_s}{\rho} \tag{6}$$

A plot of (x_m/x_v) vs $1/\rho$ is a straight line having the two points $(x_m/x_v) = 1.000$ at $\rho = \rho_s$ and $(x_m/x_v) = 1.123$ at $\rho = \rho_\ell$, corresponding to 100% and 0% quality, respectively (Figure 1). (The latter point is indeterminate, but apparently has the limit given above).

A plot of (x_m/x_v) vs ρ is a portion of a hyperbola bounded by the physical limits of ρ, namely $\rho_s \geq \rho \geq \rho_\ell$ (Figure 2).

Approximate forms of these two expressions appear on curves, following.

It is also possible to express $x_m = f(x_v,$ constants). Combining and reducing equations (6) and (3), we obtain:

$$x_m = \frac{1}{1 + \left(\frac{1-x_v}{x_v}\right)\frac{\rho_\ell}{\rho_s}} \qquad (7)$$

An approximate form of this function appears in Figure 3.

2.1 Conclusion

In heterogeneous mixtures of phases, two quality terms are available to us: one a mass fraction and one a volume fraction. Both have their use. That care in their application is required is so obvious as to not bear discussion.

Since x_m and x_v are easily related, [Equation (7)], one may elect to measure either and determine the other analytically. The choice is simply one of ease and availability of means. Equation(3)may be manipulated to indicate how a measure of the bulk density of the system leads to a measure of the volumetric quality:

$$\rho = x_v \rho_s + (1 - x_v)\rho_\ell \qquad (3)$$

$$\rho = x_v \rho_s + \rho_\ell - x_v \rho_\ell \qquad (8)$$

$$\rho = x_v (\rho_s - \rho_\ell) + \rho_\ell \qquad (9)$$

$$\rho - \rho_\ell = x_v(\rho_s - \rho_\ell) \qquad (10)$$

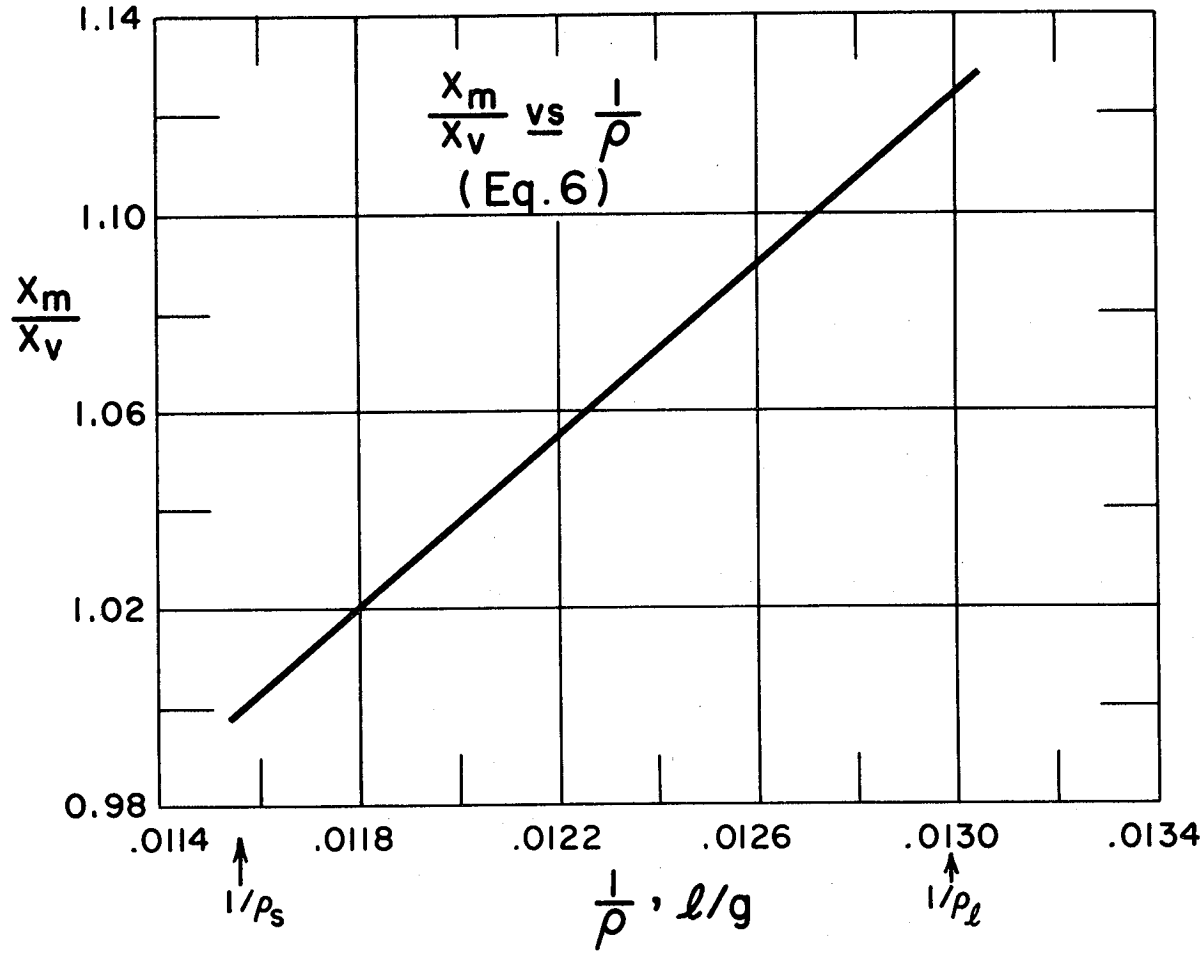

Figure 1. Ratio of Mass-Quality to Volumetric-Quality vs. the Reciprocal of the Bulk Density

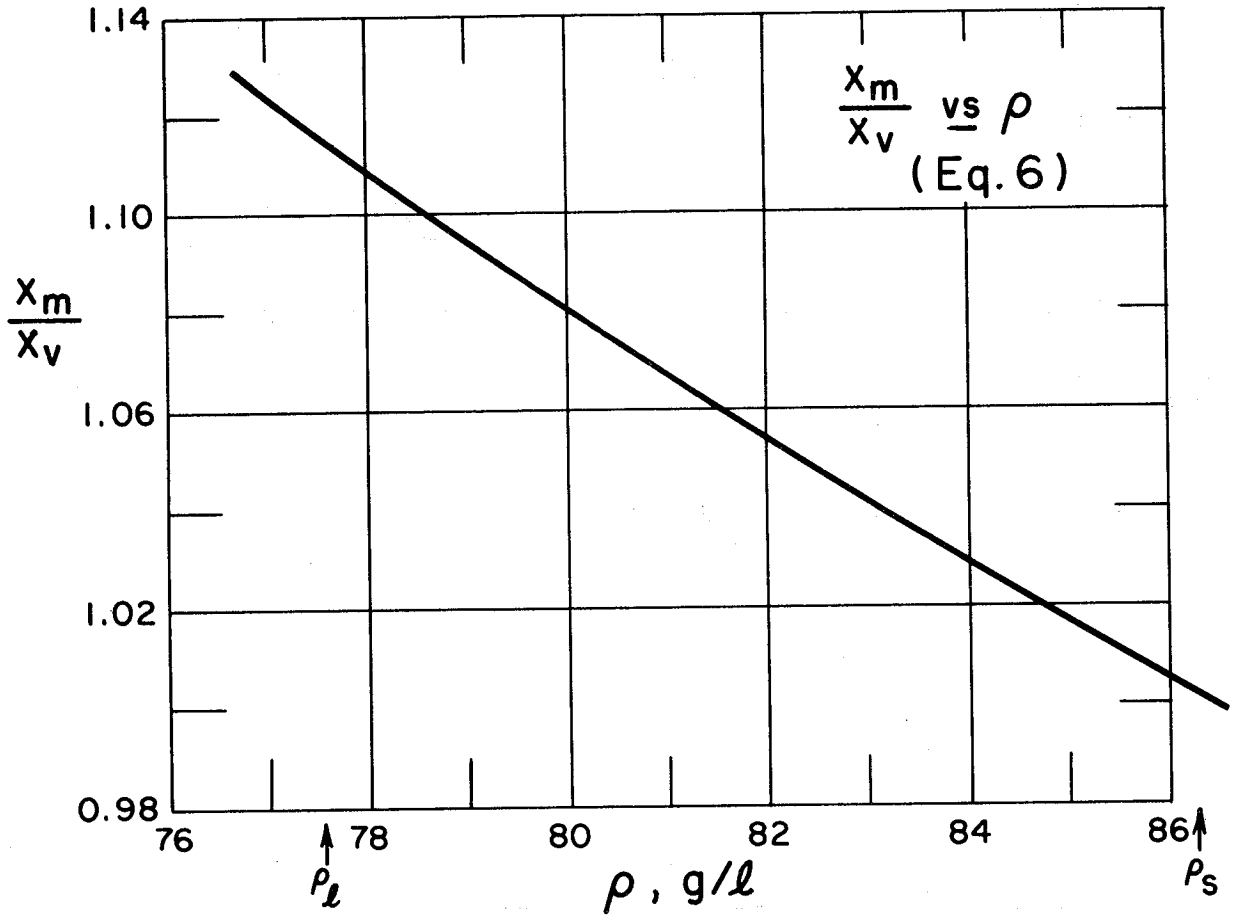

Figure 2. Ratio of the Mass-Quality to Volumetric-Quality vs. Bulk Density

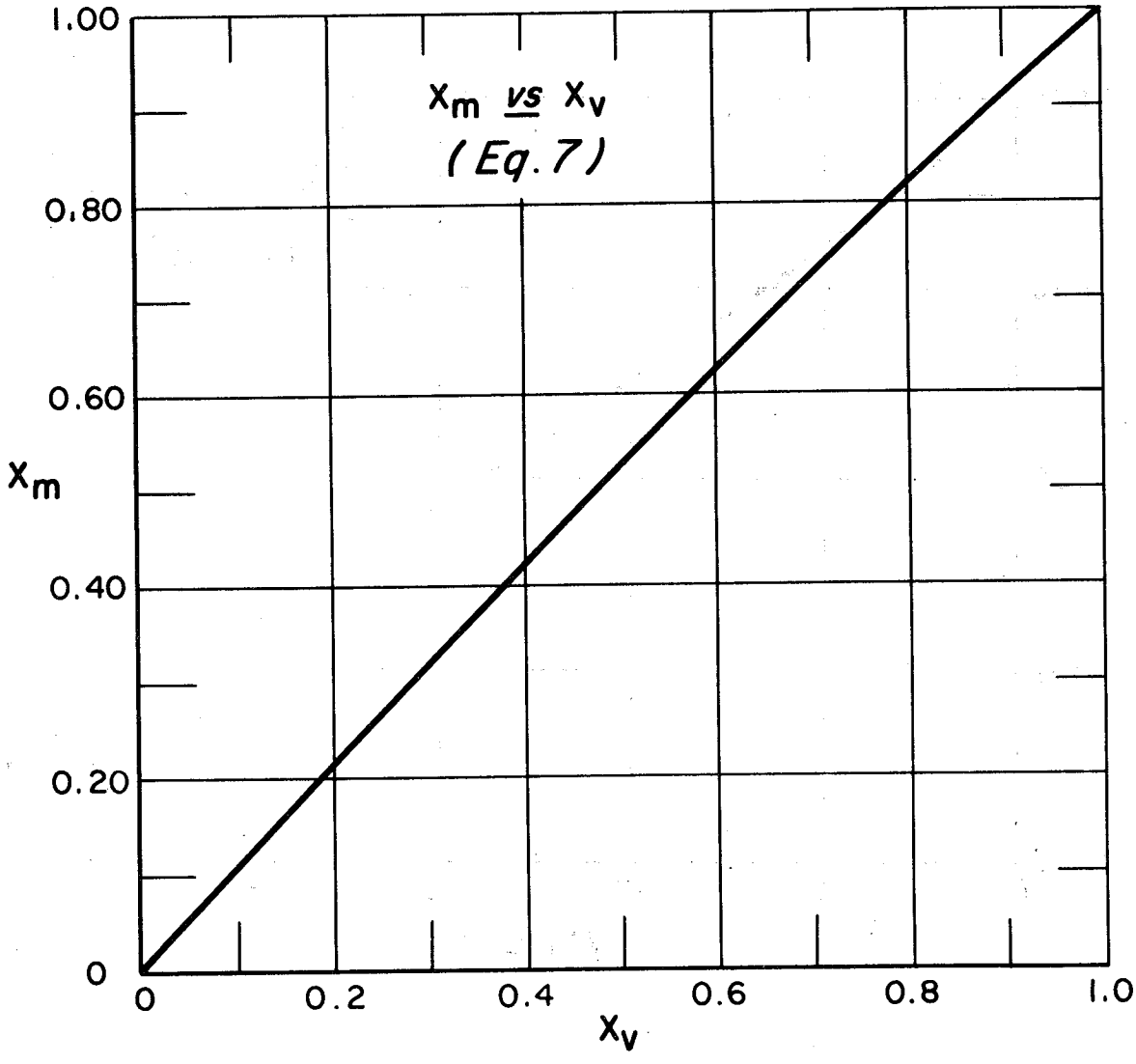

Figure 3. Mass-Quality vs. Volumetric-Quality

$$x_v = \frac{\rho - \rho_\ell}{\rho_s - \rho_\ell} = \frac{\rho}{\rho_s - \rho_\ell} - \frac{\rho_\ell}{\rho_s - \rho_\ell} \tag{11}$$

but since ρ_ℓ and ρ_s are simply constants, properties of the components of the system, then equation (11) reduces to:

$$x_v = A\rho + B \tag{12}$$

where A and B are defined by Equation (11).

Thus, a measure of the bulk density of the system is a measure of the quality of the system.

2.2 List of Symbols

Quantities		Subscripts	
M	mass	s	solid
V	volume	ℓ	liquid
v	specific volume	v	volume basis
x	quality	m	mass basis
ρ	density	(none)	total system

2.3 Tabulated Values

$\rho_s = 86.504$ gms/ℓ

$\rho_\ell = 77.029$ gms/ℓ

ρ	$\left(\frac{x_m}{x_v}\right)$	$1/\rho$
86.504 (ρ_s)	1.000	0.011560
85	1.017	
84	1.029	
83	1.042	
82	1.054	
81	1.067	
80	1.081	
79	1.094	
78	1.109	
77.029 (ρ_ℓ)	1.123	0.012982

x_v	x_m
1.00	1.00
0.90	0.9095
0.80	0.8171
0.70	0.7227
0.60	0.6263
0.50	0.5277
0.40	0.4268
0.30	0.3238
0.20	0.2183
0.10	0.1104
0.00	0.00

3. Selection of Quality Measurement Technique

The previous section led to the conclusion that a measure of the bulk density of the system is a measure of the quality of the system. Accordingly, the selection of the techniques which appear to be feasible methods of accomplishing the program objective has been primarily one of evaluating techniques of density measurement. These techniques have been evaluated according to three general criteria. First, does the physical law upon which the system is based provide a sufficient measurement coefficient to permit measurement to the degree of accuracy required? Second, are extraneous coefficients sufficiently small to permit the measurement coefficient to be utilized? Third, is the system within the present state-of-the-art?

The solid-liquid mixture of hydrogen gives rise to a number of conditions which have great bearing on the selection of a method of measurement. Among these conditions are: solid settling, solid packing, solid crystalline structure and aging, method of manufacture, collection of solid particles on probes, particle size, and the effect particle size may have on the measurement. A limitation which has great bearing on selection is the known degree of accuracy of the property of the mixture upon which the technique is based, e.g., relaxation time of the mixture for NMR techniques. Some methods of measurement, such as the acoustic method, are eliminated simply by the presence of two phases.

3.1 Measurement Method Summary

Methods of density determination include the following techniques: direct weighing, buoyancy, differential pressure, capacitance, optical, acoustic, ultrasonic, momentum, rotating paddle, transverse momentum, nuclear radiation attenuation, and nuclear magnetic resonance. Each of the principles involved will be discussed along with its relative merits

and shortcomings.

3.1.1 Direct Weighing Method

The direct weighing method of density determination measures the volume and weight of the mixture to give density. Although direct weighing is not considered a field-type instrument, it could serve as a primary calibration standard. Some of the advantages of this method are the simplicity of the equipment, repeatability, good frequency response, and the lack of dependence of pressure, temperature, and inhomogeneity effects of the fluid on the measurement. Disadvantages of direct weighing include poor sensitivity, windage and the fact that the entire system must be weighed or nulled out.

3.1.2 Buoyant Force Method

Density of a fluid may be measured by the buoyant force of the mixture upon a submerged plummet. This method is ideally suited for static laboratory use and involves relatively simple equipment. The drawbacks of the buoyancy method are slow response, poor sensitivity, and the need for a homogeneous mixture.

3.1.3 Differential Pressure Method

The differential pressure method measures the pressure of a vertical column of the mixture which, along with the height of the column, gives the density. Advantages of this method are: relatively simple equipment, small component size, and the possibility of application as a field type instrument. Disadvantages include the following: Low sensitivity, (accuracy depends upon two measured quantities, pressure and level), and complex electronics to compute actual density.

3.1.4 Capacitance Method

The capacitance method of slush density measurement utilizes the

difference in the dielectric constants of solid and liquid hydrogen. If the dielectric constant of the mixture is measured, it can be related to the density. The advantages of this method include no moving parts, good response, sensitivity, and repeatability. Disadvantages are the complex electronic equipment required and the requirement of a homogeneous solid-liquid mixture.

3.1.5 Optical Method

The optical method of density determination involves a light beam which is passed through the container and whose intensity is measured on the other side. This spectral absorption of light can be related to the density of the mixture. Although there are many good points in this system, it is felt that the scattering of light by the solid hydrogen particles and the present stage of development makes this system impractical.

3.1.6 Acoustic Method

The acoustic method utilizes the fact that the velocity of propagation of a sound wave in a fluid is directly related to the fluid density. Here also, there are several advantages, but fluid motion and the presence of solid particles in the fluid could cause spurious echoes and invalidate this method.

3.1.7 Ultrasonic Method

The ultrasonic method measures the impedance of a vibrating crystal in a fluid which can be related to the fluid s density. This method is not suitable for inhomogeneous mixtures or for a turbulent medium.

3.1.8 Momentum Method

Density can be measured by the momentum method, which can be related to the density of the fluid, by measuring fluid flow rate and fluid flow momentum. This system is not applicable to static density measure-

ments. (Note: Another technique which falls into this category is the vibration method.)

3.1.9 Rotating Paddle Method

The rotating paddle method is based on the principle that an aerodynamic foil, if rotated through a fluid, will experience a measurable drag which can be related to density. The rotating paddle serves a two-fold purpose; density measurement and stirring of the mixture. The equipment required is relatively simple. Disadvantages include low frequency response and sensitivity, and the presence of moving parts in the fluid.

3.1.10 Angular Momentum Method

Density of a fluid can be measured by the angular momentum method, which measures the angular momentum of a rotating fluid and relates this momentum to density. As in the rotating paddle method, the angular momentum method measures the density and stirs the mixture. The equipment required is relatively simple. Should this method prove feasible, it could be conveniently applied to slush hydrogen mass flow metering. Disadvantages of this method include the presence of bulky, moving parts in the fluid and the lack of previous investigation into the method's applicability to a static fluid density measurement.

3.1.11 Nuclear Radiation Attenuation Method

The nuclear radiation attenuation method utilizes the absorption of radiation energy by a fluid interposed between a radiation source and a radiation detector. This attenuation of radiation when passed through a fluid can be related to the fluid density. Advantages include no moving parts, repeatability, low power requirements, and apparent independence from fluid inhomogeneities. Disadvantages include that often a long measurement time is required, gradual decrease in the strength of the source,

complex electronic equipment, bulk size and the influence of fluid geometry.

3.1.12 Nuclear Magnetic Resonance Method

The nuclear magnetic resonance method measures density by counting the excess nuclei of a fluid in a magnetic saturated condition. This method exhibits good frequency response, sensitivity, and repeatability. Shortcomings of the system include the need to know fluid temperature and hydrogen ortho-para concentration, and the bulky and complex equipment required.

3.2 Analysis of Methods Selected

After a preliminary review of techniques, the following methods of density measurement were considered as the most promising and were analytically investigated further: direct weighing, buoyancy, differential pressure, capacitance, rotating paddle, and angular momentum. Of the six, three (weighing, buoyancy, differential pressure), are primarily for laboratory application and calibration, and the other three are field-type, secondary methods which must be calibrated against a standard.

The density is related to percent solid by Equations (3), (11) and (12).

$$\rho = \rho_s x_v + (1-x_v)\,\rho_\ell \qquad (3)$$

$$x_v = \frac{\rho - \rho_\ell}{\rho_s - \rho_\ell} \qquad (11)$$

$$x_v = A\rho + B \qquad (12)$$

where:

ρ = density of mixture

ρ_s = density of solid

ρ_ℓ = density of liquid

x_v = volume fraction solid in mixture

$A = 1/(\rho_s - \rho_\ell)$

$$B = - (\rho_\ell)/(\rho_s - \rho_\ell)$$

The sensitivity of the instrument can be evaluated analytically to determine whether or not the system can be made to the degree of accuracy desired. In general form:

$$dM = \sum_{1}^{i} \frac{\partial M}{\partial P_i} dP_i \tag{13}$$

where:

dM = observed measurement change, in our case, Δx, where x is the quality.

$\frac{\partial M}{\partial P_i}$ = measurement coefficients, how the quantity measured, M, depends upon system parameters, P

dP_i = variable parameters, for example the total weight, liquid level, etc.

In the following sections, it is shown that all of the sensitivity expressions developed are of the form:

$$dM = \frac{dP}{\theta(\rho_s - \rho_\ell)} \tag{14}$$

Where M and P are as before and

θ = geometrical parameters of the specific system, i.e., volume, height, area.

For our specific case, the general M is replaced by the quality, x:

$$dx = \frac{1}{\theta} \frac{dP}{\rho_s - \rho_\ell} \tag{15}$$

or:

$$\log dx = \log\left\{\frac{dP}{\rho_s - \rho_\ell}\right\} - \log \theta \tag{16}$$

Thus the sensitivity (Δx) of a large number of different measurement systems can be conveniently represented at the same time in a log-log presentation, once the P and θ of each system is determined. Further-

more, once θ is determined for a particular set of conditions, the dependence of dx upon all θ may be found by constructing a line of minus one (-1) through that particular θ [Eq. (16)].

The P and θ of six different density measuring systems are developed analytically in the following sub-sections. The results are then presented in Figure 4.

Thus it is possible to see at once, without experimental evaluation of every system, the following:

(a) how the ultimate sensitivity, Δx, of one technique compares with another.

(b) how the ultimate sensitivity of any one technique depends upon its particular set of parameters. Thus one can tell beforehand what changes in a particular system will lead to improved sensitivities.

(c) how the ultimate sensitivity of any system depends upon the quality, x, being measured. Figure 4 was constructed for x = 50%. A third dimension could be added to Figure 4 to show the dependence of sensitivity upon x.

(d) In those cases requiring two measurements, i.e., the direct weighing method requires weight and liquid level measurements to infer density, we can see which measurement is the limiting one.

Thus the following development and Figure 4 permit us to make an analytical judgment of how one measurement system potentially compares with another, and what should be done to improve the sensitivity.

3.2.1 Direct Weighing

In this method, the fluid and fluid vessel are weighed and the mixture volume is measured to give fluid density:

$$\rho = \frac{W - F}{V} = \frac{W - F}{hA} \qquad (17)$$

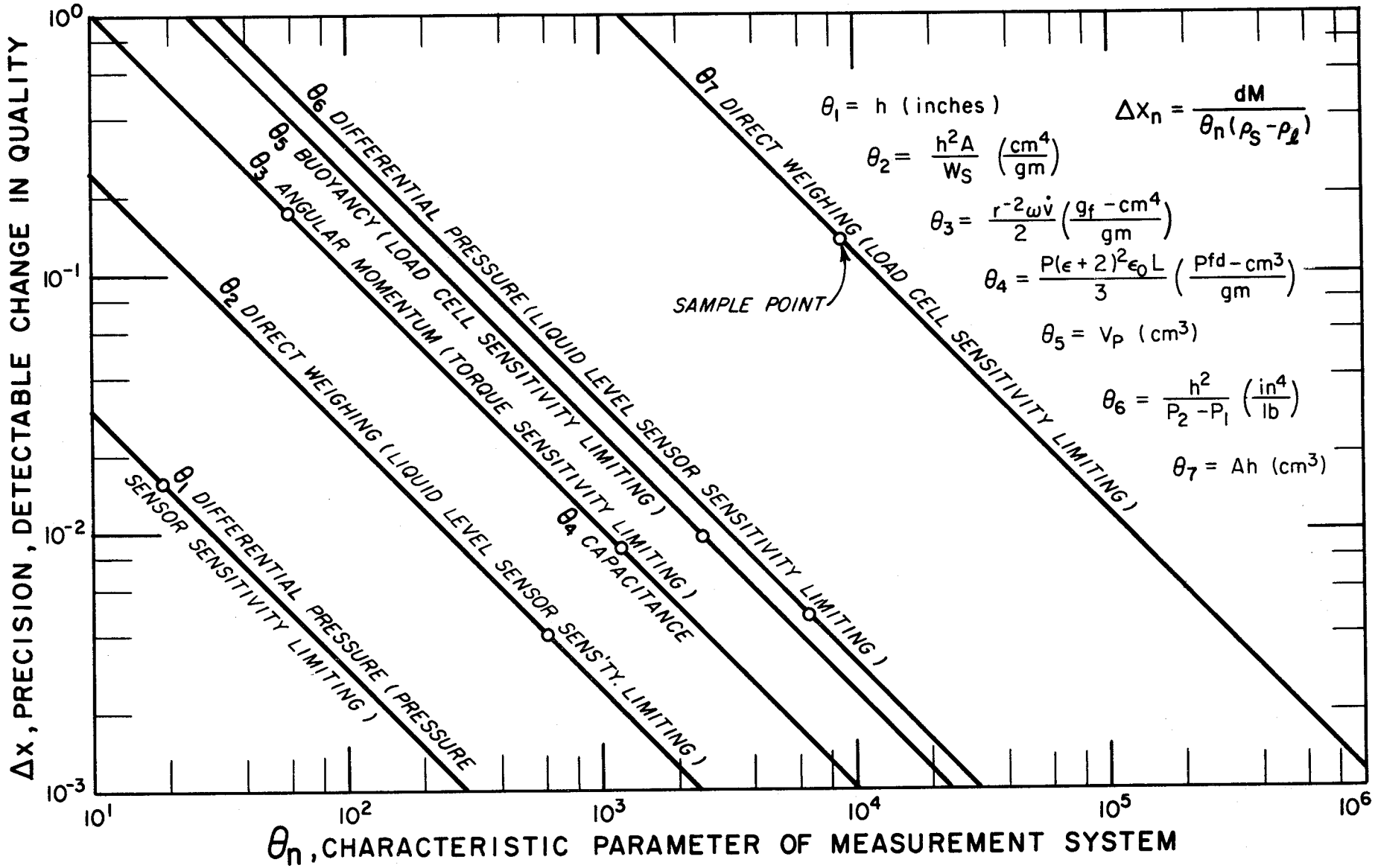

Figure 4. Measurement Sensitivity as a Function of the Parameter θ at 50% Solid Content

where:

W = total weight of vessel and fluid

F = weight of vessel (tare weight)

V = volume of fluid

A = cross-sectional area of vessel

h = height of mixture in vessel

Let us drop the subscript from x, but understand that we are speaking of the volumetric quality, x_v, and return to equation (11)

$$x = \frac{\rho - \rho_\ell}{\rho_s - \rho_\ell} \qquad (11)$$

Substituting the expression for ρ from Eqn. (17) into Eqn. (11), we have:

$$x = \frac{\left(\frac{W - F}{hA}\right) - \rho_\ell}{\rho_s - \rho_\ell} \qquad (18)$$

$$x = \frac{\left(\frac{W-F}{A}\right) - h\,\rho_\ell}{\left(\rho_s - \rho_\ell\right) h} \qquad (19)$$

The variable parameters in this method are total weight (W) and liquid level (h). From Eqn. (13), the sensitivity of a direct weighing method of density measurement can be expressed as:

$$dx = \left(\frac{\partial x}{\partial W}\right)_h dW + \left(\frac{\partial x}{\partial h}\right)_W dh \qquad (20)$$

The partial derivatives are found from differentiating Eqn. (19) to be:

$$\frac{dx}{dW} = \frac{1}{Ah\,(\rho_s - \rho_\ell)} \qquad (21)$$

and:

$$\frac{dx}{dh} = -\left[\frac{W-F}{(\rho_s - \rho_\ell)h^2 A}\right] \qquad (22)$$

Substituting this result into Eqn. (20), we have:

$$dx = \left[\frac{1}{Ah\,(\rho_s - \rho_\ell)}\right] dW - \left[\frac{W - F}{(\rho_s - \rho_\ell)\,h^2 A}\right] dh \qquad (23)$$

Compare this result with Eqn. (14):

$$dM = \frac{dP}{\theta(\rho_s - \rho_\ell)} \qquad (14)$$

We see that the variable parameters, "dP", are in this case dW and dh, and that the θ's are

$$\theta_7 = Ah, \text{ and} \qquad (24)$$

$$\theta_2 = h^2 A/(W-F) \qquad (25)$$

The subscripts on θ refer to the points on Figure 4.

3.2.1.1 Direct Weighing, Sample Sensitivity Calculations

I. Known system parameters

A. Desired sensitivity of fraction solid measurement: dx = 0.005

B. Known physical properties

ρ_ℓ = 77.029 grams/liter

ρ_s = 86.504 grams/liter

C. Assumed fraction solid, x = 0.5(ρ=81.77 $\frac{gm}{liter}$)

II. Sensitivity Calculations

A. Dimension assumptions (a nominal 6-in. diameter glass dewar is chosen)

1. Liquid height: h = 50 cm = 19.7 in.
2. Tank diameter: d = 15.2 cm = 6 in.
3. Slush total weight: $W_s = \rho Ah$ = 741 gm = 1.63 lb.
4. Tare Weight: F = 50 lb

B. Accuracy Assumptions (based on current manufacturer ratings)

1. $\Delta W = 0.025$ lb $= 11.34$ gm

2. $\Delta h = 0.01$ inch. $= 0.0254$ cm

C. Sample Calculation [from Equation (23)]

$$dx = \left[\frac{1}{Ah(\rho_s - \rho_\ell)}\right]_h dW - \left[\frac{W - F}{(\rho_s - \rho_\ell)h^2 A}\right]_W dh$$

let $$\Delta\rho = (\rho_s - \rho_\ell) \tag{26}$$

and using the values of θ from Eqns. (24) and (25), then

$$dx = \left[\frac{1}{\theta_7 \Delta\rho}\right]_h dW - \left[\frac{1}{\theta_2 \Delta\rho}\right]_W dh \tag{27}$$

$\theta_7 = Ah = 9.05 \times 10^3$ cm^3

$\theta_2 = h^2A/(W - F) = h^2A/W_s = 6.11 \times 10^2$ cm^4/gm

$\Delta\rho = \rho_s - \rho_\ell = 9.475$ gms/liter

and using the assumed values of Δw (0.025 lb) and Δh (0.01 inch) Eqn. (27) becomes

$$dx = (0.132)_h - (0.004)_W = 0.128$$

where the subscripts signify the variable being held constant.

The two limiting cases are: (a) load cell sensitivity limiting, (θ_7), and (b) liquid level sensor limiting, (θ_2). Both are shown in Figure 4.

This calculation indicates that the direct weighing method deviates from the desired sensitivity by a disturbing amount. A more accurate weighing system would increase this method's sensitivity but the system would rapidly approach state of the art. From Equation (23), it is apparent that the larger the tankage, the more sensitive is the system. The calculation does imply that for a constant weight measurement, a measure of the

liquid level would give the percent solid within the desired accuracies.

3.2.2 Buoyancy

In the buoyancy method, a weight is suspended in the fluid and its apparent weight is then a measure of the density of the fluid.

The equation for a partially submerged plummet is:

$$\rho V_s = W_p - W_r \tag{28}$$

where:

V_s = volume of submerged part of plummet

W_p = weight of plummet

W_r = apparent weight of plummet

If the value of ρ from Eqn. (28) is now substituted into the general form for x [Eqn. (11)], the fraction solid can be expressed as:

$$x = \frac{W_p - W_r - \rho_\ell A_p h}{A_p h \Delta \rho} \tag{29}$$

where:

A_p = cross sectional area of plummet

h = depth of submersion of the plummet

The variable parameters in this method are the apparent weight reading of the plummet, W_r, and the depth of submersion of the plummet, h. The sensitivity of this method of density measurement can be expressed as:

$$dx = \left(\frac{\partial x}{\partial W_r}\right)_h dW_r + \left(\frac{\partial x}{\partial h}\right)_{W_r} dh \tag{30}$$

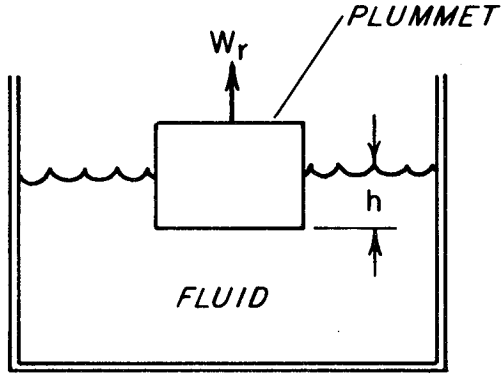

Figure 5. Schematic of Buoyancy System

$$= -\left[\frac{1}{A_p h \Delta \rho}\right] dW_r - \left[\frac{W_p - W_r}{A_p h^2 \Delta \rho}\right] dh \qquad (31)$$

Should the plummet be completely submerged, then h is constant and $A_p h$ becomes V_p. The above equations then simplify to:

$$x = \frac{W_p - W_r - \rho_\ell V_p}{V_p \Delta \rho} \qquad (32)$$

and

$$dx = -\left[\frac{1}{V_p \Delta \rho}\right] dW_r \qquad (33)$$

by comparison with Eqn. (14) we see that in this case the variable parameter dP is dW_r, and that the θ of this system is

$$\theta_5 = V_p$$

where the subscript on θ refers to Figure 4.

3.2.2.1 Buoyancy, Sample Sensitivity Calculations

1. Dimension assumptions:
   a. Hollow aluminum plummet, cylindrical in shape, (4" dia. x 12" high), made of 0.030-inch aluminum.
   b. Plummet completely submerged, $V_p = 2500\ cm^3$.
2. Accuracy assumptions
   $\Delta W_r = 5 \times 10^{-4}$ lb = 0.226 gm
3. Sample calculation

$$dx = \frac{dW_r}{V_p \Delta \rho} \qquad (34)$$

$$dx = \frac{0.226 \text{ gm}}{(2.5 \text{ liter})(9.475 \frac{\text{gms}}{\text{liter}})} = 0.0095$$

The results are given in Figure 4, for

$$\theta_5 = V_p = 2500 \text{ cm}^3, \text{ and}$$

$$dx = 0.0095$$

3.2.3 Differential Pressure

The differential pressure existing across a vertical column of fluid can be related to the fluid density if the fluid height is known (see figure 6). Namely,

$$\rho = \left(\frac{P_2 - P_1}{h}\right) \tag{35}$$

where:

h = distance between station 2 and the mixture-vapor interface.

Substituting this value of ρ into Eqn. (11) and manipulating as before, we find

$$dx = -\left[\frac{P_2 - P_1}{h^2 \Delta \rho}\right] dh + \left[\frac{1}{h \Delta \rho}\right] dp \tag{36}$$

Comparison with Eqn. (14) shows that in this case the variable parameters, dP, are dh and dp. The θ's are

$$\theta_1 = h$$
$$\theta_6 = h^2/(P_2 - P_1)$$

where the subscripts refer to Figure 4.

3.2.3.1 Differential Pressure, Sample Sensitivity Calculation

1. Dimension assumptions
   a. h = 19 inches
   b. $P_2 - P_1 = h(\rho) = 0.0556$ psid

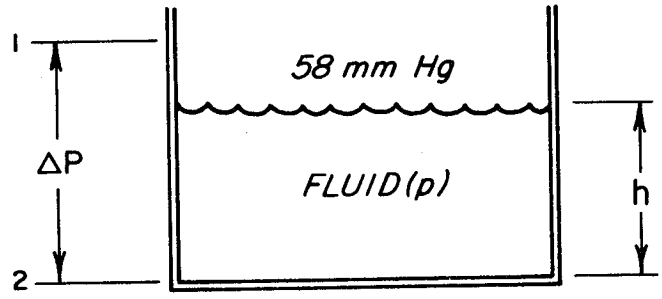

Figure 6. Schematic of Differential Pressure System

2. Accuracy assumptions

   a. $\Delta p = 10^{-4}$ psid

   b. $\Delta h = 0.01$ inch

3. Sample Calculation

$$dx = -\left[\frac{P_2 - P_1}{h^2 \Delta \rho}\right] dh + \left[\frac{1}{h \Delta \rho}\right] dp \tag{37}$$

$$\theta_1 = h = 19.0 \text{ inch}$$

$$\theta_6 = h^2/(P_2 - P_1) = 6.5 \times 10^3 \text{ in}^4/\text{lb}$$

$$dx = (4.76 \times 10^{-3})_p + (1.56 \times 10^{-2})_h = 19.8 \times 10^{-3}$$

The results are given in Figure 4, for each case limiting.

3.2.4 Capacitance

The Clausius - Mossotti equation can be written as follows:

$$\rho = \frac{1}{p}\left(\frac{\epsilon - 1}{\epsilon - 2}\right) \tag{38}$$

which relates the fluid's dielectric constant (ϵ) to the density of the fluid (ρ). Define an average dielectric constant as:

$$\bar{\epsilon} = \epsilon_s x + \epsilon_\ell (1 - x), \tag{39}$$

where:

ϵ_s, ϵ_ℓ = dielectric constant of solid and liquid phases, respectively

p = polarizability of the mixture;

then any change in the average dielectric constant would be a measure of the fraction solid (x).

Equation (38), together with (11) and (40) below, completely define the system.

$$\bar{\epsilon} = \frac{C}{\epsilon_o L} \tag{40}$$

where:

C = capacitance

ϵ_o = constant (8.85×10^{-12} fd/meter)

L = capacitor characteristic length: $\left(\frac{\text{plate area}}{\text{spacing}}\right)$.

The sensitivity of the capacitance system of density measurement is:

$$dx = \left(\frac{\partial x}{\partial \rho}\right)\left(\frac{\partial \rho}{\partial \bar{\epsilon}}\right)\left(\frac{\partial \bar{\epsilon}}{\partial C}\right) dC$$

$$= \left(\frac{1}{\rho_s - \rho_\ell}\right)\left(\frac{1}{p}\right)\left(\frac{3}{(\bar{\epsilon} + 2)^2}\right)\left(\frac{1}{\epsilon_o L}\right) dC \qquad (41)$$

(p = polarizability of the mixture, assumed constant.)

Comparison with Eqn. (14) shows that for this system the θ is

$$\theta_4 = \frac{p(\epsilon + 2)^2 \epsilon_o L}{3} \quad \frac{\text{pfd-cm}^3}{\text{gm}}$$

3.2.4.1 Capacitance, Sample Sensitivity Calculation

1. Dimension assumptions
   a. p (polarizability) = 1 cm^3 gm
   b. Ten capacitors are located horizontally in container with a characteristic length (L) of 36.5 meters.

2. Accuracy assumptions

   Δc = 0.1 picofarads

3. Sample Calculations

$$\Delta x = \left(\frac{1}{\rho_s - \rho_\ell}\right)\left(\frac{1}{p}\right)\left(\frac{3}{(\bar{\epsilon} + 2)^2}\right)\left(\frac{1}{\epsilon_o L}\right) \Delta C \qquad (42)$$

$$\Delta x = 0.0088, \quad \theta_4 = 1.2 \times 10^3 \ \frac{\text{pfd - cm}^3}{\text{gm}}$$

3.2.5 Rotating Paddle

After preliminary slush production investigations, it became apparent that due to settling of the mixture, stirring may be required. The vibrating paddle technique was considered at this point because if the rotating paddle method did, in fact, prove feasible, stirring of the mixture would also be accomplished. In principle, the drag experienced by an aerodynamic foil passing through a fluid will be proportional to the density of the fluid. A series of paddles attached to a shaft are rotated through a fluid at constant velocity. The torque required to keep the shaft rotating at a constant speed is a measure of the density.

The theoretical basis for this method is expressed in terms of the aerodynamic drag equation:

$$D\ (r, Re) = C_D(r) \left(\rho \frac{V^2}{2} \right) S \qquad (43)$$

where:

$D(r, Re)$ = aerodynamic drag

$C_D(r, Re)$ = drag coefficient or friction factor

V = instantaneous paddle velocity

S = wetted surface area

This drag is related to the torque by:

$$\tau = 2N\ D\ (r, Re)\ \bar{r} \qquad (44)$$

where:

τ = torque at constant velocity

N = number of paddles

$\bar{r}$ = drag centroid moment arm

The drag coefficient (C_D) is dependent on the dimensionless Reynolds number ($Re_x = vt/\nu$) and the form of the equation for drag varies as

the Reynolds number passes through various critical points (laminar, transition, and turbulent flow). The equations for drag coefficients at various Reynolds numbers are developed in most texts on fluid mechanics. To determine the order of magnitude of this torque and its sensitivity, a sample calculation is carried out in the following section. The exact order of magnitude cannot be determined analytically because of the lack of reliable viscosity data for liquid hydrogen at the triple point. The influence of solid particles cannot be determined except by experimentation.

3.2.5.1 Rotating Paddle, Sample Sensitivity Calculation

1. Dimension assumptions
   a. Number of paddles, $N = 6$
   b. Width of paddle, $t = 1$ cm
   c. Length of paddle, $L = 5$ cm
   d. Angular velocity, $w = 60$ rpm
2. Accuracy assumption

   $\Delta x = 0.1\ gm_f - cm$
3. Sample Calculation

$$Re_x = {}^{vt}/_{v} = 5.34 \times 10^3 \text{ (transition region)}$$

$$C_p = \frac{0.455}{(\log_{10} Re_x)^{2.58}} \text{ (for turbulent flow)}$$

$$= 0.015$$

$$D(r) = \int_o^L C_d \rho \frac{V^2}{2} S\, dr$$

$$= \frac{C_d \rho w^2 t L^3}{3}$$

$$\bar{r} = \frac{\int_o^L D(r)\, r\, dr}{\int_o^L D(r)\, dr} = \frac{\int_o^L r^3\, dr}{\int_o^L r^2\, dr}$$

$$\bar{r} = \frac{3}{4} L$$

$$\tau = 2N\, D(r)\, \bar{r}$$

$$= \frac{3N\, C_d\, \rho\, w^2\, t\, L^4}{2}$$

$$= 90 \text{ dyne - cm} = 0.092 \text{ gmf - cm}$$

After this preliminary analytical investigation, it appears that the rotating paddle does not merit further consideration as the sensitivity is non-existant due to the very low viscosity of liquid hydrogen.

3.2.6 Angular Momentum

The angular momentum of a rotating fluid can be related to the density of the fluid by the following:

$$\rho = \frac{2\tau}{(R_1^2 + R_2^2)\, \omega\, \dot{V}} \tag{45}$$

where:

τ = torque required to rotate cylinder,

R_1 R_2 = radii of inner and outer cylinders, respectively,

ω = angular velocity,

$\dot{V}$ = volumetric flow rate.

If the driving plate is rotated at a constant speed, the torque required to rotate the cylinder should vary withthe density. An analytical solution of the method cannot accurately be made, as the volumetric flow rate

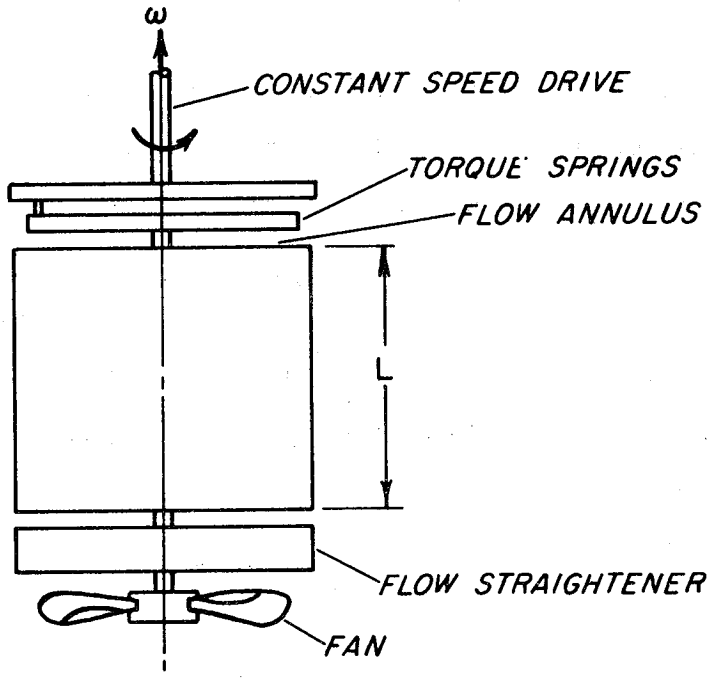

Figure 7. Schematic of Angular Momentum System

cannot be predicted to any degree of reliability. A sensitivity calculation can readily be made based on dimension and flow rate assumptions. The sensitivity can be expressed as:

$$dx = \frac{2d\tau}{(R_1^2 + R_2^2)\,\omega\,\dot{V}(\rho_s - \rho_\ell)} \tag{46}$$

3.2.6.1 Angular Momentum, Sample Sensitivity Calculation

1. Dimension assumptions.
   a. Radius of gyrations: $\frac{R_1^2 + R_2^2}{2} = 10\ cm^2$
   b. Volumetric flow rate: $\dot{V} = 944\frac{cm^3}{sec} = 2\frac{ft^3}{min}$
   c. Angular velocity $\omega = 2\pi\frac{rad}{sec}$

2. Accuracy assumption

   $\Delta\tau = 0.1\ gm_f - cm$

3. Sample calculation

$$\Delta x = \frac{2d\tau}{(R_1^2 + R_2^2)\,\omega\,\dot{V}\,(\rho_s - \rho_\ell)} \tag{47}$$

$$\Delta x = 0.174$$

$$\theta_3 = \frac{(R_1^2 + R_2^2)\,\omega\,\dot{V}}{2} = \frac{60.6\ gm_f - cm^4}{gm_m}$$

3.3 Summary

An investigation of several known methods of density measurement revealed six possible systems for measuring a mixture of solid and liquid

hydrogen. These systems have been discussed in terms of applicability, theoretical basis of measurement, and sensitivity.

An index, the Theta Parameter, has been developed which permits us to compare analytically on a common basis the several different techniques which are available. The results are presented in Figure 4. Inspection of this figure tells how the sensitivity of one technique compares, with another, and how the sensitivity of any one technique depends upon its particular system parameters (θ). A third dimension could be added to Figure 4 to permit the above comparisons to be made with respect to various qualities, x. Thus an analytical tool has been made available to screen candidate techniques before resorting to experimental comparison.

The potential performance of the capacitance technique led to its selection for experimental evaluation. Other criteria in this selection were (a) a large sample size, (b) free fluid flow into the sampling section, and (c) availability. That is, this measurement principle is available now as opposed to others requiring extensive development. Of the several available capacitance principle measurement systems, a system employing a matrix type sampling section was selected as it offered the advantages of (1) a large air capacitance value, (2) a large total sample, (3) a large space between the capacitor "plates" to accommodate large solid particles, and (4) free fluid movement into the sampling section from the top, the bottom, and the side.

Section 5 describes a test program conducted to evaluate the performance of a capacitance principle measurement system which was designed to determine slush hydrogen fraction solid content.

4. Selected Values of Density and Dielectric Constant

Since the selected fraction solid content measurement system uses the capacitance principle, the dielectric constant and density of triple point liquid and solid hydrogen must be known. Accordingly, a literature review was made to ascertain these values. The review revealed a considerable variation of these values, as follows:

(a) "A Compilation of the Dielectric Constants of Solid, Liquid, and Gaseous He, H_2, Ne, N_2, O_2, AIR, CO, F_2, A, and CH_4 Below 300°K," Hust, Germann, and Stewart, NBS Report 8252, April 7, 1964.

1. Dielectric Constant of Liquid by Graphic Means = 1.2516
2. Dielectric Constant of Solid by Guillien in 1940 at 13.90°K = 1.2808

(b) "A Compendium of the Properties of Materials at Low Temperature (Phase 1)," Johnson, WADD Technical Report 56-56, Part I, July, 1960.

1. Dielectric Constant of Liquid by Graphic Means = 1.254
2. Dielectric Constant of Solid by Graphic Means = 1.282

(c) "Theoretical, Experimental, and Analytical Examination of Subcooled and Solid Hydrogen," Prepared under Contract No. AF33(657)-10248 by Union Carbide Corporation, Linde Division, Technical Documentary Report No. APL TDR 64-22, May 1964.

1. Density of liquid = 77.03 gm/liter
2. Density of solid = 86.64 gm/liter

(d) "Slush Hydrogen Production and Handling as a Fuel for Space Projects,": Carney, Advances in Cryogenic Engineering, Volume 9, pp 529-535.

1. Density of liquid = 4.81 lbs/ft^3 = 77.038 gm/liter
2. Density of solid = 5.41 lbs/ft^3 = 86.648 gm/liter

(e) "Research On Rheologic And Thermodynamic Properties Of Solid And Slush Hydrogen," Prepared under Contract No. AF33(657)-11098 by Linde Division, Union Carbide Corporation, Twelve-Months Report, 15 June 1963-15 June 1964, October 12, 1964.

1. Density of liquid = 4.808 lbs/ft^3 = 77.006 gm/liter
2. Density of solid = 5.401 lbs/ft^3 = 86.504 gm/liter
   = 5.398 lbs/ft^3 = 86.456 gm/liter

(f) "Research Of Production Techniques For Obtaining Over 50% Solid In Slush Hydrogen," Prepared by Union Carbide Corporation, Linde Division, under Contract AF33(615)1357, Bimonthly Progress Report Number 4, October 16, 1964.

1. Density of liquid = 4.8079 lbs/ft^3 = 77.005 gm/liter
2. Density of solid = 5.412 lbs/ft^3 = 86.680 gm/liter

(g) "Liquid-Solid Mixtures Of Hydrogen Near The Triple Point," Mann, Ludtke, Sindt, and Chelton, Preprint of Paper E-4 prepared for presentation at the 1965 Cryogenic Engineering Conference, Rice University, Houston, Texas, August 23-25, 1965.

1. Density of solid = 86.5 gm/liter

(h) "Fluid Hydrogen Slush-A Review," Cook and Dwyer, Preprint of Paper E-3 prepared for presentation at the 1965 Cryogenic Engineering Conference, Rice University, Houston, Texas, August 23-25, 1965.

1. Density of liquid = 4.808 lbs/ft^3 = 77.006 gm/liter
2. Density of solid = 5.406 lbs/ft^3 = 86.584 gm/liter

(i) "Heat Of Fusion And Density Of Solid Parahydrogen At Pressures To About 400 Atmospheres," Lander, Dwyer, and Cook, Preprint of Paper to be presented at Cryogenic Engineering Conference, Rice University, Houston, Texas, August 23-25, 1965.

1. Density of solid = 5.408 lbs/ft^3 = 86.616 gm/liter

These values are listed in Table I, where the column labled "Source" is indexed to the references above.

A non-critical listing of physical constants, such as Table I, is of little value except to demonstrate forcefully that care and judgment must be exercised in selecting the most probable value. For this study, the "best" value for the required densities and dielectric constants was determined in the following way.

4.1 The Density of Solid and Liquid Parahydrogen at the Triple Point

R. B. Stewart and H. M. Roder [1964] give the density of solid parahydrogen at the triple point as 0.04291 g mols/cm^3. This value was determined as follows:

Woolley, Scott, and Brickwedde [1948] in NBS RP1932, page 467, table 38, lists the latent heat of fusion for parahydrogen at the triple point as 28.03 cal/mole.

Roder, Diller, Weber, and Goodwin [1963] list the slope of the fusion line at the triple point as 29.28 atm/°K.

By the Clapyron equation, we may calculate the volume change in fusion as:

$$\Delta V_{fusion} = \frac{L}{T}\frac{dT}{dP} = \left(\frac{28.03 \text{ cal/g mol}}{13.803 \text{ °K}}\right)\left(\frac{1}{29.28}\frac{\text{°K}}{\text{atm}}\right)$$

$$\left(\frac{4.1840 \times 10^7 \text{ dyne - cm}}{\text{cal}}\right)\left(\frac{1 \text{ atm. cm}^2/\text{dyne}}{1.013250 \times 10^6}\right)$$

$$= 2.864 \text{ cm}^3/\text{g mole.}$$

Table I. Reported Values of Density and Dielectric Constant for Solid and Liquid Hydrogen at the Triple Point

Source	Dielectric Constant		Density, gms/ℓ	
	Liquid	Solid	Liquid	Solid
a	1.2516	1.2808	-	-
b	1.254	1.282	-	-
c	-	-	77.03	86.64
d	-	-	77.038	86.648
e	-	-	77.006	86.504 and 86.456
f	-	-	77.005	86.680
g	-	-	-	86.5
h	-	-	77.006	86.584
i	-	-	-	86.616

Woolley, Scott, and Brickwedde [1948] in NBS RP1932, page 460, table 31, lists the volume of the liquid at the triple point as 26.176 cm^3/mole, or the density of the liquid at the triple point is 1/26.176 cm^3/gmole = 0.03821 gmole/cm^3. By difference then the value of the density of the solid at the triple point is,

$$V_{solid} = V_{liquid} - \Delta V_{fusion}$$

$$V_{solid} = 26.176 - 2.864 = 23.312 \text{ cm}^3/\text{g mole}$$

and $\rho_{solid} = 1/V_{solid} = 0.04291$ gmole/cm^3.

NBS RP 1932 also lists the volume change on fusion in table 34, page 461. This value was also calculated by the Clapyron equation with the calorimetrically measured heats of fusion. For normal hydrogen they reported value of 2.85 whereas the value calculated here is 2.86 cm^3/mole. The difference may be more due to the different vapor equation used for the value of dP/dT than for the differences between normal and para hydrogen.

Taking the molecular weight of hydrogen as 2.01594 gms/gmole, the following values of density are calculated:

(a) triple point liquid parahydrogen

$$\rho_\ell = \left(0.03821 \frac{\text{gm mole}}{\text{cm}^3}\right)\left(2.01594 \frac{\text{gm}}{\text{gm mole}}\right)\left(\frac{10^3 \text{ cm}^3}{\ell}\right)$$

$$\rho_\ell = 77.029 \text{ gm}/\ell$$

and

(b) triple point solid parahydrogen

$$\rho_s = \left(0.04291 \text{ gm}/\text{cm}^3\right)\left(2.01594 \text{ gm}/\text{gm mole}\right)\left(10^3 \frac{\text{cm}^3}{\ell}\right)$$

$$\rho_s = 86.504 \text{ gm}/\ell.$$

4.2 The Dielectric Constant of Solid and Liquid Parahydrogen at the Triple Point

The dielectric constant and density are related for simple fluids, such as hydrogen, by the well-known Clausius - Mossotti function:

$$P = [(\epsilon - 1)/(\epsilon + 2)] (1/\rho)$$

Where P is the macroscopic polarizability in units of induced dipole moment per unit mass per unit applied field, and ϵ and ρ are the dielectric constant and density in cgs units.

Stewart [1964] determined the dielectric constant over the density range 0.0024-0.0796 g/cm^3 (2.6-326 atm and 24°-100°K) in both liquid and gas. The recent completion of PVT measurements on fluid parahydrogen in this laboratory by Goodwin, Diller, Roder, and Weber [1963] has made available density values considerably more precise than heretofore. The absolute accuracy of these results is estimated to be better than 0.1% and the relative precision 0.02%.

Stewart's measurements combined with those of Goodwin and others permit the Clausius - Mossotti function to be calculated with 0.05% precision. In the range considered, the CM function, or polarizability, instead of being constant, initially rises with density to a maximum 0.2% above the low density value of 1.00427 cm^3/g, and then falls. The data in this range can be represented within experimental error by a quadratic function of density. The results were presented in tabular form. Also the dielectric constant at any desired density can easily be calculated to an accuracy better than 0.1% in ϵ - 1 from the function fitting the polarizability.

Accordingly we shall combine this work of Stewart with the density values determined above to find the corresponding dielectric constants.

Stewart suggested that the reciprocal of the CM function rather than the function itself should be used. Accordingly, a least-squares fit was

made of

$$1/P = A + B\rho + C\rho^3$$

by him. The coefficients in this second-degree equation are customarily called the first, second, and third dielectric virial coefficients, by analogy with the usual procedure for handling departures from the ideal gas law in PVT work. They have no relation to the PVT virial coefficients. The values of the CM function and density at all of his 205 data points were fed into a computer and treated with a multiple regression and correlation program to determine the best values of A, B, and C. In addition to the best values of A, B, and C, a Student's "t" test for the confidence levels for nonzero values of B and C was made by Stewart.

The results were

$$A = (0.99575 \pm 0.00132)\ g/cm^3,$$

$$B = (-0.09069 \pm 0.02463) \qquad t = -3.683,$$

$$C = (1.1227 \pm 0.2895)\ cm^3/g \qquad t = 3.878.$$

The t values correspond to confidence levels of at least 99.97% for both B and C. From these it would appear that the parabolic fit is a satisfactory one. The rather uncertain values of the B and C coefficients arise from the extreme flatness of the function, which has a total rise of only 0.2% of its mean value over the density range considered. Evidently, the use of higher order polynomials would not substantially improve the fit.

We may now combine the previously found values of ρ, together with the expression for P, $1/P = A + B\rho, + C\rho^2$, the values for A, B, and C, above, and the Clausius - Mossotti relations solved for ϵ,

$$\epsilon = (1 + 2P\rho)/(1 - P\rho),$$

to obtain the desired dielectric constants.

(a) Triple Point Liquid Parahydrogen

The density of triple point liquid parahydrogen was found to be

0.03821 gm moles/cm^3 or 0.077029 gms/cm^3.

$$\text{From } \frac{1}{P} = A + B\rho + C\rho^2,$$

$$\frac{1}{P} = \left(0.99575 \frac{gm}{cm^3}\right) - \left[(0.09069)\left(0.077029 \frac{gm}{cm^3}\right)\right] + \left[\left(1.1227 \frac{cm^3}{gm}\right)\left(0.077029 \frac{gm}{cm^3}\right)^2\right]$$

$$\frac{1}{P} = 0.99543$$

$$P = 1.00459$$

$$\text{From } \epsilon = (1 + 2P\rho)/(1 - P\rho),$$

$$\epsilon_\ell = \left[1 + 2(1.00459)(0.077029)\right] / \left[1 - (1.00459)(0.077029)\right]$$

$$\epsilon_\ell = 1.15476/0.92262$$

$$\epsilon_\ell = \underline{1.2516}$$

(b) Triple Point Solid Parahydrogen

The density of triple point solid parahydrogen was found to be 0.04291 gm moles/cm^3 or 0.086504 gm/cm^3.

$$\text{From } \frac{1}{P} = A + B\rho + C\rho^2,$$

$$\frac{1}{P} = \left(0.99575 \frac{gm}{cm^3}\right) - \left[(0.09069)\left(0.086504 \frac{gm}{cm^3}\right)\right] + \left[\left(1.1227 \frac{cm^3}{gm}\right)\left(0.086504 \frac{gm}{cm^3}\right)^2\right]$$

$$\frac{1}{P} = 0.996306$$

$$P = 1.00371$$

$$\epsilon = (1 + 2P\rho)/(1 - P\rho)$$

$$\epsilon_s = \left[1 + 2\,(1.00371)(0.086504) \right] / \left[1 - (1.00371)(0.086504) \right]$$

$$\epsilon_s = 1.17365/0.913175$$

$$\epsilon^s = \underline{1.2852}$$

4.3 Summary of Selected Values of the Density and Dielectric Constant of Solid and Liquid Parahydrogen at the Triple Point

The Table below summarizes the selected physical constants which were calculated in the previous sections according to the methods and sources indicated there. The complete list of References follows in Section 4.4.

Table II. Selected Physical Constants of Parahydrogen at the Triple Point.

	Liquid	Solid
Specific Volume	0.03821 g mol/cm^3	0.04291 g mol/cm^3
Density	77.029 gms/ℓ	86.504 gms/ℓ
Dielectric Constant	1.2516	1.2852

The measurement system was then designed on the basis of the above values; that the system would indicate 0% solid content with a fluid sample dielectric constant of $\epsilon = 1.2516$ and would indicate 100% solid content with a fluid sample dielectric constant of $\epsilon = 1.2852$.

4.4 References to Physical Properties

Woolley, H. W., Scott, R. B., and Brickwedde, F. G., (1948), Compilation of Thermal Properties of Hydrogen in its Various Isotopic and Ortho-Para Modifications, J. Res. NBS 41, 379-475.

Stewart, R. B., and Roder, H. M. (1964), Properties of Normal and Parahydrogen, in the book Technology and Uses of Liquid Hydrogen, edited by Scott, Denton, and Nicholls, Pergamon Press, Ltd.

Roder, H. M., Diller, D. E., Weber, L. A., and Goodwin, R. D. (1963), The Orthobaric Densities of Paryhydrogen, Derived Heats of Vaporization, and Critical Constants, Cyrogenics, 3, No. 1, 16-22.

Stewart, J. W. (1964), Dielectric Polarizability of Fluid Parahydrogen, J. Chem. Phys., 40, No. 11, 3297-3306.

Goodwin, R. D., Diller, D. E., Roder, H. M., and Weber, L. A. (1963), Pressure - Density - Temperature Relations of Fluid Parahydrogen from 15 to 100°K at Pressure to 350 Atmospheres, J. Res. NBS 67A (Chem. and Physics), 173-192.

5. Matrix Capacitance Quality Sensor

We have seen in Section 2 that a measurement of slush hydrogen density will infer the fraction solid content, and in Section 3, many different density measurement principles were reviewed for a slush hydrogen application. Of the many principles, the capacitance type was selected. Criteria in this selection were (a) a large sample size, (b) free fluid flow into the sampling section, and (c) availability, i. e., this measurement principle is available now as opposed to one requiring extensive development. Of the several available capacitance principle measurement systems, one employing a matrix type sampling section was selected as it offered the advantages of: (1) a large air capacitance value, (2) a large total sample, (3) a large space between the capacitor "plates" to accommodate large solid particles, and (4) free fluid movement into the sampling section from the top, the bottom, and the side.

This section concerns a test program conducted to evaluate the performance of a capacitance principle measurement system designed to determine slush hydrogen fraction solid content.

5.1 Objectives of Test Program

To evaluate the performance of the selected capacitance principle fraction solid content measurement system, the following test program objectives were established:

(a) Observation of slush flow into the matrix sampling section for both stirred and unstirred slush. The purpose of this was to determine if the solid particles would freely circulate into and within the matrix sampling volume.

(b) Observation of slush fluid reaction when the matrix sampling section was withdrawn from settled, unstirred slush. The purpose of this was the simulation of an application where the slush level was reduced, as in the case of emptying a storage vessel.

Figure 8. Slush Hydrogen Generator, Laboratory Area

(c) Calibration of the fraction solid measurement system. The purpose of this was system design verification.

(d) Make conclusions and recommendations concerning the measurement of fraction solid content.

5.2 Apparatus and Procedures

5.2.1 Slush Generator

The slush hydrogen generator used is shown in Figure 8 and Figure 9. A complete description of the operation of the slush generator is contained in NBS Report 8881, "Characteristics of Liquid-Solid Mixtures of Hydrogen at the Triple Point", by D. B. Mann, P. R. Ludtke, C. F. Sindt, D. B. Chelton, D. E. Daney and G. L. Pollack. As shown in Figure 8, the matrix sampling section was located in a 6 - inch diameter by 30-inch deep glass dewar. The glass dewar was mounted on a 2 - foot long section of 6 - inch diameter copper pipe. This glass dewar-copper pipe assembly was located adjacent to a 6 -inch diameter vacuum pumping connection between the assembly and the vacuum pumping stack.

One end (top) of the copper pipe section was blanked off by a brass plate which served as a mounting base for a gas-driven mixer motor, a lift rod, and a vent line. Stand-offs were used to minimize the heat conduction to these components. A hydrogen fill line valve was located at the side of the copper pipe section. Electrical leads entered the side of the copper pipe section through Kovar-seals.

Veeco fittings were used at the top end of the stand-offs to permit vertical movement of the mixer shaft and the lift rod when raising and lowering the matrix sampling section. Ambient air leakage into the low pressure hydrogen was prevented by helium gas pressurized chambers installed between the Veeco fittings and the stand-offs.

A liquid nitrogen filled glass dewar and a clear plastic shield surrounded the test dewar. The liquid nitrogen served to reduce heat input

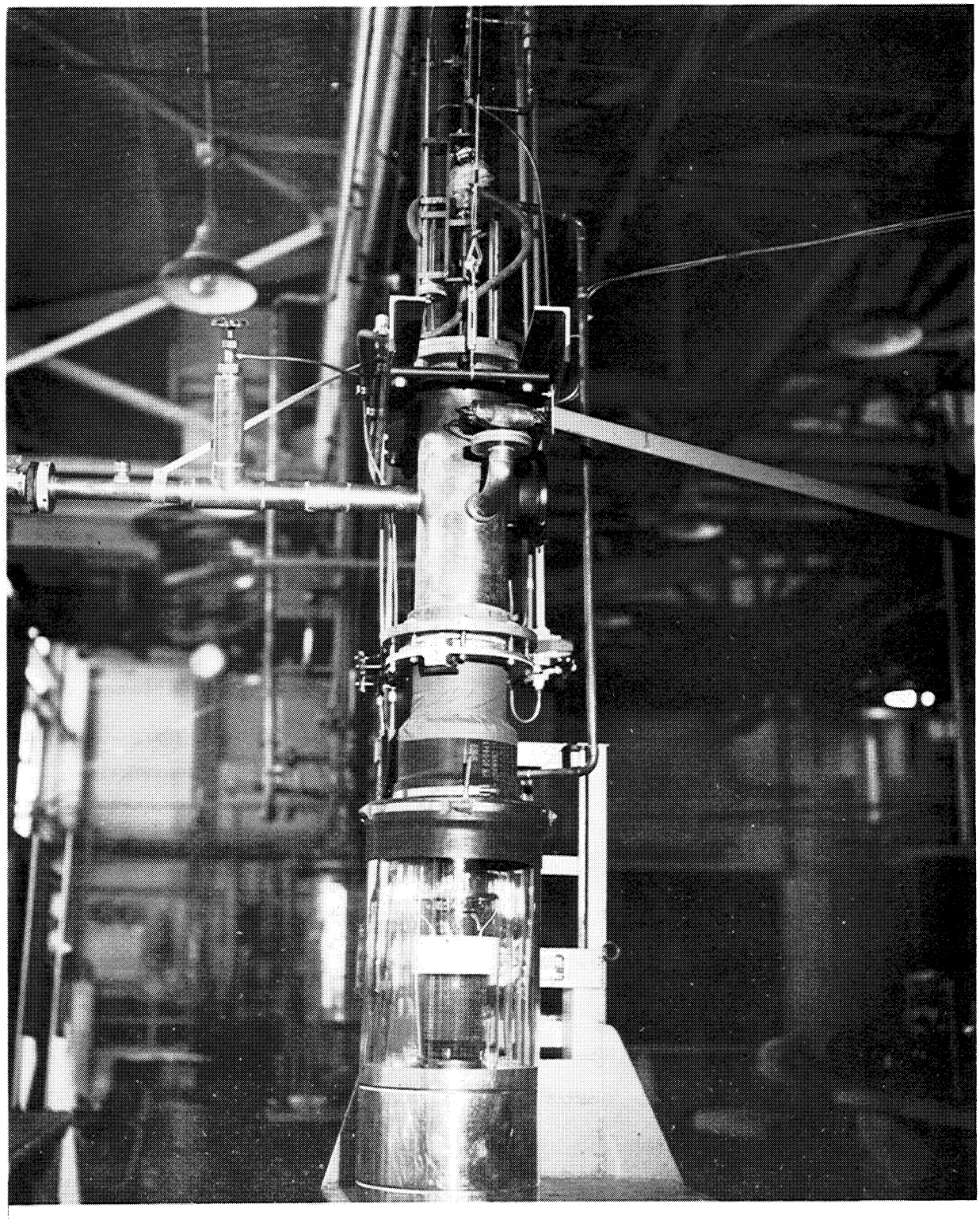

Figure 9. Slush Hydrogen Generator

B- 57713

to the hydrogen while the plastic shield served as a safety measure in case of a glass dewar failure.

An electrical heater was located in the bottom of the test dewar. The heater provided for controlled melting of the solid hydrogen. Electrical leads to the heater were encased in helium filled tubing while the heater was encased in a helium filled chamber. Heater heat capacity was variable from 0 to 100 watts.

Liquid hydrogen filling of the slush generator was controlled by manually operated valves located at both the slush generator and the hydrogen supply dewar. Approximately 10 to 15 liters of liquid hydrogen were used for slush hydrogen generation. Except for a few cases, slush generation was by the "freeze-thaw" technique (see NBS Report 8881, p. 36) using a large capacity vacuum pump. Appropriate control valves and bias gas were used in conjunction with the vacuum pump to generate slush hydrogen.

Withdrawal and immersion of the matrix sampling section was by means of a manually operated gear drive mechanism, located at the top of the matrix sampling section. The mixer was a four-bladed plastic propeller.

5.2.2 Capacitance Sensor and Readout

The capacitance sensor used to measure the slush hydrogen dielectric constant had a matrix configuration. The matrix configuration minimizes the effects of a two-phase fluid geometry distribution by dividing the sample volume into a large number of capacitive cubes which are electrically paralleled. Since capacitors in parallel add, the capacitance of the entire matrix is the sum of all these small capacitive cubes, and therefore is proportional to the dielectric constant of the slush hydrogen within the confines of the matrix.

The matrix is a three-dimensional wire matrix fabricated by IKOR,

the measurement system supplier, under a license from Liquidometer Corporation. The matrix consists of alternate flat wire mats or screens interconnected by longitudinal wire uprights. Adjoining mats and uprights are electrically isolated and maintained at different potentials. Alternate mats and uprights are electrically interconnected and maintained at the same potential. Wire spacing of the mats and uprights is approximately 1/4 inch. Matrix dimensions, including the teflon tube, were 5.9 inch diameter by 7 inch length. Figures 10, 11, and 12 show the matrix.

The upper portion of the matrix is contained by a teflon tube and retainer ring. The lower portion of the matrix is uncovered to facilitate slush circulation and flow visualization.

Matrix radial and axial alignment is maintained by a slotted teflon spacer placed between the two topmost mats. The lower matrix end is unrestrained to allow for differential contractions between the matrix and the teflon tube during cool down. Adequate diametrical clearance is provided at room temperature between the upper end of the matrix and its teflon holder to permit thermal contraction without matrix deformation.

Figure 13 shows the electronic system schematic. A four-arm capacitor birdge is used with the active side of the bridge consisting of the matrix C1 and capacitor C2, and the inactive side consisting of capacitors C3 and C4. The excitation for the bridge is a 1-kHz square wave with controlled rise and fall times.

The high side of the matrix is connected to the center conductor of a 20-foot shielded cable. The opposite end of this cable enters the Mode Switch chassis through a connector. The Mode Switch, when set on Operate, connects the center conductor of this cable to the junction of C2 and the Base of Q1. When the Mode Switch is set to one of the test positions, it connects one of three variable condensers to the junction of C2 and C1. These condensers are adjustable to correspond to 0%, 50%, and 100% solid content.

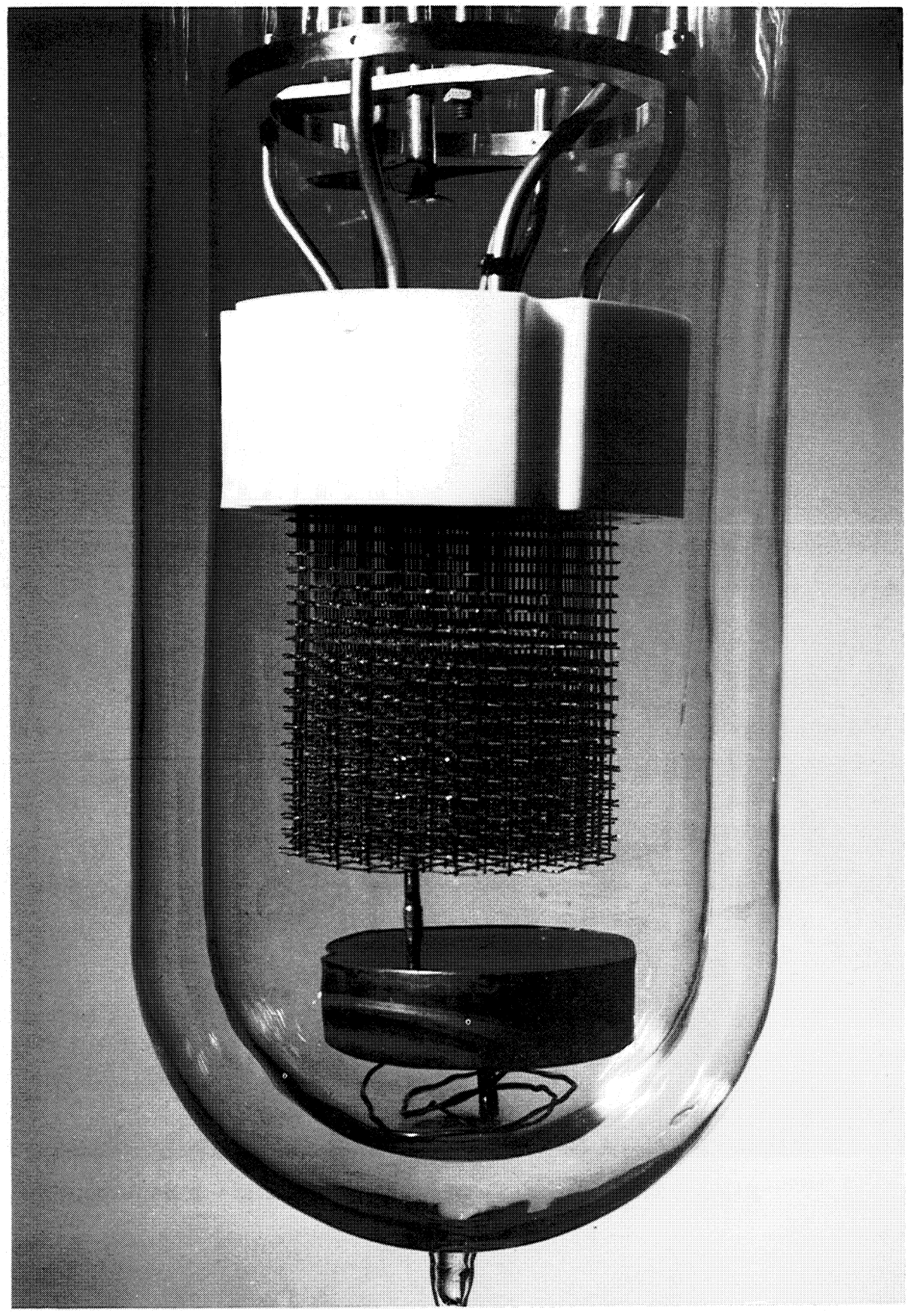

Figure 10. Matrix Capacitance Sensor Installed in Slush Generator

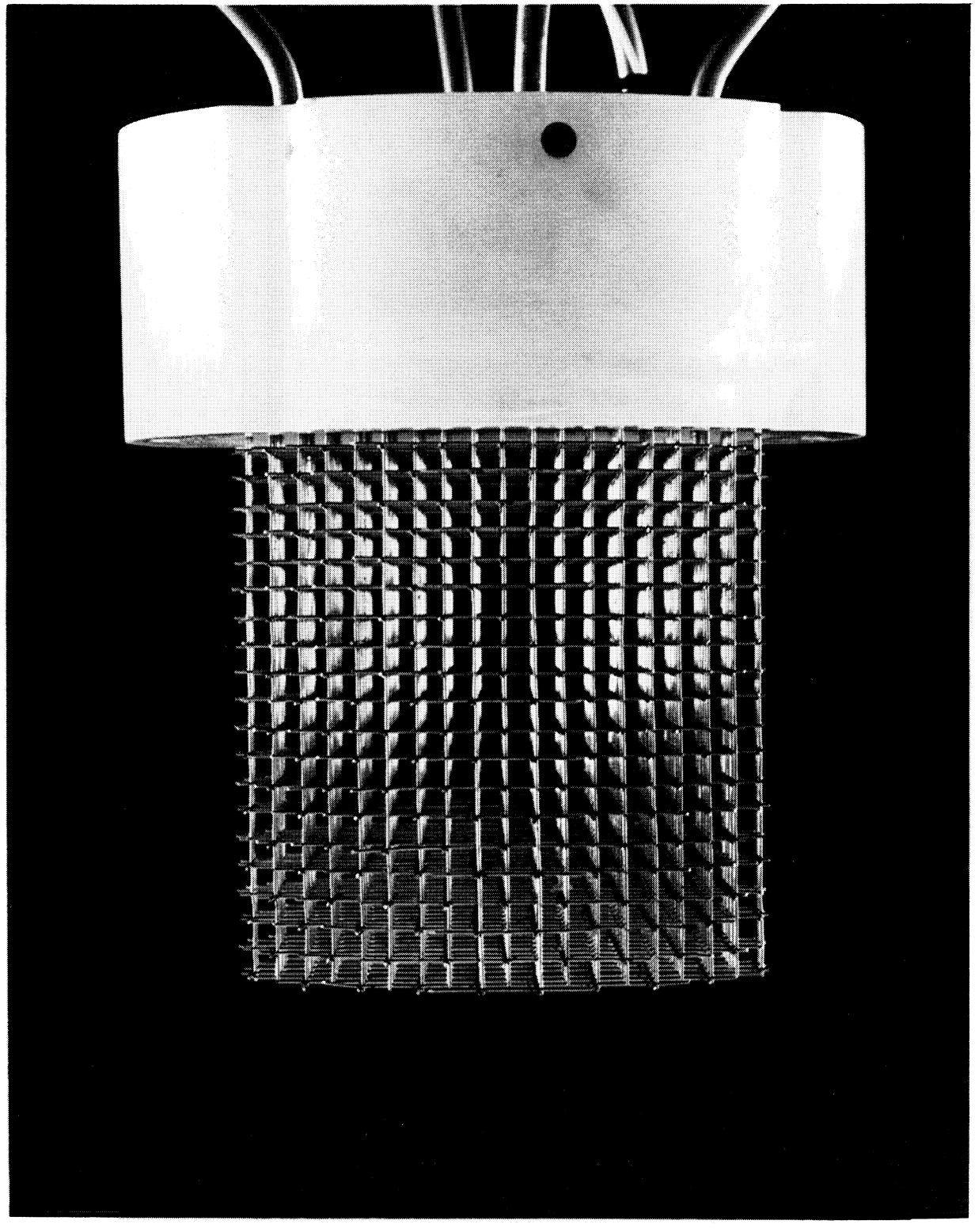

Figure 11. Side View of Matrix Capacitance Sensor

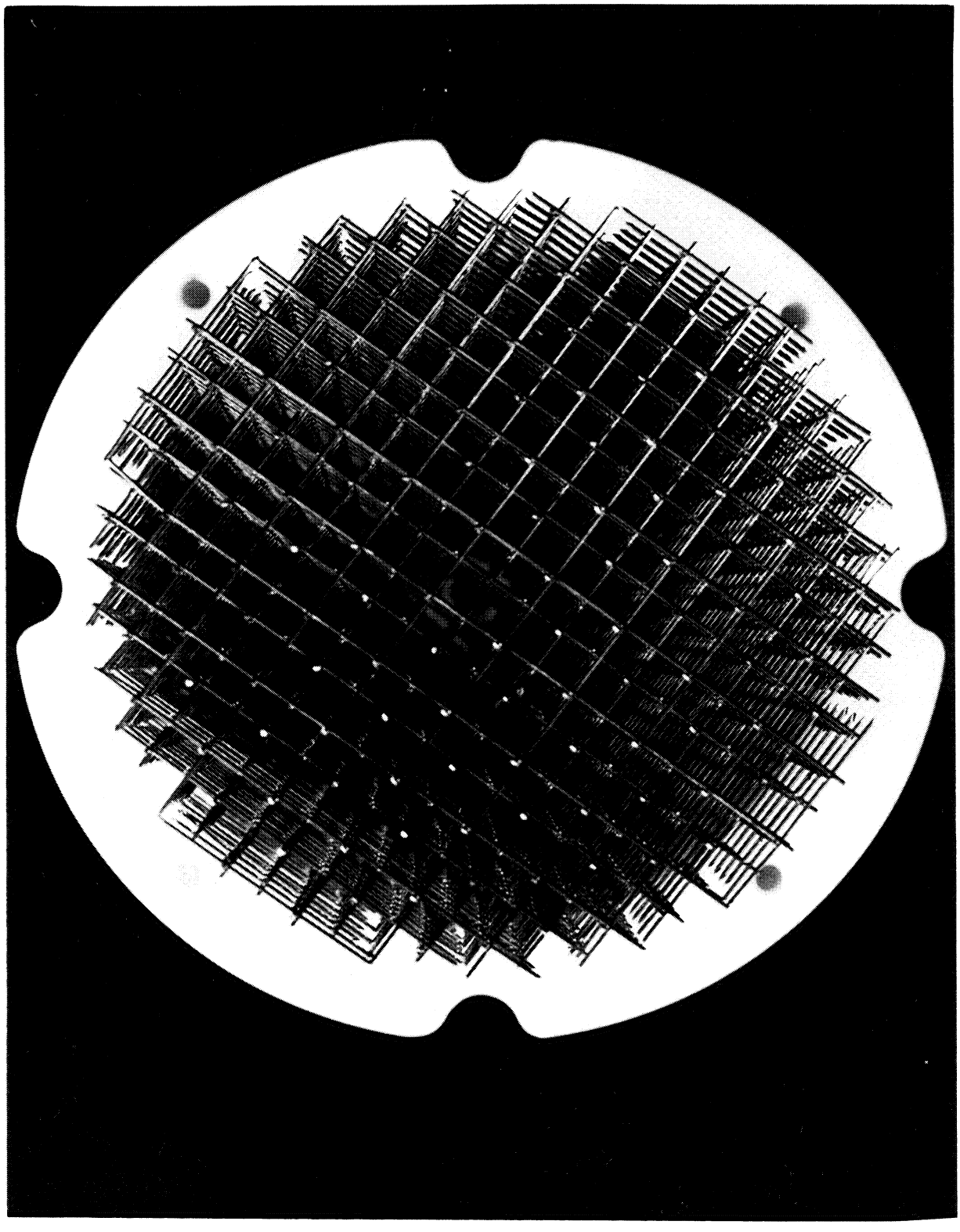

Figure 12. Bottom View of Matrix Capacitance Sensor

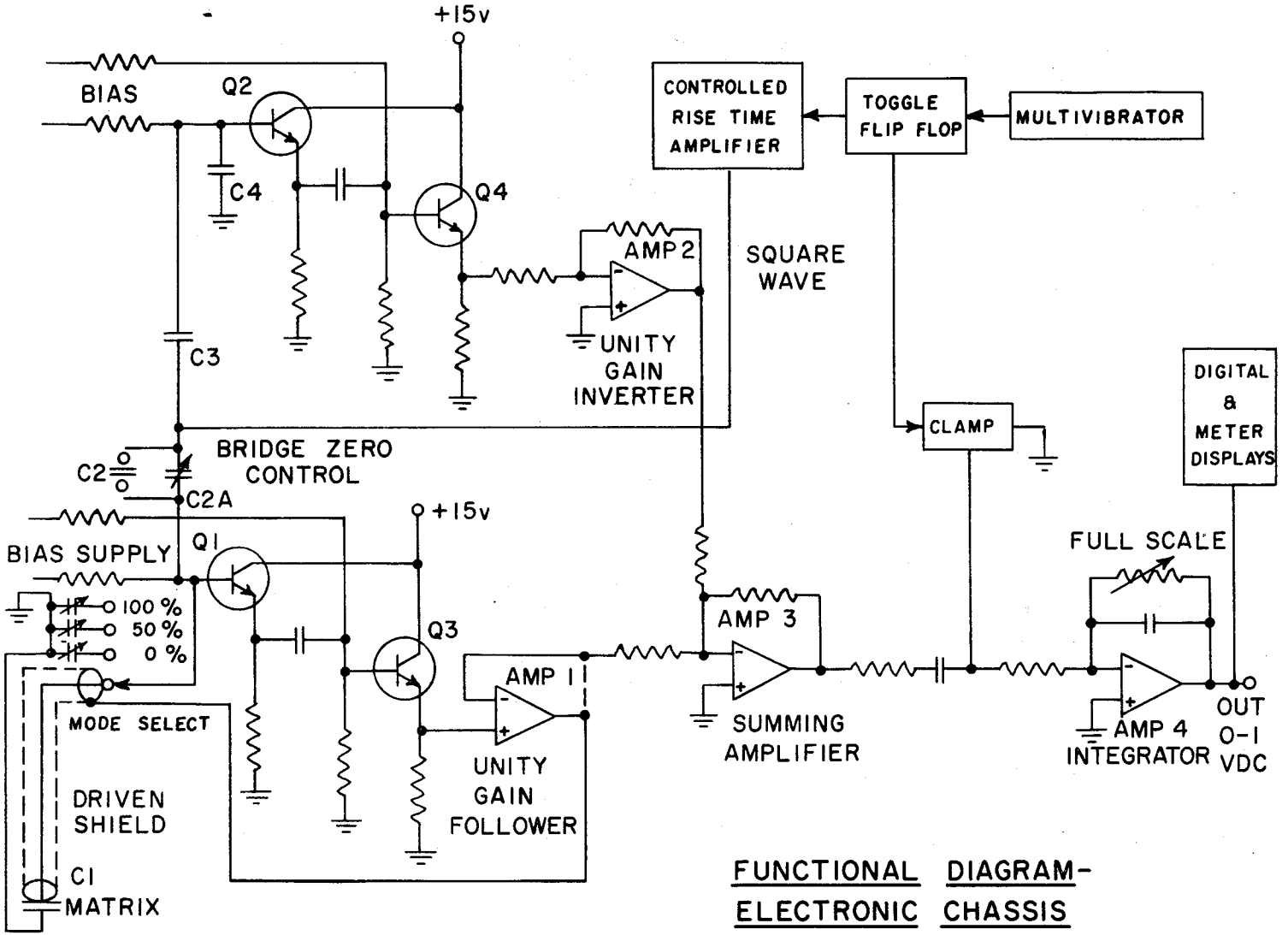

Figure 13. Schematic of Capacitance Electronic System

The low side of the matrix is connected to signal ground within the Mode Switch chassis by means of a wire running alongside the shielded cable and connected to the chassis by a pinjack. Both shielded cable and matrix return are, in turn, protected by a ground shield and flexible plastic sleeving.

The junction of C1 and C2 is coupled to emitter follower Q1 and then to emitter follower Q3. The output of Q3 is fed to a special operational amplifier (Amp 1) connected as a unity gain follower. The output of this follower is used to drive the shield around the cable connecting the matrix capacitor C1 to the bridge. This allows for an approximate 20 foot separation between the matrix sampling section and the bridge. Cable and other stray capacitances are attenuated by about two orders of magnitude by the driven shield.

The signal at the junction of C3 and C4 is fed through emitter followers Q2 and Q4 and then to a unity gain inverter (Amp 2). The outputs of the unity gain inverter and follower are summed and amplified by Amp 3. This signal is proportional to the difference between signals at the bases of Q1 and Q2 and is thus proportional to bridge unbalance. The output of Amp 3 is clamped to ground during each negative half-cycle of the input square wave and integrated by Amp 4 during each positive half-cycle. The integrator has a long time constant related to the square wave, and provides a low ripple, low impedance, dc signal at the output. The integrator is offset by a dc current at the error point to operate the clamp Q5 in a linear region.

The output of the integrator is 1 Vdc full scale. This voltage is displayed by a digital readout and by a large panel meter, both indicating percent solid content.

Figure 14 shows the front panel and controls of the capacitance principle measurement system readout. Some of these controls and their functions are:

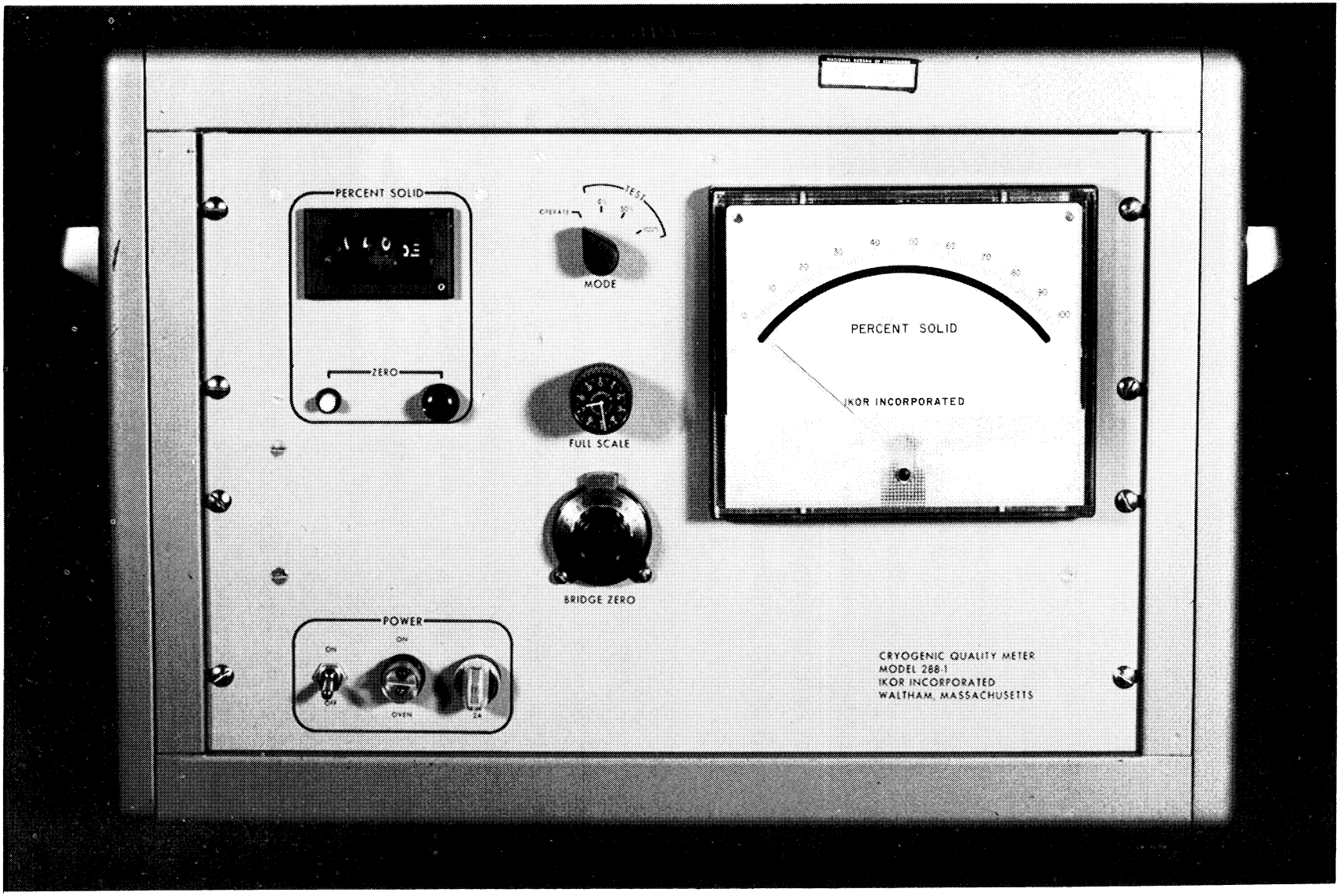

Figure 14. Front Panel of Quality Indicator

1. Mode Switch - selects as input either the matrix or one of three test capacitors.
2. Full Scale Control - allows adjustment of system gain for different ratios of solid/liquid dielectric constants for a variety of cryogens.
3. Bridge Zero Control - adjusts electronic bridge balance for zero reading with zero solid fraction content.

5.2.3 Level Measurement

As a clear glass dewar was used to contain the slush hydrogen, fluid levels were determined with a precision cathetometer. The cathetometer was a Wild model No. 59 and was located approximately 8 feet from the glass dewar. Fluid level measurements were made to within 0.1 mm. Figure 15 is a photograph of the cathetometer.

Fluid level measurements were made to determine fluid volume. To relate level to volume, the dewar was calibrated with water. In these water calibrations, the matrix sampling section was in its test position within the dewar.

5.2.4 Slush Generation

In most cases, slush production was by the "freeze-thaw" technique in which the absolute pressure of the hydrogen was alternately varied from just above to just below the triple point pressure. Slush produced by this technique when unstirred settled to the bottom of the dewar.

In a few cases, it was desired to produce a maximum amount of solid hydrogen. In these few cases, the slush was produced by the "slow-freeze" technique. This technique differs from the "freeze-thaw" technique in that an absolute pressure, slightly below the triple point pressure, is continuously maintained. Solid hydrogen thus generated "grows" downward from the liquid-vapor interface. Using this production technique, solid hydrogen was made until the solid material filled the dewar; that is,

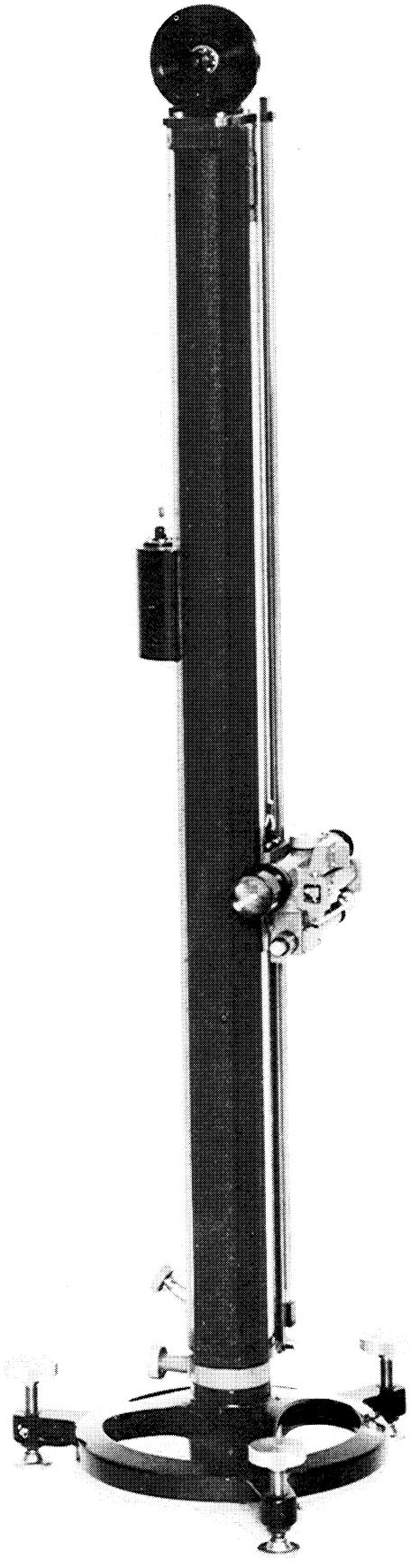

Figure 15. Cathetometer Used for Differential Level Measurement

no visible liquid remained. Approximately three hours were required to generate the solid hydrogen desired when using this technique.

5.2.5 Flow Observations - Freeze - Thaw Slush

When the matrix sampling was in its test position, well below the liquid level, slush produced at the liquid-vapor interface settled downward and into the matrix. Visual observations and movies were made of this fresh, unstirred slush flow into and about the matrix. This same procedure was followed with fresh, stirred slush. With stirring, the solid particles were kept in suspension and flowed freely through the matrix as long as stirring was maintained.

To observe fluid reaction when the matrix was withdrawn from and immersed into a settled slush, the matrix was located in its normal immersed position and the slush was generated by the "freeze-thaw" technique and allowed to settle. The slush production was accompanied by stirring to break up any large particles and to ensure a free fluid circulation into and around the matrix. When sufficient slush was made, stirring ceased and the slush was allowed to settle. The settled slush-liquid interface was near the top of the matrix. Withdrawal from and immersion into the settled slush of the matrix was by manual operation of the gear drive lift mechanism. Visual observations and movies were made of the fluid reaction during this test. The results of these tests are given in Sections 5.2.7 and 5.2.8.

5.2.6 Calibration Procedure

To verify the measurement system design it was necessary to establish a calibration procedure. The initial selected procedure consisted of:

(a) Adjusting the system readout to 0% solid content when the fluid sample existed at the triple point. Operationally this consisted

of slowly reducing the pressure of the fluid sample until a thin crust of solid appeared at the liquid-vapor interface. At this time the system readout was adjusted to indicate 0%.

(b) Making slush hydrogen by the "freeze-thaw" techinque.

(c) Melting the solid hydrogen by means of the heater.

(d) Using the heat of fusion of the solid and the measured total heat input, calculate the percent solid content present and compare this calculated solid content to the indicated solid content.

Such a calibration procedure would reveal calculated solid content end points; the end points being the percent solid content at the start of the melt and the percent solid content at the end of the melt, 0%.

This calibration procedure was unsatisfactory since it depended upon a visual observation of the end of the melt. This observation was subject to human error; different observers made different judgements of when the solid was completely melted. Also, near the end of the melt, while solid particles were still clearly visible, some of the heat input was heating the liquid. Thus, instead of a homogeneous triple point liquid at the end of the melt, some of the liquid existed at a temperature above that of the triple point. Such a liquid has a dielectric constant below that of a triple point liquid; thus, at the end of the melt, the indicated percent solid content was less than the desired 0%.

The final selected calibration procedure consisted of:

(a) Adjusting the system readout to 0% solid content when the fluid sample existed at the triple point. Operationally this consisted of slowly reducing the pressure of the fluid sample until a thin crust of solid appeared at the liquid-vapor interface. At this time the system readout was adjusted to indicate 0%.

(b) Making slush hydrogen by the "freeze-thaw" technique.

(c) Melting the solid hydrogen by means of the heater

(d) Measuring the fluid volume change by a cathetometer and recording the indicated percent solid content at discrete time intervals during the melt.

(e) Using the measured fluid volume change during a discrete time interval of the melt, calculate the percent solid content change during the time interval.

(f) Compare the indicated percent solid content from the sensor with that calculated percent solid content obtained from the volume change.

In this procedure, volume was determined by liquid level measurements, as measured by the cathetometer. The dewar was originally volume calibrated using water and the cathetometer. To avoid the previous problem of heating the liquid during the melt, volume readings and indicated percent solid content readings were taken only during the period when the heat input was melting the solid. This was determined by noting a linear volume change for a fixed amount of heat input during a fixed time interval. In this calibration procedure, the fluid was stirred to ensure as honogeneous a fluid as possible.

5.2.7 "Freeze-Thaw" Slush Flow

Observations of slush flow into and around the matrix sensor were, for the most part, concerned with slush generated by the "freeze-thaw" technique. Slush generated in this manner was aged for approximately 30 minutes; and as a consequence, was of a "light downy" appearance.

When slush was generated by the "freeze-thaw" technique, and with no stirring, the solid particles would settle downward from the surface. At first these particles were observed to flow downward through the matrix sensor and then collect at the bottom of the test dewar. With continued slush generation, the solid particles were then observed to build up or "bridge" over the top end of the matrix sensor, thus preventing any further

solid particle flow into and through the matrix. When this "bridging" of fresh solid particles was slightly stirred, by means of the propeller mixer which was located approximately 2 inches above the top of the matrix, the solid particles were observed to once again flow freely into and through the matrix. With still further slush generation, accompanied by stirring, it was observed that the solid particles still continued to freely flow into and through the matrix. At the cessation of slush generation, and with mixing stopped, the solid particles were observed to settle downward through the mixer until the resultant settled slush filled and covered over the top end of the matrix.

A number of tests were conducted to observe the settled slush flow reaction when the matrix sensor was withdrawn from and immersed into the settled, 30 minutes old, fresh slush.

When the matrix sensor was withdrawn from the settled slush and into the clear liquid it was observed that the slush freely flowed downward through the matrix. No "hang-up" of solid particles was observed in the matrix. This test was conducted to simulate the emptying of a slush hydrogen storage vessel where the fluid level would be dropping; hence, the slush level would traverse a fixed position matrix sensor in a downward direction.

When the matrix sensor was immersed into the fresh settled slush from the clear liquid sone, no flow of the slush was observed into the matrix. Instead of a free flow into the matrix, the slush appeared to be compacted by the lower end of the matrix. In addition, the settled slush that was not acted on, that is the settled slush between the outside of the matrix and the dewar wall, did not collapse and flow into the matrix. This reaction was similar to "boring a hole" in the settled slush.

5.2.8 "Slow-Freeze" Slush Flow

In addition to observations of slush flow in the matrix using "freeze-thaw" slush, observations were made of slush flow into and through the matrix using slush generated by the "slow-freeze" technique. The purpose of this particular test was to observe the slush flow when the slush had a

high percentage of solid content. The solid hydrogen generated by this "slow-freeze" technique was made in such a quantity that no discernible liquid remained in the test dewar. The solid thus generated was almost a solid cake. Approximately 3 hours were required for this production of solid hydrogen. This solid hydrogen, although generated at an absolute pressure just slightly below the triple point pressure, hence at a slow rate, was not clear in appearance, thus indicating the presence of vapor inclusions or voids. Observations of the matrix during the formation of this solid revealed that the solid formed within the matrix and appeared to completely fill the matrix. With the matrix sensor filled with the generated solid hydrogen, it was noted that the percent solid content indication of the sensor readout was registering a value below zero percent. This reading was attributed to the fact that a fluid mixture of solid and triple point liquid (slush) did not exist within the matrix. Instead, a fluid mixture of solid, liquid, vapor and possibly vacuum voids existed. Such a fluid mixture could have a dielectric constant below that of a triple point liquid (zero percent solid content) and thus the sensed capacitance value is low and will drive the readout to a below zero reading.

After the formation of the solid cake in the test dewar, the absolute pressure was raised to a pressure slightly above the triple point pressure, thus causing a slow melt of the solid. During this melt, attempts were made to drive the mixer propeller. The mixer propeller however was "frozen" in the solid cake. After a while, however, melting of the solid had progressed to such a point that the mixer propeller became free and stirring was then accomplished. At this point, the fraction solid content sensor readout registered a near 50% solid content. The accuracy of this reading was however questionable because of the possibility of vapor inclusions or voids still remaining in the solid particles. Observations of the slush flow revealed that the mixer was breaking up the solid which then appeared to freely flow into and through the matrix.

5.2.9 Calibration of Measurement System

Upon the initial receipt of the measurement system from the contractor, several trial runs were made using both nitrogen slush and hydrogen slush for system familiarization. These runs revealed that the system readout had drift, so the system was returned to the contractor for repairs. The contractor determined that the heater controls in the Bridge Zero required redesign. These trial runs also revealed that when the heater, located at the bottom of the test dewar, was energized, extraneous capacitance was generated which then affected the matrix sensor thus causing the system readout to oscillate. This meant that capacitance readings, thus percent solid content, could only be taken when the heater was not energized.

The calibration procedure used has already been described in the previous Calibration Procedures, Section 5.2.6. Briefly, the procedure followed consisted of:

(a) Establish the zero percent solid content indication on the system readout.

(b) Make "freeze-thaw" slush with stirring.

(c) Make slush until seemingly a maximum value was reached.

(d) Record fluid level, readout indication, and time.

(e) Apply heat (typically 29 watts) for 30 seconds with stirring to melt the solid hydrogen. Maintain absolute pressure in dewar at slightly above triple point pressure.

(f) Stir for a total of 50 seconds.

(g) At 60-second time interval; record fluid level, readout indication, and time.

(h) Repeat cycle as shown in (e), (f), and (g) until fluid level ceases to increase.

From the recorded data of the above procedure a plot was made of the fluid volume versus time. Figure 16 shows such a plot in which

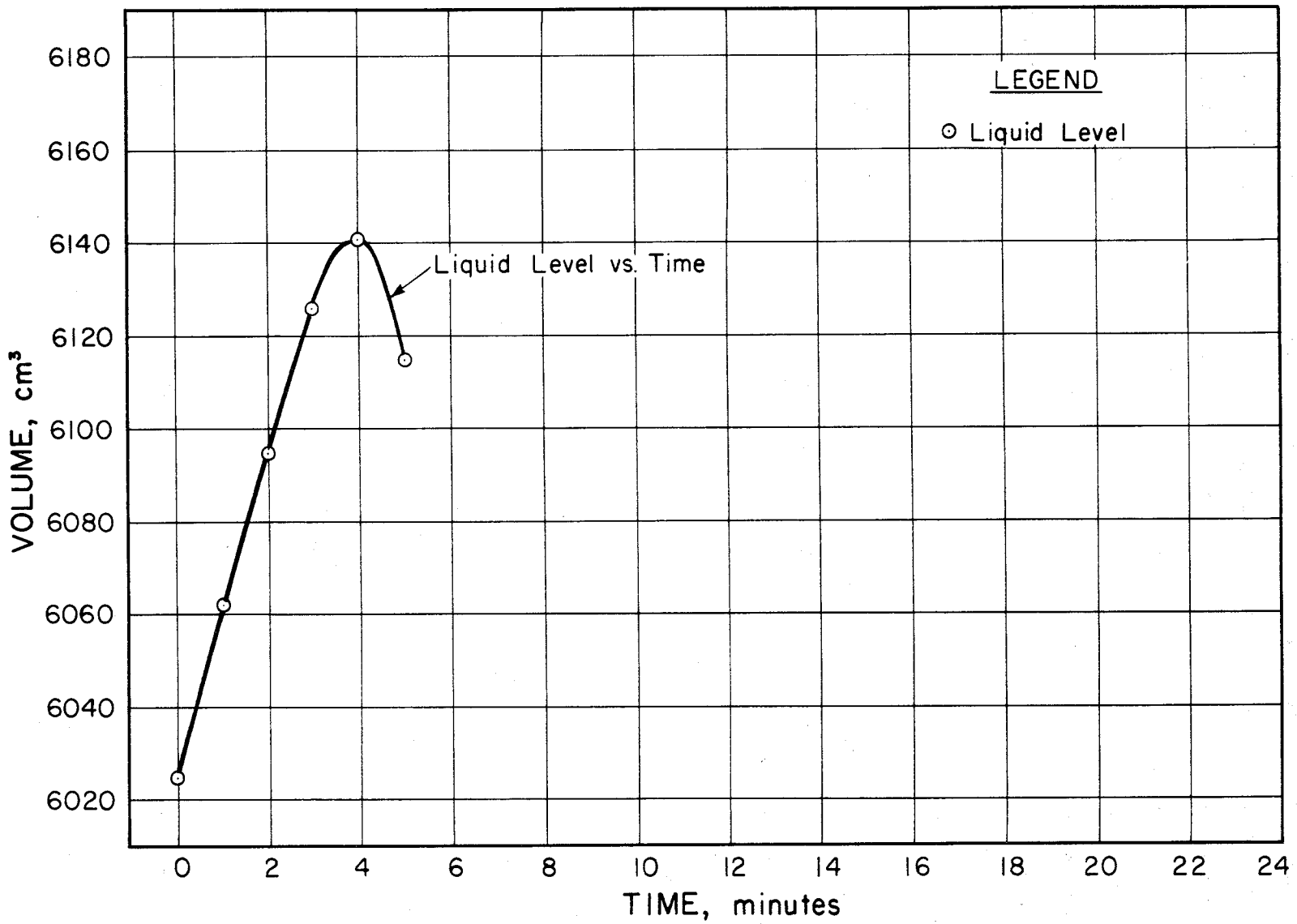

Figure 16. Change in Fluid Volume vs. Time, Typical Run

the volume increase with time is very near a straight line until a maximum volume is reached after which the volume decreased. This maximum volume is assumed to be the point at which the solid content is completely melted. The onset of the decrease in liquid level corresponds to liquid vaporization. Observations of the slush tended to verify this as the solid particles were seen to be just melted at this point.

Knowing the fluid volume end points, the start of the melt where the maximum solid content is present, and the end of the melt where the solid content is zero, calculations were made to determine the solid content at the start of the melt. These calculations depend upon the following relations.

From the definition of specific volume, (V/M), the mass of any material is $M = V/\bar{v}$, where V = total volume, M = mass, and $\bar{v}$ = specific volume. Consider now the problem of determining the unknown mass of a solid from its change of volume upon melting. The mass will be unchanged by this process, thus:

$$M = M_\ell = M_s = \frac{V_\ell}{\bar{v}_\ell} = \frac{V_s}{\bar{v}_s}$$

Where the subscript s refers to the solid originally present, and the subscript ℓ refers to the liquid formed from melting the solid.

From the definition of specific volume, again, we have

$$M\bar{v}_s = V_s$$

and

$$M\bar{v}_\ell = V_\ell$$

Where no subscript is required on M, since the mass is unchanged by melting, or $M = M_s = M_\ell$.

Taking the difference of these last two relations, we have

$$V_\ell - V_s = M\bar{v}_\ell - M\bar{v}_s = M(\bar{v}_\ell - \bar{v}_s)$$

$$\text{now let } \Delta V = (V_\ell - V_s)$$

$$\text{and } \Delta \bar{v} = (\bar{v}_\ell - \bar{v}_s)$$

If these two definitions of ΔV and $\Delta \bar{v}$ are used in the equation immediately above them, then

$$\Delta V = M(\Delta \bar{v})$$

$$\text{or } M = \frac{\Delta V}{\Delta \bar{v}}$$

$$\text{but } M = M_\ell = M_s$$

$$\text{so } M_s = \frac{\Delta V}{\Delta \bar{v}}$$

Using the above, $M_s = \frac{\Delta V}{\Delta \bar{v}}$, a sample calculation, referenced to the fluid volume versus time plot of Figure 16 is as follows:

$$\underline{\underline{\Delta V}} = 6141 \text{ cm}^3 - 6025 \text{ cm}^3 = 116 \text{ cm}^3$$

$$M_s = \frac{\Delta V}{\Delta \bar{v}}$$

$$\text{where } \Delta \bar{v} = (\bar{v}_\ell - \bar{v}_s)$$

$$= (12.98 \text{ cm}^3/\text{gm} - 11.56 \text{ cm}^3/\text{gm})$$

$$\Delta \bar{v} = 1.42 \text{ cm}^3/\text{gm}$$

$$\underline{\underline{M_s}} = 116 \text{ cm}^3/(1.42 \text{ cm}^3/\text{gm}) = \underline{\underline{81.69 \text{ gm}}}$$

$$V_\ell = V - V_s$$

$$V_\ell = 6025 \text{ cm}^3 - \left(\frac{81.69 \text{ gm}}{.086504 \text{ gm/cm}^3}\right)$$

$$\underline{\underline{V_\ell}} = \underline{\underline{5080.65 \text{ cm}^3}}$$

$$\% \text{ solid content} = x_m = \frac{M_s}{M_s + M_\ell}$$

$$x_m = \frac{81.69 \text{ gm}}{81.69 \text{ gm} + \left[\left(5080.65 \text{ cm}^3 \right) \left(.077029 \frac{\text{gm}}{\text{cm}^3} \right) \right]}$$

$$x_m = 17.3\%$$

Repeating this calculation procedure using the intermediate recorded fluid volumes, a plot was made of the calculated percent solid content and fluid volume. Figure 17 shows such a plot derived from Figure 16.

In this figure we display the Quality (% solid content) calculated from the volume change. This is considered to be our standard, or actual quality present. It is shown as the dashed line and dark circles.

The data points, x, are the corresponding qualities indicated by the instrument. Associated with each of them is the tolerance allowed in the measurement system, namely ± 2%.

Therefore, as long as the calculated quality line falls within the boundaries of the indicated quality points, the system is said to be within specification. We see that this is the case in Figure 16 for all the points but one, namely that one taken at the start of the run.

Figures 18and 19 are similarly paired (as were Figures 16 and 17), and the above discussion applies directly to Figure 19.

It was felt that the indicator system (Figure 14) was perhaps limiting the measurement precision. Accordingly, as experimental run was also made in which a General Radio type 1615 A capacitance bridge was substituted for the contractor readout. This bridge was used in conjunction with the contractor supplied matrix capacitance sensor. Experimental and analytical procedures were the same as before except that the GR bridge capacitance readings had to be converted to a percent solid content reading.

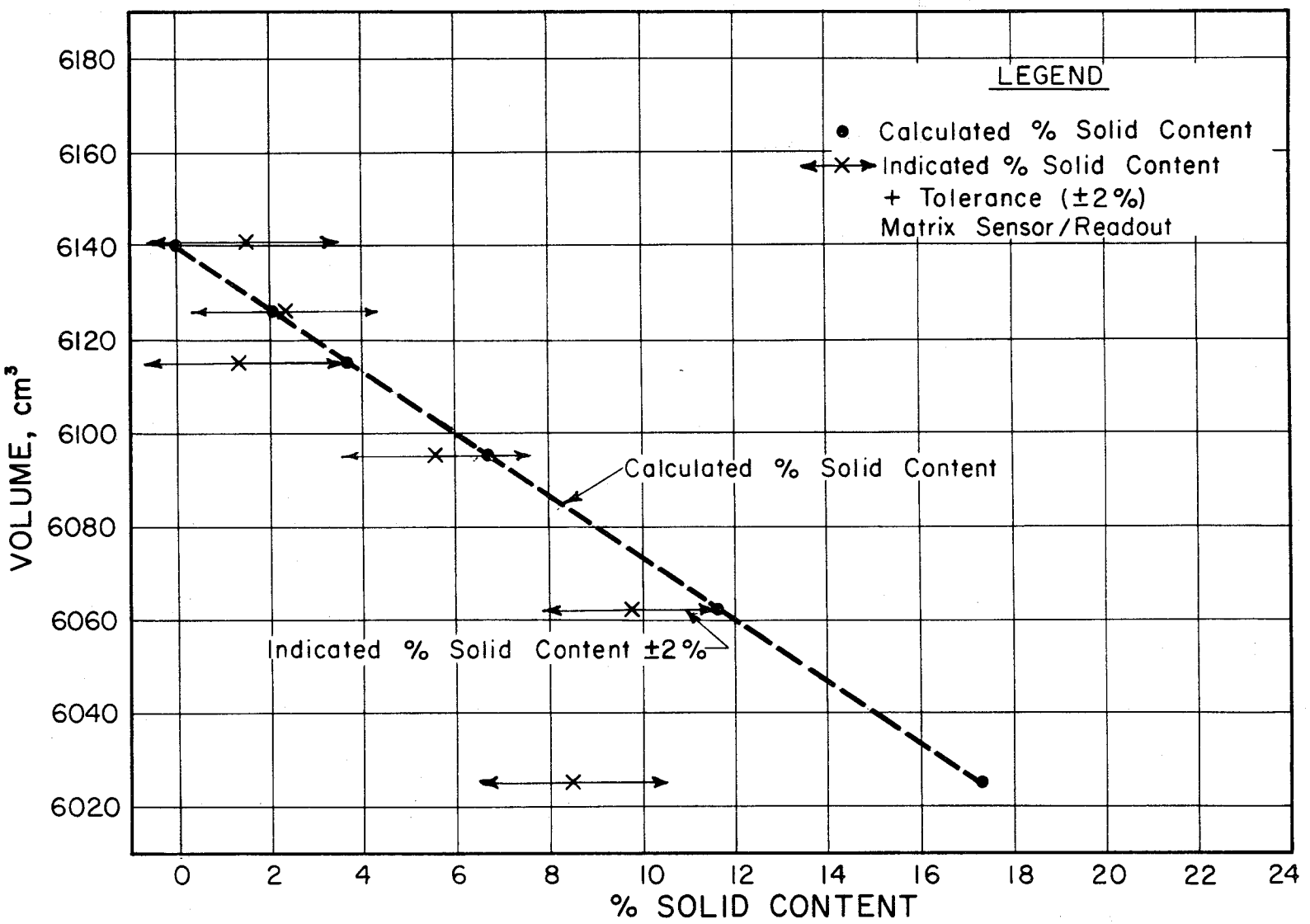

Figure 17. Volume Change, Calculated Quality and Indicated Quality, Typical Run

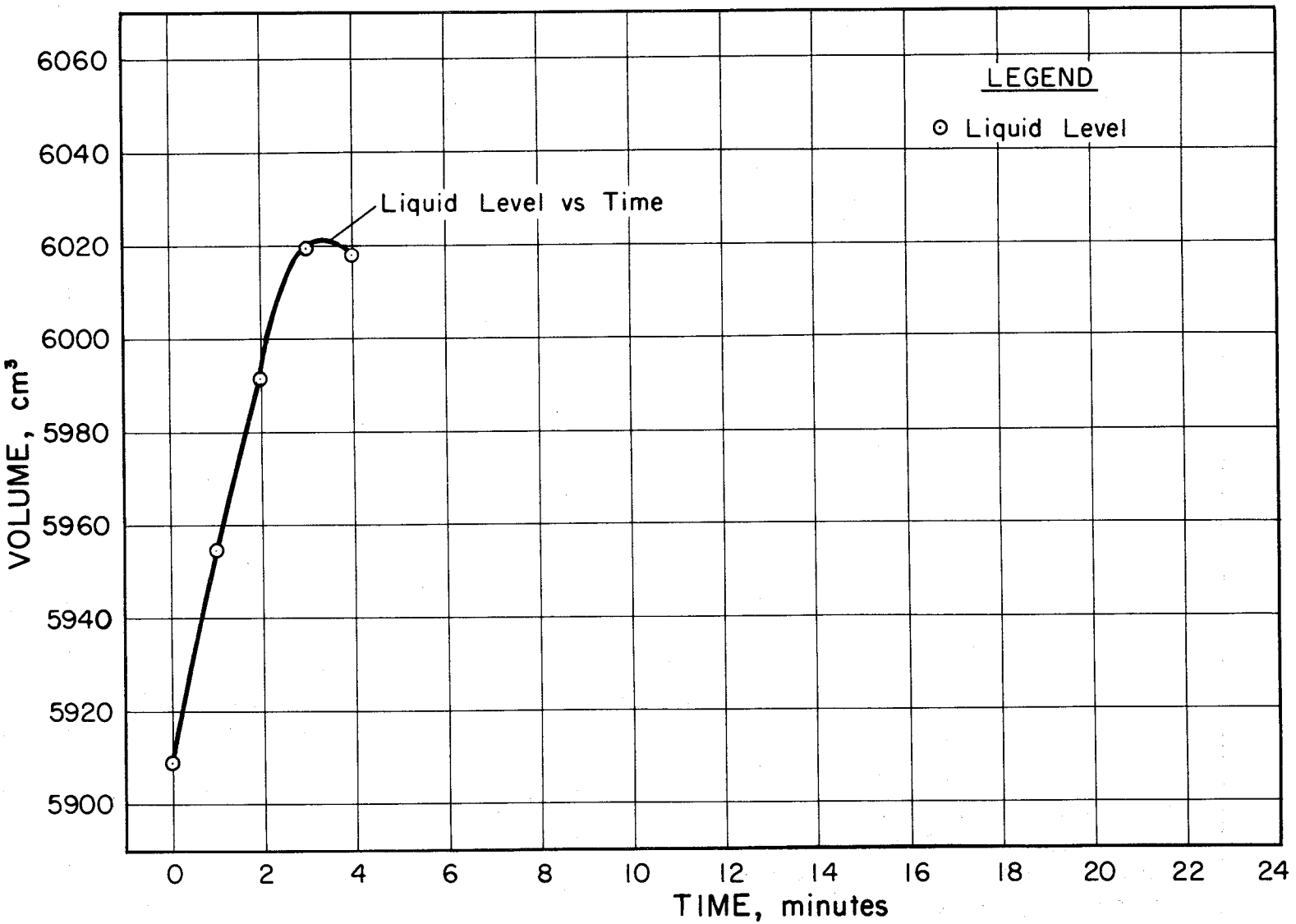

Figure 18. Change in Fluid Volume vs. Time, Second Typical Run

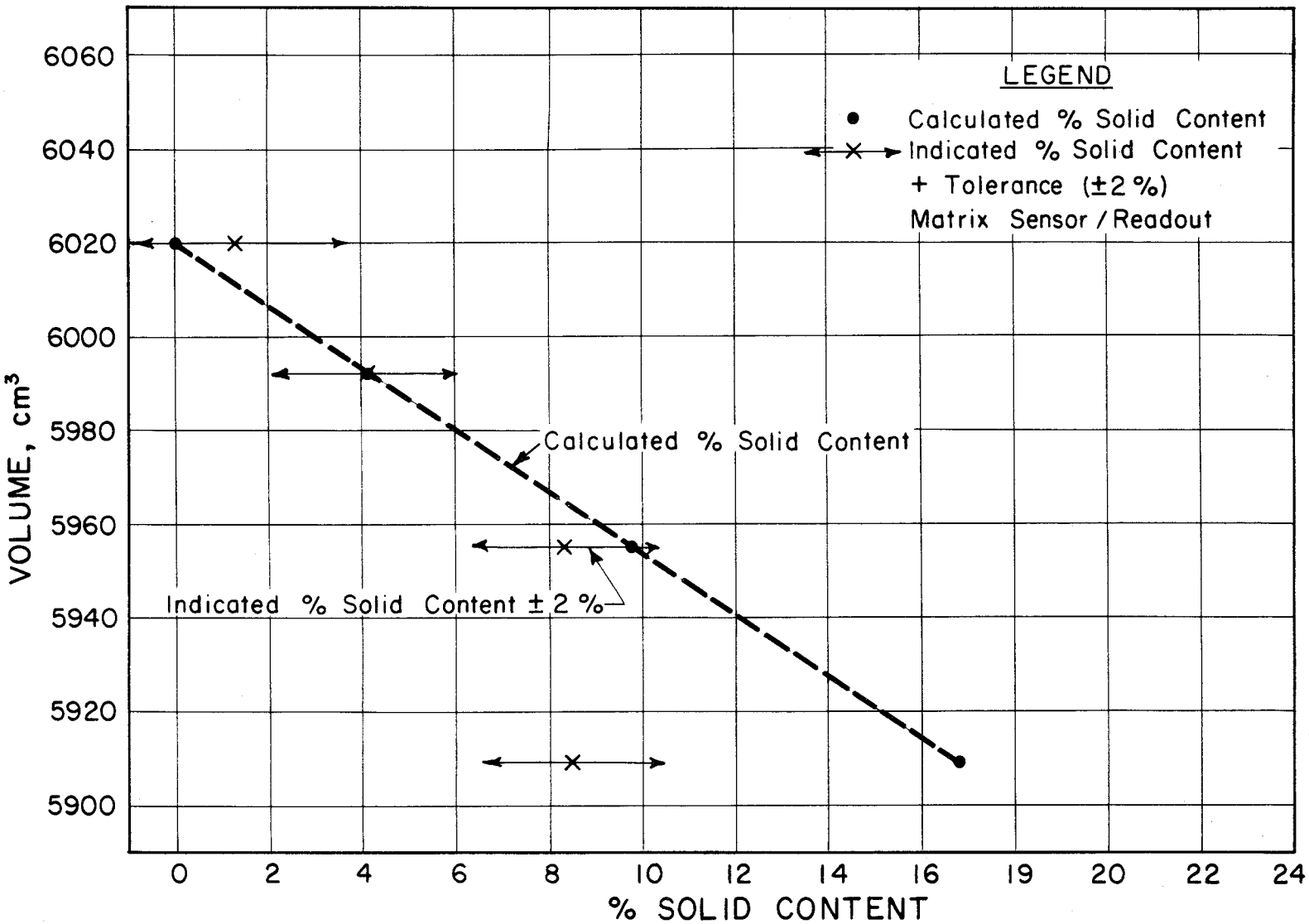

Figure 19. Volume Change, Calculated Quality and Indicated Quality, Typical Run

The results of this experimental run are shown in Figures 20 and 21.

Performance of the contractor measurement system, as shown in Figures 17 and 19, and of the GR bridge-contractor matrix sensor combination, as shown in Figure 21, is acceptable, being within the specification tolerance except at the start of the experimental runs. All measurements at this point are low in relation to the calculated percent solid content for this point. It is felt that these low measurement readings could be due to insufficient mixing of the slush within the test dewar at the beginning of the run. The propeller mixer did not appear to evenly stir the slush fluid when the percent solid content exceeded the 10% level. Good stirring was evident, by observation, when both the propeller mixer was running and the heater was energized. Thermal agitation and mixing of the slush fluid were observed when the heater was energized, at points other than the initial one of the run.

5.3 Conclusions and Recommendations

The results of this test program indicated that the selected capacitance principle measurement system performed to specification tolerances in measuring the solid content of slush hydrogen. Also, visual observations of slush flow into and through the matrix sensor of "freeze-thaw" generated slush was satisfactory, in particular when the slush was stirred. A simulated field type application revealed that the flow of a settled slush out of the matrix was satisfactory when the settled slush level was lowered.

Performance of the capacitance principle measurement system is dependent upon the slush hydrogen existing as a homogeneous liquid-solid mixture. Vapor inclusions or vacuum voids in the solid will adversely affect the measuring accuracy. This is because the measurement is based on the dielectric constant of triple point liquid representing zero percent solid content and the dielectric constant of triple point solid representing 100 percent solid content.

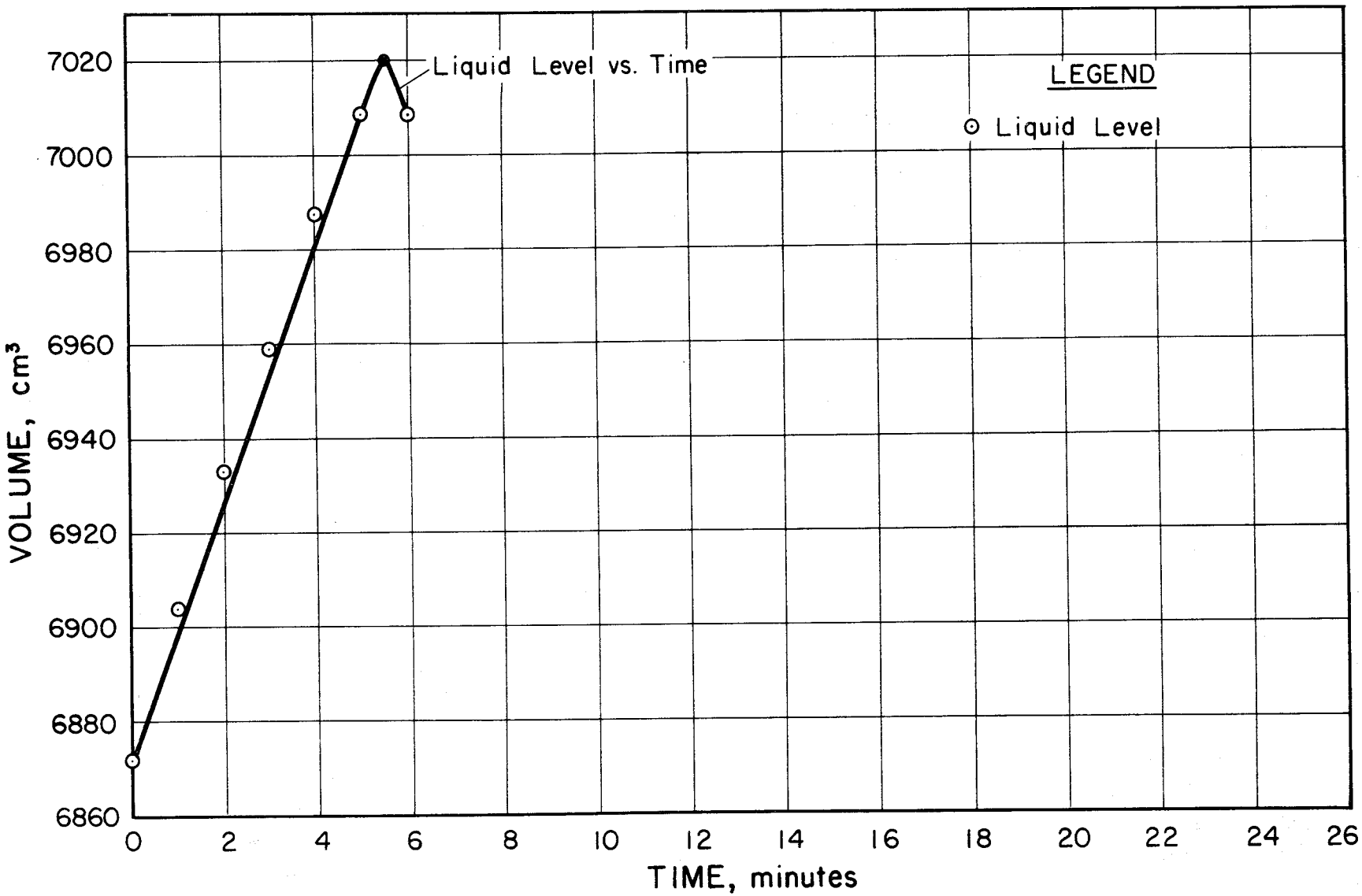

Figure 20. Change in Fluid Volume vs. Time
Run with GR Bridge

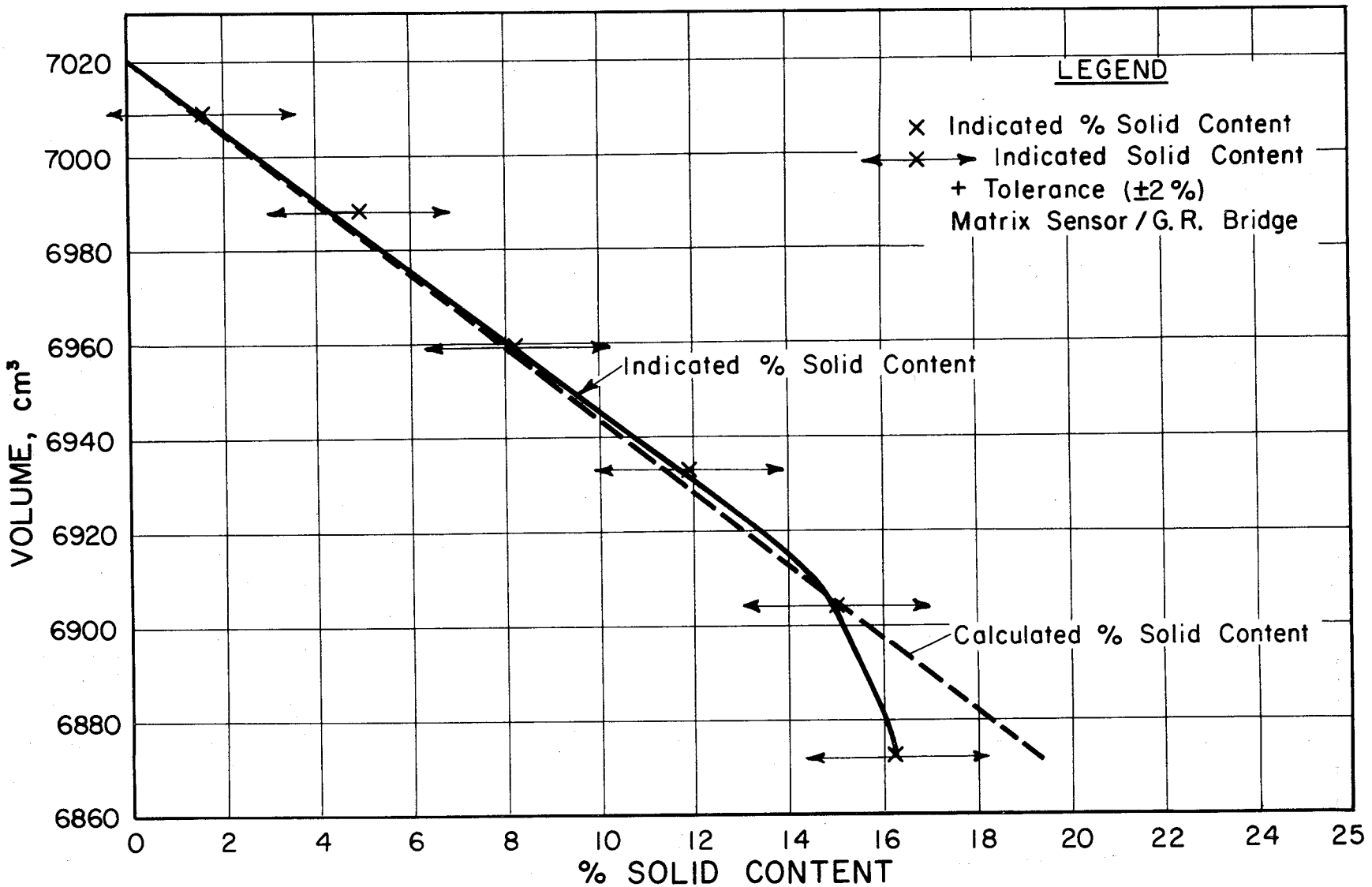

Figure 21. Volume Change, Calculated Quality and Indicated Quality, Run with GR Bridge

It was also demonstrated that the use of a stable, precision capacitance bridge, as represented by a General Radio type 1615 A capacitance bridge, in combination with the IKOR matrix capacitance sensor will infer the measurement of the solid content of slush hydrogen satisfactorily.

The calibration of the measurement system was difficult and tedious. Level measurements, hence fluid volume measurements, by use of the cathetometer were difficult due to the necessity of observing the fluid level through the glass walls of two dewars plus the wall of the plastic shield. Also, level measurements had to be made only when the fluid was quiet.

As the heater, used to melt the solid, was located near the bottom of the test dewar, hence below the matrix sensor, it was necessary that the heater lead wires pass in close proximity to the side of the matrix sensor. Thus, when the heater was energized, extraneous capacitive effects were present that consequently affected the matrix sensor causing oscillation of the measurement system readout. As a consequence, no readings of capacitance, thus percent solid content, were possible when the heater was energized.

Referring to Figures 17, 19, and 21, it can be seen that in no case was more than twenty percent solid content generated. During these "freeze-thaw" slush generations, attempts were made to increase the solid content above this point by varying the mixer speed and the total time of generation but these variations were unsuccessful in increasing the solid content. It may be that the large volume of the matrix sensor had the effect of reducing slush circulation and also the effect of hindering solid particle settling, thus limiting the percent of solid generated.

As solid content instrumentation is required for the further development of slush hydrogen technology the following recommendations are offered:

A. Electronic circuit improvements are recommended for the contractor furnished measurement system readout. In particular, im-

provements in readout stability, drift, and ease of zero and range adjustment are recommended. That such improvements are possible is evident from the performance of the matrix sensor when used with the General Radio, type 1615 A, precision capacitance bridge (Figure 21).

B. With the above measurement system readout improvements, it is recommended that the grid spacing of the matrix sensor be increased to allow for an increased ease of slush flow into and through the matrix. Increasing the grid spacing will, of course, decrease the matrix sensor vacuum capacitance. However, this does not appear to offer significant degradation of measurement if an improved readout is available.

C. Improved calibration and proving techniques for solid content instrumentation are urgently needed and therefore urgently recommended. There are several solid content measurement systems that appear feasible within available technology, however the present means to prove these systems is marginal.

As the solid content of slush hydrogen is directly related to the slush density, it is evident that the solid content of slush can be measured if a slush hydrogen "density calibrator" were available. The development of such a "density calibrator", using a measure of the fluid mass and a measure of the fluid volume, appears feasible. Fluid volume measurement can be determined by using a volume calibrated slush container in combination with liquid level measurement. Cryogenic fluid mass, heretofore, has been measured by weighing the storage container, with its ancillary fill lines and vent lines, and the contained fluid. For liquid hydrogen applications this technique has not been sufficiently accurate due to the low mass of the hydrogen in comparison to the high tare mass of the container. A recent weighing concept however appears to offer a very nearly zero container tare mass. Such a concept may offer a highly accurate liquid hydrogen (and slush hydrogen) mass measurement. Obviously, with accurate volume measurement and accurate mass mea-

surement it would be possible to have an accurate bulk fluid density measurement, hence, accurate bulk percent solid content of slush hydrogen.

In view of this distinct possibility of a slush hydrogen "density calibrator" it is recommended that its development be pursued.

D. The capacitance principle of measuring the percent solid content of slush hydrogen is by no means the only measurement principle. Other principles appear feasible, however they do require further development. Such other principles include nuclear radiation attenuation and nuclear magnetic resonance. These principles were not examined experimentally in this study, for they do require a long lead time for development. They do offer possible advantages for future use, however, e. g. improved sampling, and absence of obstructions in the container or transfer line. It is recommended that these principles be investigated.

These above recommendations have been offered to provide improved measurements of the solid content of slush hydrogen. Such measurements are already needed in current slush hydrogen technology research and they will be needed even more so in future research and development programs. Of the offered recommendations, the recommended development of a slush hydrogen "density calibrator" merits first attention as such a device is required to prove or calibrate any type of measurement system.

6. Analysis of a Proposed Typical Weighing Scheme to Determine Fraction Solids in Slush Hydrogen

This analysis was stimulated by a request to determine the precision of a quality measurement made by the direct weighing of an existing slush tank. The problem was both real and typical and hence deserved attention. The tank is a 1000-gallon capacity vacuum insulated hydrogen storage vessel. The weighing system consists of four 3000-pound capacity compression strain gage load cells, water jacketed for thermal stability, and an instrument case. This weighing system is said to have an accuracy of plus or minus 0.5 pound, which is considered to be quite good. Therefore, the following analysis was undertaken in order to determine the ultimate precision, or, loosely, accuracy, of this system for determining quality.

6.1 Storage Tank and Weighing System

The cryogenic storage tank is a double-walled, vacuum insulated vessel whose inner container is a 78-inch diameter sphere. See Figure 22. The volume capacity of the inner container is, by calculation, 1075.7 gallons, tare weight of the tank is reported to be 9000 pounds.

Weighing of the tank and its slush hydrogen contents is by four 3000-pound capacity compression load cells which are assumed to be so placed that no individual load cell is overstrained.

6.2 Tank Volume Calculations

The volume of the spherical inner container of the tank is determined by:

$$V = 4.189\, r^3$$

where:

V = volume

r = tank radius = 39 inches

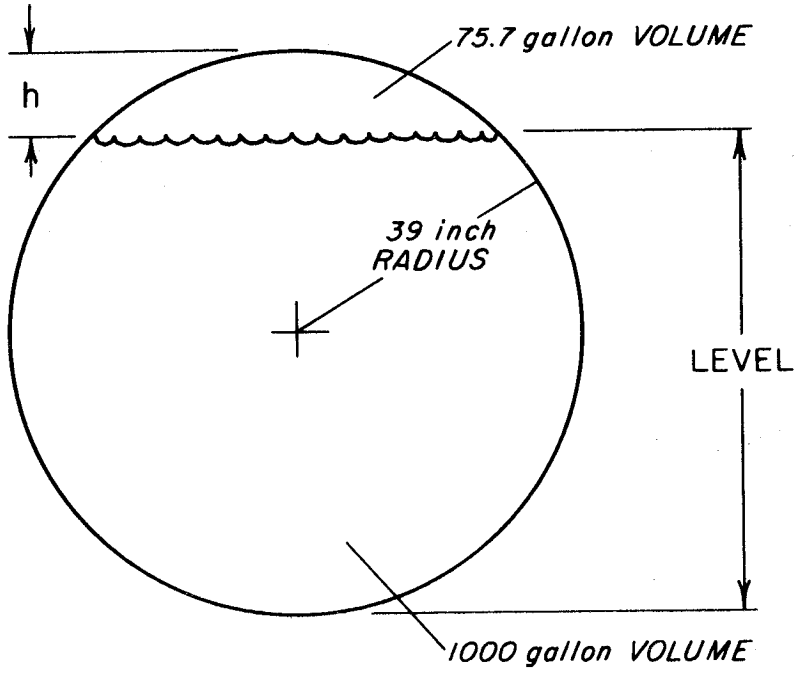

Figure 22. Slush Storage Tank for Weighing System

hence:

$$\text{Volume} = 1075.7 \text{ gallons (U.S.)}.$$

To determine the liquid level in the vessel when 1000 gallons are stored in the tank consider the following.

Volume of a spherical sector is:

$$V = 2.0944\, r^2 h$$

where:

V = volume

r = spherical radius

h = height of sector

Solving for the dimension h of the 75.7 gallon empty volume:

$$h = \frac{(75.7 \text{ gallon})\,(231 \text{ in}^3/\text{gallon})}{2.0944\,(39 \text{ inches})^2}$$

$$\underline{h = 5.489 \text{ inches.}}$$

Thus, the liquid level for 1000 gallons is:

$$78 \text{ inches} - 5.489 \text{ inches} = \underline{72.511 \text{ inches.}}$$

Using the same procedure, the liquid level for 500 gallons is <u>36.253 inches.</u>

6.3 Fluid Density

The density of the slush hydrogen is given as a function of the quality by our fundamental equation

$$\rho = x\rho_s + (1 - x)\,\rho_\ell$$

$$\text{or} \quad \rho = \rho_\ell + x\,(\rho_s - \rho_\ell)$$

Where the symbols are as before.

The triple point liquid density of hydrogen was found to be 77.029 grams per liter while that of triple point solid density of hydrogen was

86.504 grams per liter. Using these values, the density of various solid fraction contents slush hydrogen is as shown in the following table, for qualities up to 60%, the maximum expected in this particular system.

Table III.

Quality and Density of Mixture

% Solid Fraction Content	Density Grams/Liter
0	77.029
10	77.9765
20	78.924
30	79.8715
40	80.819
50	81.7665
60	82.714

6.4 Weight of Slush Hydrogen at Various Volumes

In order to analyze the weighing system accuracy in the measurement of slush hydrogen fraction solids content, it is necessary to know the weight of the slush hydrogen. This weight is determined by:

$$\text{weight} = \text{volume} \times \text{density}$$

$$\text{weight (pounds)} = (\text{gallons})\left(3.785 \frac{\text{liter}}{\text{gallon}}\right)\left(\frac{\text{pound}}{453.6 \text{ gram}}\right)\left[\text{density}\left(\frac{\text{gram}}{\text{liter}}\right)\right]$$

A sample calculation of the weight of 500 gallons of 50% slush is:

$$\text{weight} = 500 \text{ gals.} \times 3.785 \frac{\text{liter}}{\text{gallon}} \times \frac{\text{pound}}{453.6 \text{ gram}} \times 81.7665 \frac{\text{gram}}{\text{liter}}$$

$$\text{weight} = 341.13 \text{ pounds.}$$

Using the above equation, the weight of hydrogen at various fraction solids contents and at various tank volumes is shown in Table IV.

Table IV.

Weight of Mixture for Various Volumes and Qualities

Volume (Gallons)	Weight of Hydrogen (Pounds)						
	Fraction Solids Content						
	0%	10%	20%	30%	40%	50%	60%
100	64.27	65.06	65.85	66.65	67.44	68.23	69.02
200	128.55	130.13	131.71	133.29	134.88	136.45	138.03
300	192.82	195.19	197.56	199.94	202.32	204.68	207.05
400	257.09	260.26	263.42	266.58	269.76	272.90	276.07
500	321.37	325.32	329.27	333.23	337.20	341.13	345.09
600	385.64	390.38	395.12	399.87	404.64	409.36	414.10
700	449.91	455.45	460.98	466.52	472.08	477.58	483.12
800	514.18	520.51	526.83	533.16	539.52	545.81	552.14
900	578.46	585.58	592.69	599.81	606.96	614.03	621.15
1000	642.73	650.64	658.54	666.45	674.40	682.26	690.17

6.5 Slush Measurement Error Due to Weighing Error

With a tank tare weight of 9000 pounds and with a weighing system accuracy of plus or minus 0.5 pound the slush measurement error can be calculated. As an example, consider the following case (see Figure 23):

1. Total force on load cells = 9000 + 341.13 pounds

   where: tare weight = 9000 pounds

   500 gallons = 341.13 pounds
   50% slush

2. Assume weighing is in error by -0.5 pounds

3. Total indicated weight = 9341.13 - 0.5

   = 9340.63 pounds

4. Hence, indicated weight of slush = 340.63 pounds.

From:

Indicated weight = Volume x Density

or

$$\rho\left(\frac{\text{grams}}{\text{liter}}\right) = \frac{\text{Indicated Weight (pounds)}}{\text{Volume (gals.)} \times 3.785 \frac{\text{liter}}{\text{gallon}} \times \frac{1}{453.6 \text{ gram/pound}}}$$

Substituting:

$$\rho = \frac{(340.63\#)\,(453.6 \text{ gram/pound})}{(500 \text{ gals})\,(3.785 \text{ liter/gal})}$$

$$\rho = 81.64321 \text{ grams/liter}$$

Using the basic equation for quality vs. density, the fraction solids content equivalent to a density of 81.643 grams/liter can be determined:

$$\rho = \rho_\ell + x\,(\rho_s - \rho_\ell)$$

$$\text{or} \quad \rho = 77.029 \frac{\text{grams}}{\text{liter}} + x\,(9.475 \text{ grams/liter})$$

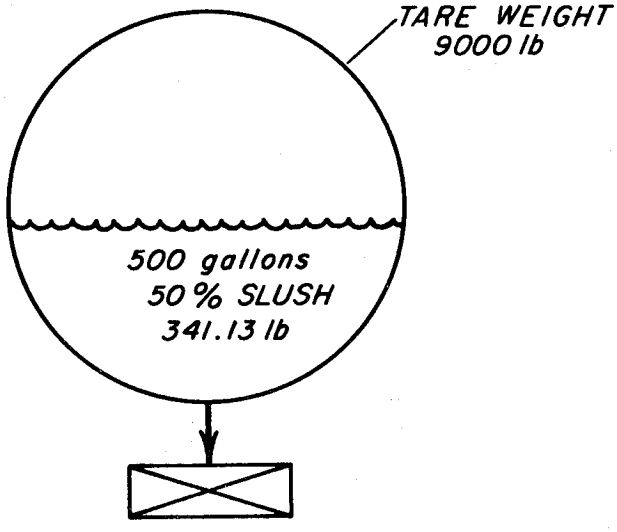

Figure 23. Slush Storage System, 50% full, at 50% Quality

$$x = \frac{81.643 - 77.029}{9.475} \times 100\%$$

$$x = 48.70\%$$

Since the true fraction solids content is 50%, the indicated measurement error due to a weighing error of -0.5 pound is:

$$50\% - 48.70\% = 1.3\%$$

Total measurement error is thus:

$$\frac{1.3}{50} \times 100\% = 2.6\%.$$

Similar calculations were made for various tank volumes of slush hydrogen at various fraction solids contents. From these calculations the curves of Figure 24 were plotted, which displays the measurement error vs. the volume of mixture in the 1000-gallon tank, with the true quality of the mixture as the parameter. One can see that the error is greatest at the lowest volumes (tare weight is more significant) and smallest qualities (least difference in densities to be measured).

6.6 Volume Measurement Error Due to Level Measurement Error

A fluid level measurement is required with a tank weighing system to determine slush hydrogen fraction solids content. Consider the following sample situation (see Figure 25).

Cryogenic liquid level sensors typically are accurate to within plus or minus 0.010 inch. By calculation, the depth of level for 500 gallons is 41.747 inch. If to this measurement the error of a liquid level sensor is added the indicated depth will be

$$41.747 + 0.010 = 41.757 \text{ inches.}$$

The equation for the volume of a spherical sector can be written as:

$$\text{Volume} = (h)\,(2.0944)\,(r^2)$$

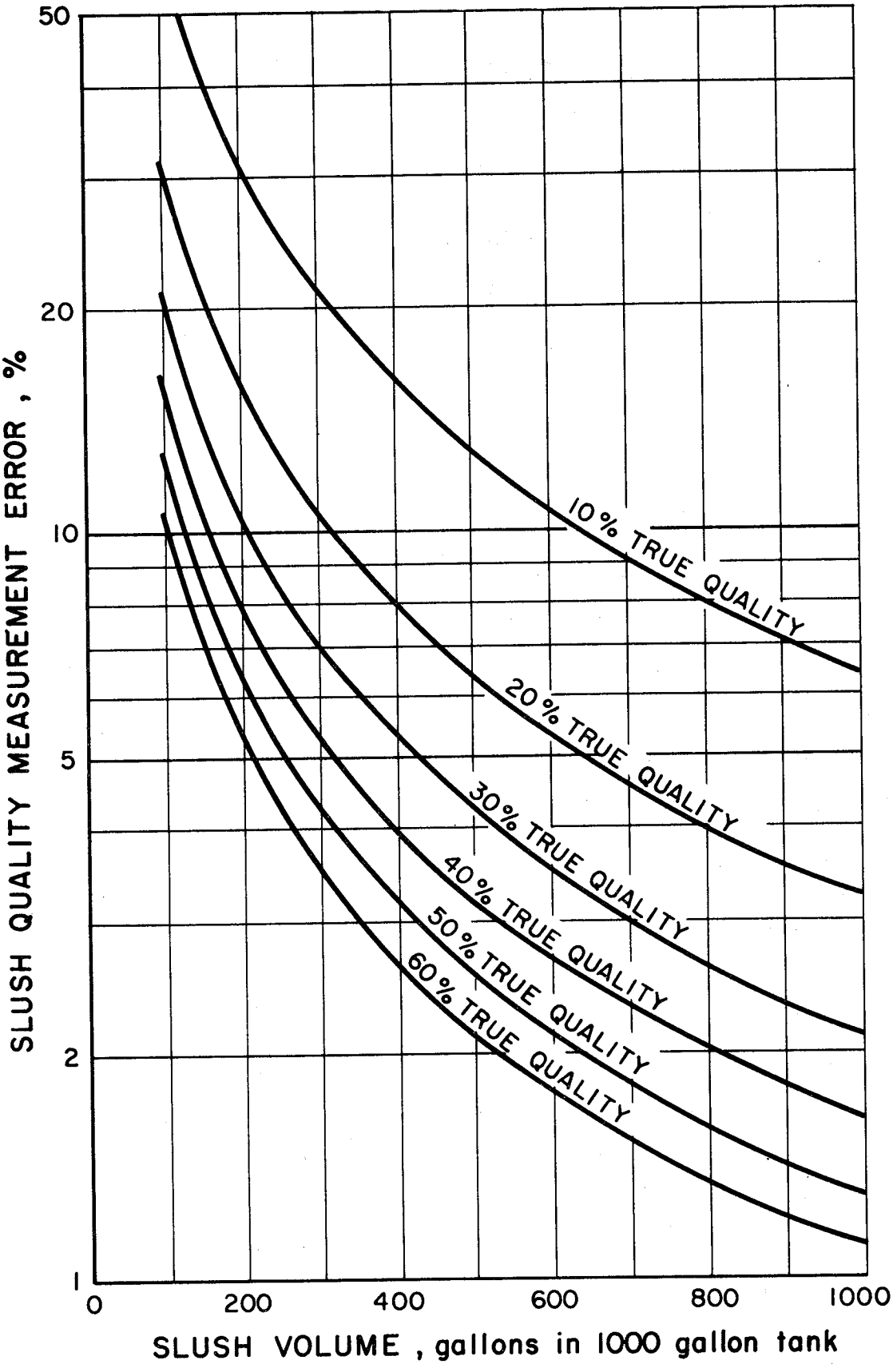

Figure 24. Quality Measurement Error vs. Volume of Container Filled, True Quality as Parameter

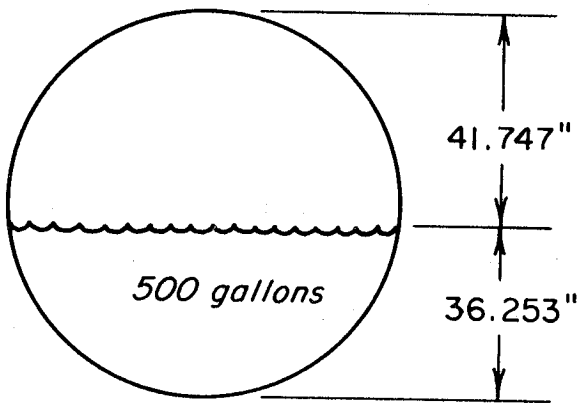

Figure 25. Slush Storage System, Level Measurement Error

Substituting:

$$\text{Volume} = (41.757 \text{ inch})(2.0944)(39 \text{ inch})^2$$

$$\text{Volume} = 575.84 \text{ gallons.}$$

From a previous calculation, the total tank volume is 1075.70 gallons. Thus, the indicated fluid volume is:

$$1075.70 - 575.84 = 499.86 \text{ gallons.}$$

As the actual volume is 500 gallons, the volume measurement error is:

$$500 - 499.86 = 0.14 \text{ gallons.}$$

The volume measurement error due to the error in level measurement is thus:

$$\frac{.14}{500} \times 100\% = .03\%$$

The volume measurement error in this case represents a "worst case" because the fluid level is near the center of the tank where a level measurement error would produce the maximum volume measurement error. Hence as we saw in Section 3.0, it is the load cell sensitivity which limits the accuracy of a direct weighing system, and not the liquid level sensor sensitivity.

6.7 Conclusions

It is obvious from the curves of Figure 24 that maximum measurement accuracy is obtained when large fluid volumes and high fraction solids content slush hydrogen are used. This measurement accuracy shown is the best possible because errors due to windage, fluid dynamic effects, and piping have been ignored. Even so, the measurement errors shown in Figure 24 are probably intolerable.

As mentioned earlier, the load cell resolution for this case is considered quite good. The fault with this system lies in the high tare weight, e.g., most of the range of the load cells is being used to measure tare

weight and is not available for exercise by the difference in solid/liquid densities. This is nearly always the case in direct weighing systems for liquid hydrogen. An improvement in measurement accuracy is possible if the tank is counterpoised in some fashion to reduce the tare weight. As an example, a reduction of tare weight to 900 pounds would mean a reduction in error by a factor of 10.

7. Flow Measurement

One phase of the slush hydrogen instrumentation effort was to "Investigate the feasibility of a slush hydrogen mass flowmeter development program."

This section concerns such an investigation and covers the following:

1. The need for slush hydrogen flow measurement.
2. The particular problems of slush hydrogen flow measurement.
3. A review of several candidate techniques for slush hydrogen flow measurement.
4. A summary of this investigation
5. Recommendations for future plans to accomplish slush hydrogen flow measurement.

7.1 The Need For Slush Hydrogen Flow Measurement

It is first necessary to establish the need to measure slush hydrogen flow, the benefits of such a measurement, and its economics. To answer this question, let us look at current and proposed slush hydrogen research activities and also at that time when slush hydrogen technology may be common practice.

7.1.1 Research Activities

Since slush hydrogen can be made, it follows that research will next be concerned with moving the mixture through transfer lines. This research effort will be as important as the present research efforts of slush hydrogen production and storage. Transfer of the slush mixture will be through straight pipe sections, transfer line elbows, and valves. Knowledge of the amount transferred through these plumbing components will be needed. A flowmeter could supply this knowledge. To move the slush mixture through a transfer line, either a pump or a gas drive system, or both, will be required. The performance, including the efficiency, of these transfer systems can be determined if the amount of mixture transferred is known, e. g., by means of a flowmeter. Slush hydrogen density, hence fraction solids content, at the exit end of a transfer line is an important parameter in transfer studies. A mass flowmeter at this location in the transfer line would supply this knowledge, provided a volumetric tank gaging system is also used.

7.1.2 Future Applications

Slush hydrogen technology could be employed in both chemical and nuclear rocket applications to obtain the benefits of both storage and density increase. Some specialized ground support handling and transfer systems may be required to accomodate the slush mixture, and flow measurements will be required in these systems. A flowmeter is often

the best means of providing many measurements. For example, to fuel the rocket, tanking procedures to insure the correct, pre-determined fuel load will be employed. Vehicle weighing or volumetric tank gaging to determine the mass of fuel aboard the vehicle may not suffice for the accuracy required. Totalized mass flow from a mass flowmeter can provide the required accuracy.

7.1.3 Commercial Custody Transfer

The advantages of slush hydrogen storage are certain to be used in commercial custody transfer applications. In such commercial applications, the custody transfer, hence customer billing, will be on the basis of the amount of fluid transferred from the suppliers transport to the customers storage facility. One of the best methods of determining the amount of fluid transferred is to employ totalizing mass flowmeters. Customer billing can then be computed on a mass basis. When a mass basis is used, there can be little or no dispute between the two parties over the amount of fluid transferred. The customer will pay for only the mass he received whereas the supplier will be paid for the mass that he delivered.

7.2 The Problems Of Slush Hydrogen Flow Measurement

Now that the need for slush hydrogen flow measurement has been established, a review of the problems associated with making such a measurement is pertinent.

7.2.1 Volume vs. Mass Flow

Volume flow measurement or mass flow measurement is an important question. Each measurement has its merits and also its demerits. To be brief, volumetric flow measurement is more generally employed today than is mass flow measurement. This is the case in most flow measurement applications, including cryogenic service applications. The reasons for this are manifold but it can be generalized as due to the lower cost, extensive experience, and probably most important, the relative recent appearance of mass flowmeters with their attendent limited experience. In spite of the fact that volumetric flow measurement systems are popular, most users would much prefer to use direct mass measurement systems. In the case of aero-space applications, the ultimate desired flow measurement is mass flow. Direct mass flow measurement, meaning not an inferred measurement from multiple measurements such as pressure, temperature, volume, etc., is desired for fluid transfer, vehicle loading, and propellant management during flight. Future aero-space missions will call for stringent accuracy requirements for propellant loading and propellant management that can best be met by reliable and accurate direct mass measuring flowmeters. In this light then, the question of volume flow measurement or mass flow measurement is answered -- mass flow measurement is overwhelmingly preferred.

7.2.2. Slush Hydrogen Properties and Flow Measurement

All flow measurement techniques are dependent upon a wide variety of fluid and operational parameters. These techniques are dependent upon fluid properties such as viscosity, conductivity, specific heat, density, etc., in addition to being dependent upon fluid state, flow range, pressure drop, etc. Therefore, when considering a particular flow measurement system, all such parameters must be examined in detail to determine if the technique is applicable. Let us examine, in detail, some particular properties of slush hydrogen and their influence upon the choice of a flow measurement technique.

Slush hydrogen is a two-phase fluid composed of both liquid and solid hydrogen having a variable ratio of liquid to solid content. Very little is known about the flow measurement of a fluid existing in this particular two-phase condition. There is, however, experience with the flow measurement of two-phase fluids when the fluid exists as a vapor-liquid fluid. This experience, however, indicates that conventional volumetric measurement techniques are inadequate in terms of high accuracy. This is partially due to the fact that flow coefficients, or metering factors, are unknown or variable depending on the fluid quality. In the case of boiling two-phase cryogenic fluids, some experience has been gained in the use of volumetric turbine type flowmeters. Because slush hydrogen exists as a solid-liquid mixture, a flow measurement technique must be selected that is fully capable of handling such a fluid. Analysis of some of the mass flow measurement techniques indicates that these techniques are capable of handling such a fluid.

Because the solid fraction of slush hydrogen is more dense than the liquid fraction, the solid fraction may tend to "settle out" unless agitated. When agitated, the fluid may still not be a homogeneous mixture, depending on the mixing technique. Many flow measurement techniques

require that the fluid being measured is indeed a homogeneous fluid. These techniques thus must be excluded from slush hydrogen service. Several of the mass flow measurement techniques do not require a homogeneous fluid, therefore they may be considered for slush hydrogen service.

7.2.3 Calibration And Testing Of Flowmeters

Any measurement system, be it temperature, pressure, volume, density, flow, etc., requires calibration to some standard reference. To prove out stability, response, life, etc., requires testing to some standard reference. In the case of low temperature measurements, cryostats having calibrated temperature references are employed. In the case of pressure measurements in the cryogenic regime, cyostats having calibrated pressure references are employed. Similarly, flow measurements require flow stands having calibrated mass or volume references.

Cryogenic flow stands, also known as flow facilities, are unfortunately few in number and limited in scope. Except for a modest flow facility at one government agency, the flow facilities are all managed by commercial sources who are primarily engaged in aero-space activities, such as engine testing. See Table V.

These cryogenic flow facilities have all been designed solely for liquid cryogen service. For the case of liquid-vapor service, a common occurrence in cryogenic flow, these facilities have a most difficult if not impossible task of providing adequate flow measurement calibration to some standard reference. Now, if slush hydrogen service is considered, we find that these facilities are at present inadequate to handle such a fluid. It may be that an extensive facility modification could provide such a capability. But, the fact remains that as of now there is no known flow facility that can either handle slush hydrogen or provide slush hydrogen calibrations.

TABLE V.

Cryogenic Flow Facilities

Site and Reference	Fluids	Primary Standard	Capacity Rate & Range	2 Phase	Bi-Directional Flow Capability	Accuracy
Wyle (1)	LH_2	Platform scale with beam balance	5#/sec. May be able to get 10#/sec	Helium gas in liquid hydrogen	Yes, for filling purposes	±0.23% max. error at flow of 5#/sec
	LO_2	"	5.6 to 56#/sec (350-3500 gpm)			±0.28% volumetric ±0.17% mass
Pratt and Whitney (2)	LH_2	Load cells	4.5 to 7.4#/sec (450 to 750 gpm)	?	Yes	±0.36%
	LO_2	"	16 to 40#/sec (100 to 250 gpm)	?	?	±0.30%
Aerojet-General (3)	LH_2 LN_2 LO_2 RP-1	Time-volume	1000#/sec	No	No	±0.18%
NASA-Lewis (4)	LH_2	Buoyant force	0.05 to 1.0#/sec	No	Yes	±0.14%
NAA Rocketdyne	LO_2	Time-volume	850#/sec (5400 gpm)	No	No	±0.25% volumetric
	LH_2		97#/sec (10,000 gpm)	No	No	±0.25% volumetric

In view of the lack of an appropriate flow facility for slush hydrogen service, we are faced with a peculiar dilemma. On the one hand there are possible techniques that can operate in slush hydrogen service if calibrated, while on the other hand, no flow facility exists to provide such calibration. The answer to this dilemma is to provide a slush hydrogen flow facility at which these flow measurement techniques can be calibrated and tested. Nothing will be gained if flowmeters are developed for such service if calibration means are non-existant.

To sum up the problems of slush hydrogen flow measurement, we find that a direct mass flow measurement is preferred to a volumetric flow measurement. There are at present only a limited number of cryogenic flow facilities, all of which are inadequate for slush hydrogen service. If candidate mass flowmeters for slush hydrogen service are to be tested and calibrated, an appropriate flow facility is required.

7.3 Candidate Flow Measurement Techniques

The selection of candidate slush hydrogen flow measurement techniques involved a review of practical techniques in cryogenic flow measurement, and a review of recent and current research and development efforts in cryogenic flow measurement. From this broad review, we have selected certain techniques; that, in our judgment, may hold promise for successful operation with slush hydrogen. The techniques selected include mass flowmeters that have had limited cryogenic experience, and mass flowmeters that have no cryogenic experience but which, however, look promising. A discussion of the turbine type flowmeter is also included, primarily because of its cryogenic service popularity. The candidate techniques will be discussed in detail, particularly for their slush hydrogen applicability.

7.3.1 Turbine Type Flowmeter

The turbine type flowmeter is a popular means to measure cryogenic fluid flow. It has had extensive cryogenic experience from which design improvements have resulted. Because of both the extensive experience and the popularity, a discussion of this technique is included in this report even though the measurement is volumetric flow, not mass flow. To infer mass flow, the desired measurement, attempts have been made to couple the meter's volume flow measurement with fluid temperature and fluid pressure measurements. Then, by computation, an inference of mass flow is made. This inferred mass flow has not been highly accurate. This is understandable when one considers that three separate measurements, with their attendant inaccuracies, are combined in a computation which is then referred to fluid P-V-T data which, in itself has uncertainties. In the case of slush hydrogen, since

the mixture is at a fixed (triple) point, temperature and pressure measurements are redundant. However, a density measurement would have to be made and coupled with the volumetric flow measurement to determine mass rate. Density measuring devices are still in the development stage.

As a true volume flow measurement technique, the turbine flowmeter is an excellent device having excellent repeatability. To achieve this excellence, it must however be used correctly. All too frequently, the turbine flowmeter is misapplied. That is to say, it is used where the flow range is too great, it is used for flow rates lower than which it is designed for, and it is used in two-phase fluid applications.

The turbine type volumetric flowmeter is a simple mechanism that consists of a freely rotating bladed rotor, supported by bearings inside a housing, and an electrical transducer that senses rotor speed. Refer to Figure 26. Rotor speed is a direct function of flow velocity. A mathematical description of the turbine type flowmeter is given by

$$\omega = \frac{V \tan \alpha}{R} = \frac{Q}{A_h - A_r} \quad \frac{\tan \alpha}{R} \tag{7-1}$$

where:

ω = rotor angular velocity

V = average flow velocity at the rotor blades

α = rotor blade angle with the pipe axis

R = average radius of rotor blade center of pressure

Q = volumetric flow rate

A_h = internal cross-sectional area of housing

A_r = maximum cross-sectional area of rotor

Deviations from this idealized mathematical expression can be expected to be due to (1) retarding forces on the rotor such as fluid drag, mechanical friction from rotary and thrust bearings, and transducer magnetic drag, (2) velocity profile variations, and (3) swirl of the incoming fluid stream.

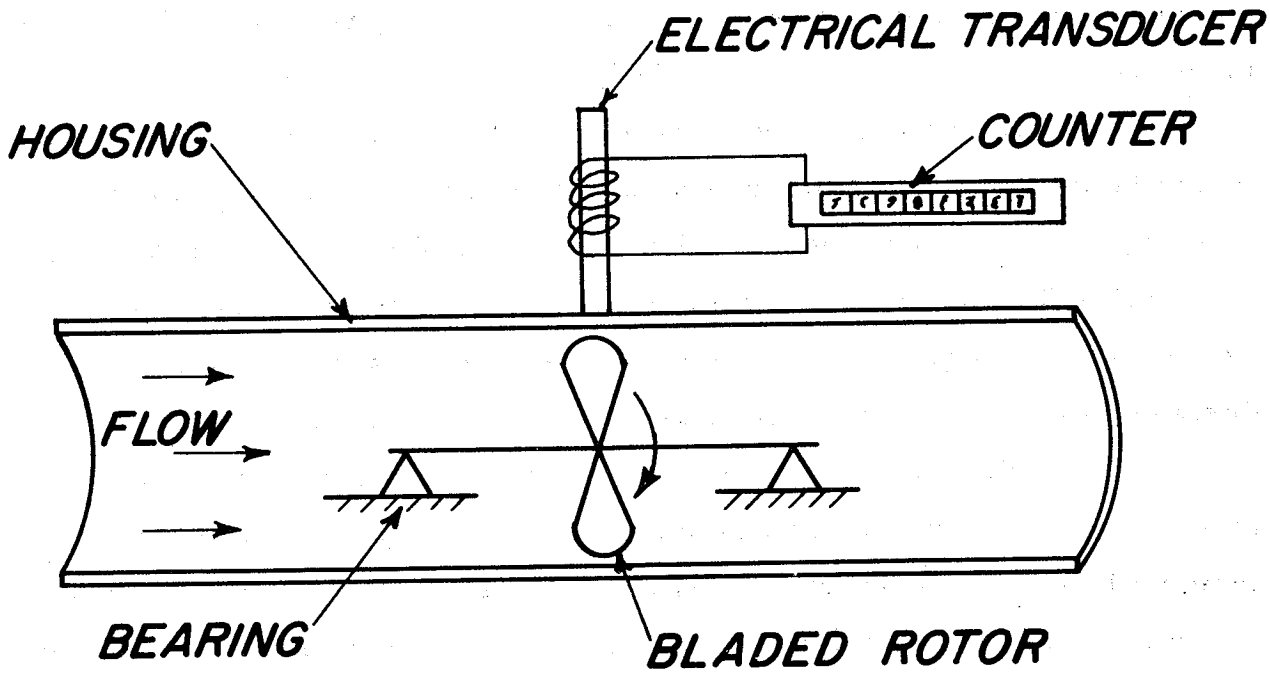

TURBINE TYPE FLOWMETER

Figure 26

The turbine type flowmeter is designed for use with a homogeneous fluid. Experience when used with a liquid-vapor fluid has resulted in measurement errors and, in a few cases, has also resulted in dangerous turbine "run-away." In these cases of turbine "run-away," the end result has been catastrophic.

The advantages of the turbine type flowmeter include:

1. Small size - thus a minimum mass to cool down
2. Lightweight
3. Generally, a 10 to 1 flow range
4. Linear calibration
5. Excellent repeatability
6. Digital type output signal
7. Requires no shaft seals
8. Self propelled - fluid flow supplies the driving force
9. Excellent response.

The disadvantages of the turbine type flowmeter include:

1. Volumetric measurement - not mass measurement
2. Designed for single phase fluids
3. Overspeed will cause turbine "run-away"
4. Rotating mechanical component
5. Requires upstream flow straightening to eliminate fluid swirl effects
6. Attitude sensitive-requires mounting in same position as when calibrated.

Figures 27 through 33 show calibrations of various turbine type flowmeters for both water and liquid hydrogen fluids. These calibration curves show the variable correlation that exists between the water calibration and the liquid hydrogen calibration. These curves further indicate the need to calibrate each and every turbine flowmeter using liquid hydrogen as the calibration media. This requirement of calibration is true for any flow measurement technique.

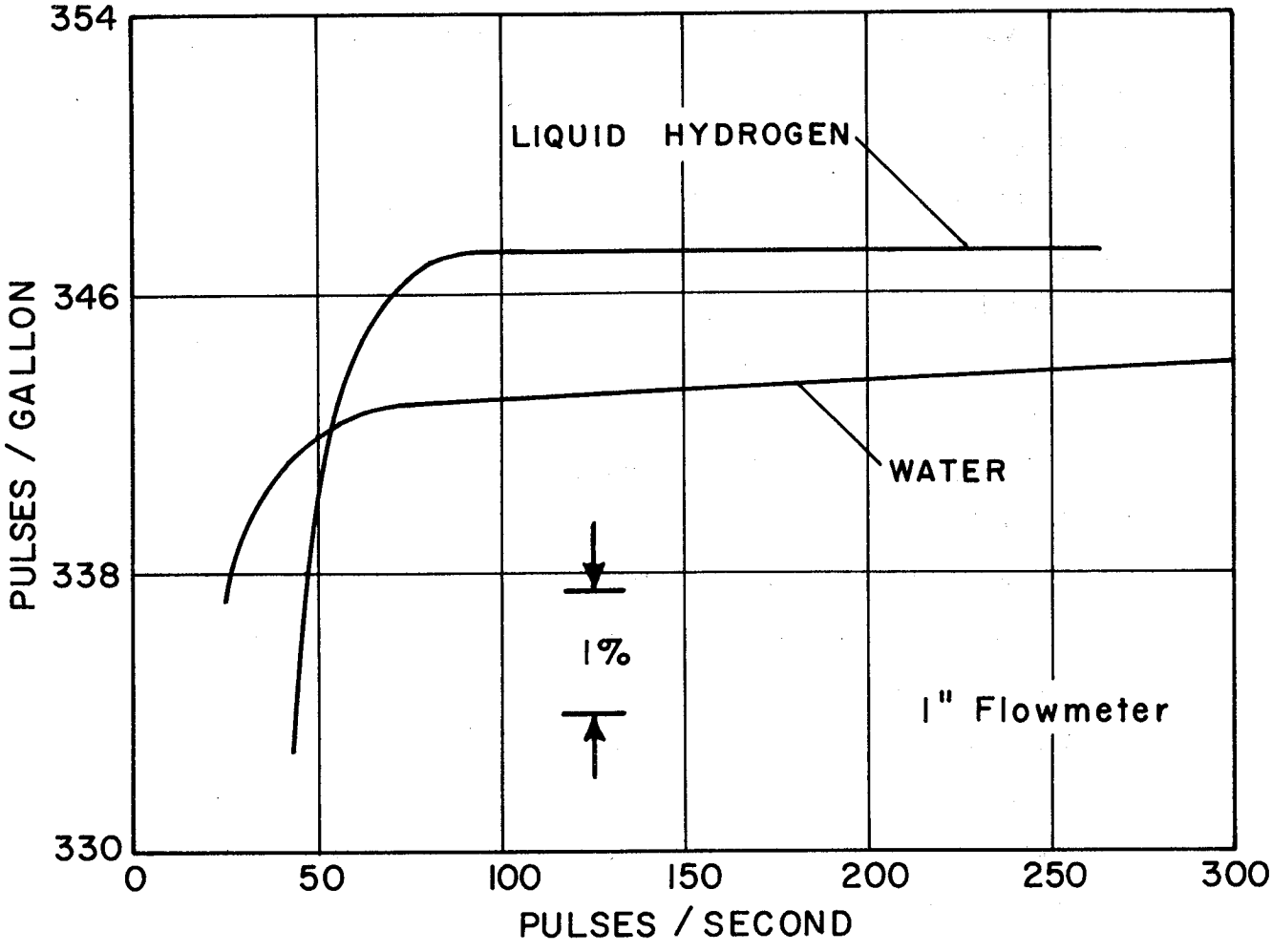

Calibration Of Turbine - type Flowmeter With Liquid Hydrogen And Water

Figure 27

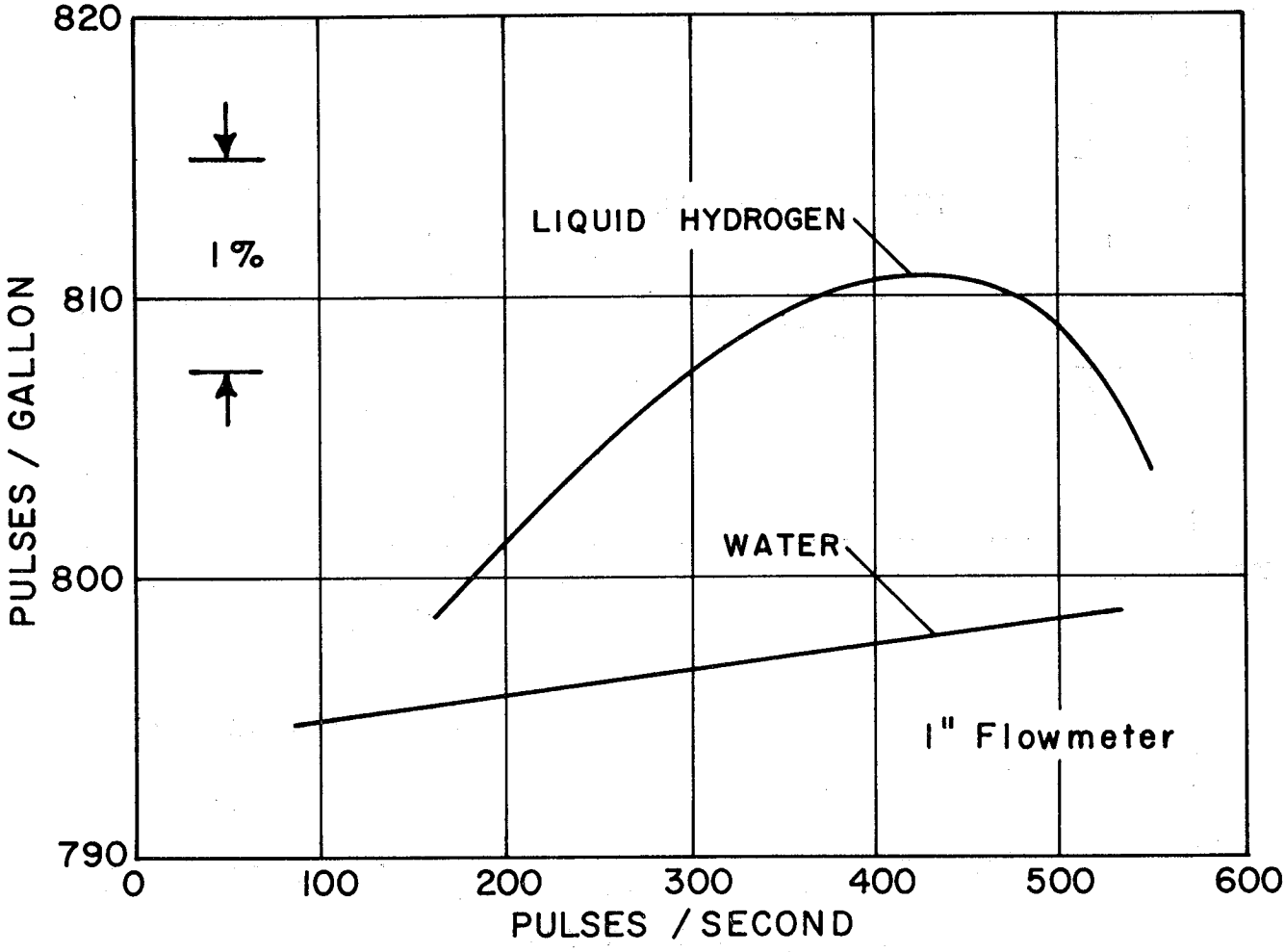

Calibration Of Turbine-type Flowmeter With Liquid Hydrogen And Water

Figure 28

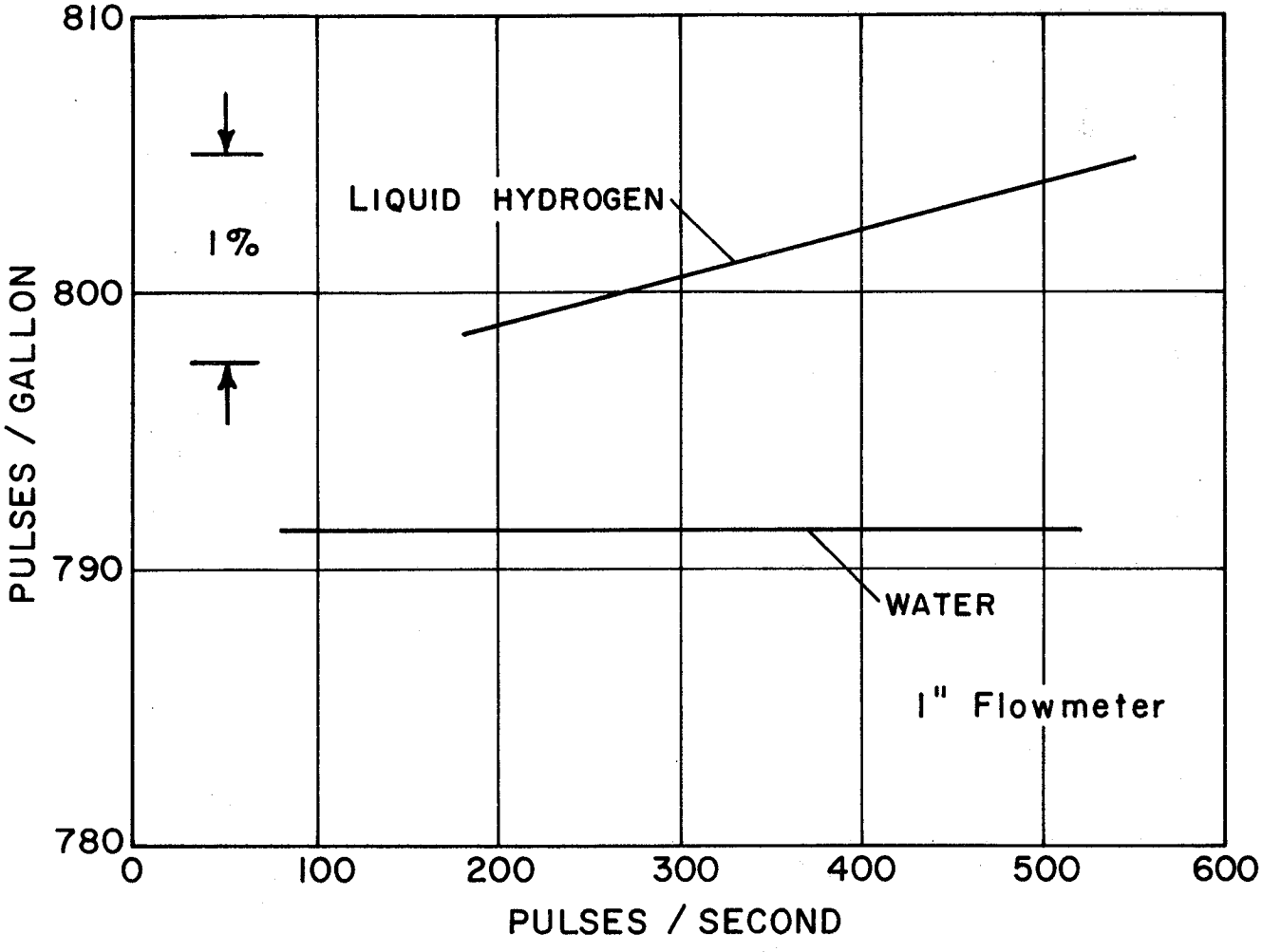

Calibration Of Turbine-type Flowmeter With Liquid Hydrogen And Water

Figure 29

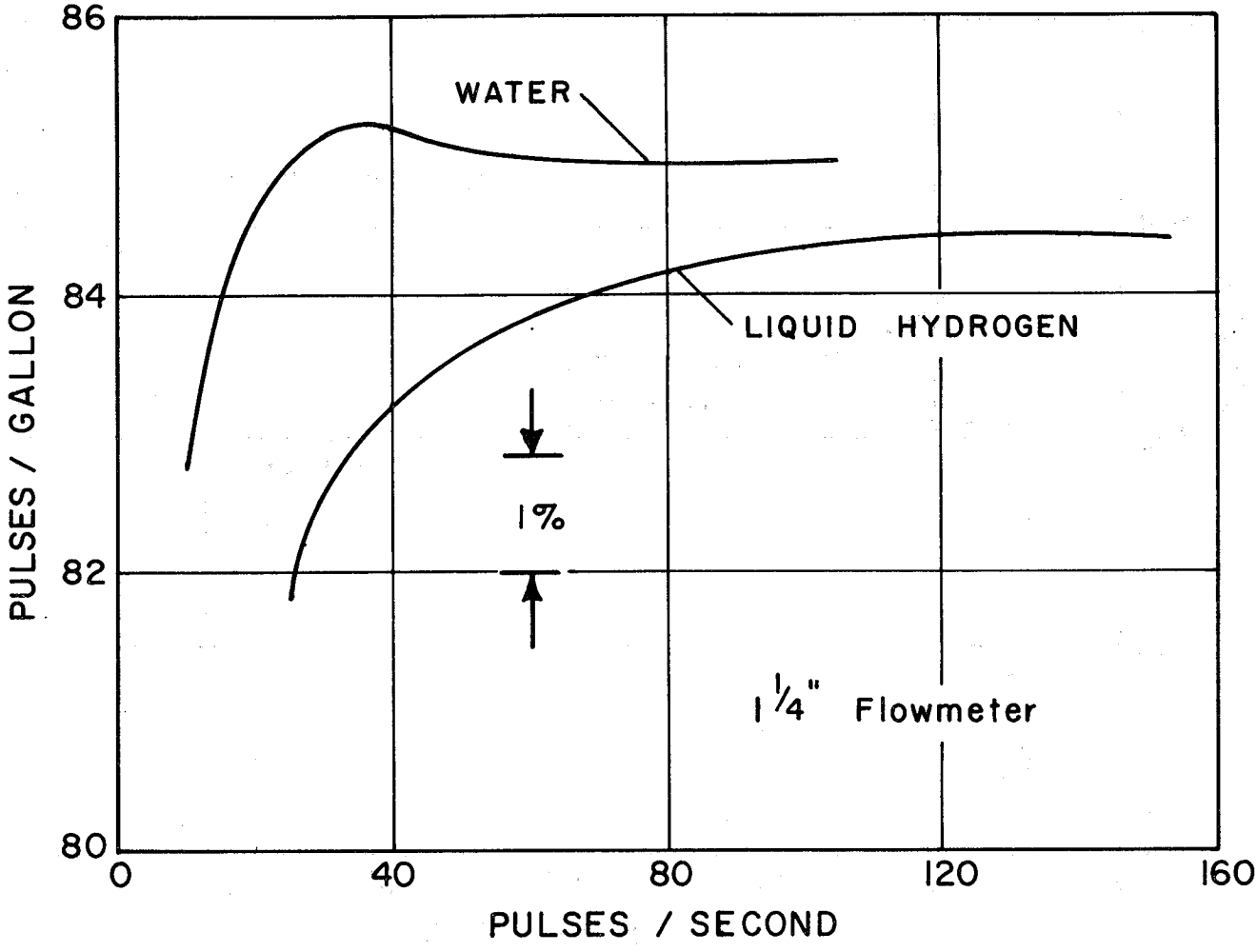

Calibration Of Turbine-type Flowmeter With Liquid Hydrogen And Water

Figure 30

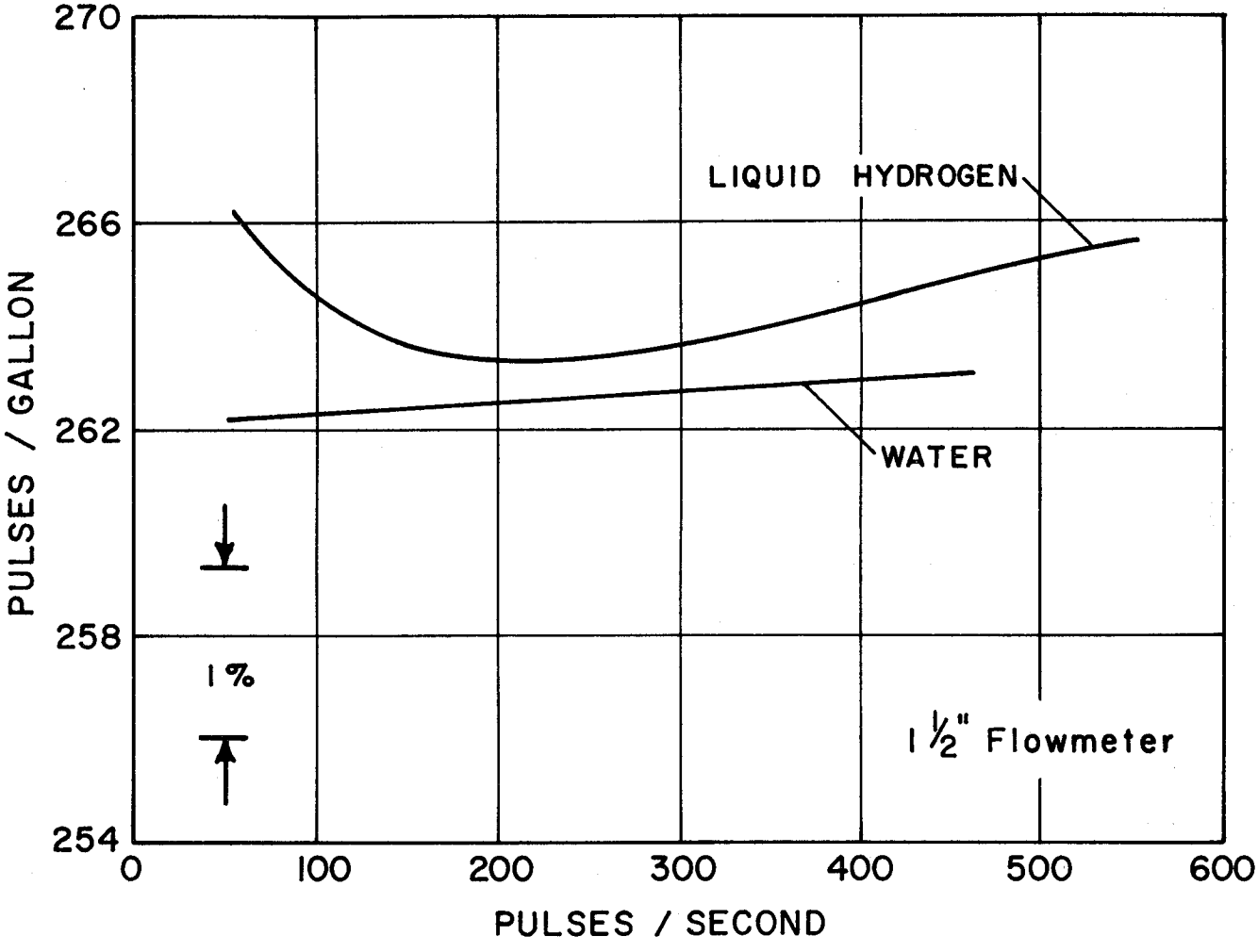

Calibration Of Turbine-type Flowmeter With Liquid Hydrogen And Water

Figure 31

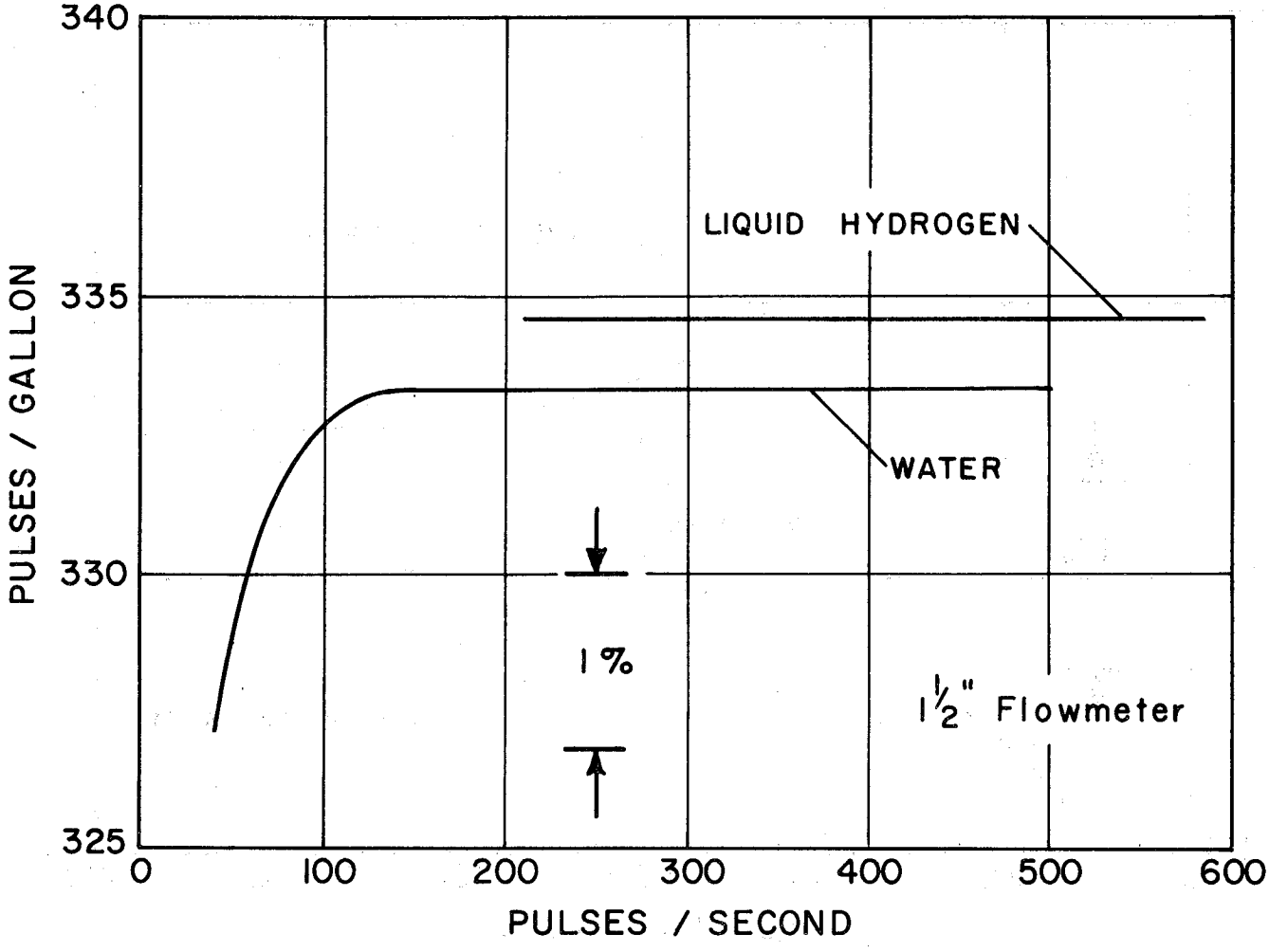

Calibration Of Turbine-type Flowmeter With Liquid Hydrogen And Water

Figure 32

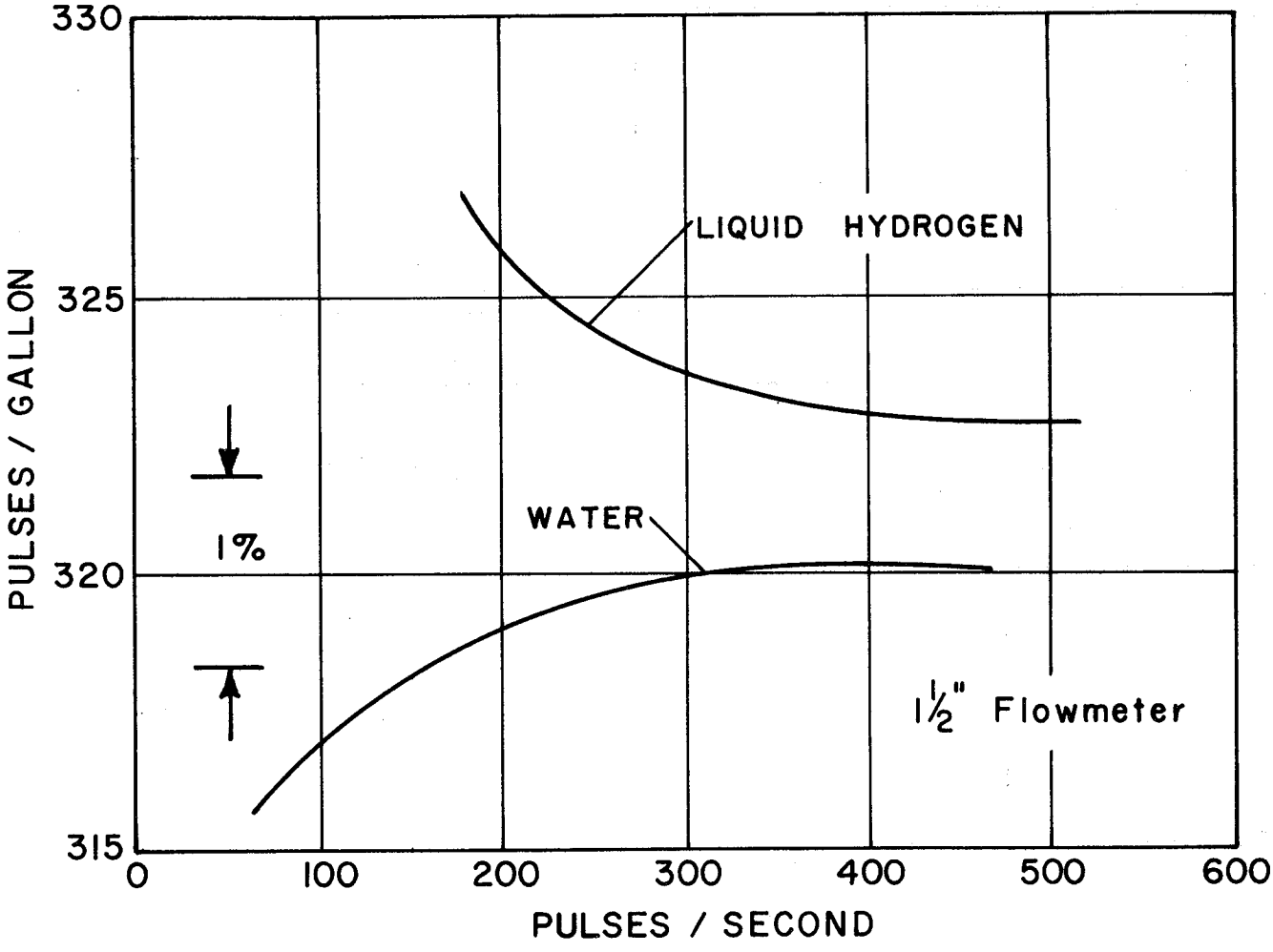

Calibration Of Turbine - type Flowmeter With Liquid Hydrogen And Water

Figure 33

For slush hydrogen service, the use of a turbine type flowmeter is of questionable value. First of all, the turbine type flowmeter will measure only the volumetric flow rate, not the desired mass flow rate. Secondly, because the slush mixutre is a two-phase, liquid-solid fluid, having a variable solid content, the calibration would be difficult. Finally, the accuracy of flow measurement in this media is questionable, since no experience or calibration facility exists. Countering these points, however, is the availability and general acceptance of the turbine meter.

7.3.2 Transverse Momentum Mass Flowmeter

Several types of mass flowmeters can be classed as transverse momentum mass flowmeters. All such meters are direct mass flowmeters since the reaction of their primary element is proportional to the momentum of the stream. Each of these flowmeters imposes on the fluid stream a momentum (velocity) transverse (at right angles) to the axial (longitudinal) flow of the stream. These transverse momentrum flowmeters can be classified as (a) axial flow, (b) radial flow, and (c) gyroscopic. Since each of these classes is basic, several variations on mechanical design and primary element reaction-detection have been devised. Some variations will be discussed under each class.

7.3.2.1 Axial-Flow Transverse Momentum Mass Flowmeter

Figure 34 is a schematic of an axial flow transverse momentum flowmeter. The General Electric Company "angular momentum" mass flowmeter uses this design. Substantially all fluid flow passes through both the impeller and the turbine. The impeller and the turbine are geometrically similar cylinders mounted in a cylindrical flow conduit on an axis coinciding with the conduit centerline. Each element is mounted on a separate shaft. Both impeller and turbine are composed of several straight vanes located at the periphery of the elements and parallel to the centerline of the conduit. A means is provided for measuring the torque on the turbine shaft. If the impeller were locked (not rotating), the torque on the turbine shaft should be zero.

Now, suppose the impeller is rotated at some angular speed, ω. As the fluid stream enters the impeller, it is picked up and set to rotating at an angular speed equal to the angular speed of the impeller. A stipulation to achieve this condition is that the vanes must be sufficiently long and spaced sufficiently close together. This imposed velocity results in the fluid stream having an angular (or transverse) momentum in addition to the normal axial momentum of the stream.

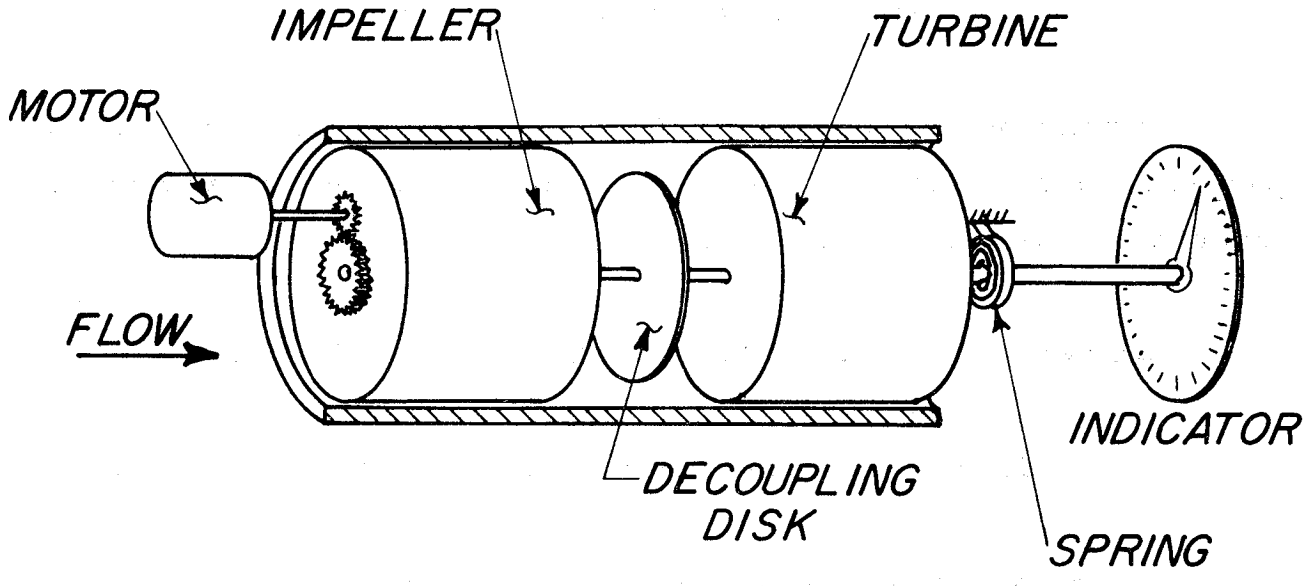

AXIAL FLOW TRANSVERSE MOMENTUM
MASS FLOWMETER

Figure 34

Located adjacent to the impeller is the turbine. Since it is restrained and does not rotate, the turbine straightens the fluid stream; that is, the turbine removes all of the angular momentum from the fluid stream that was supplied by the impeller.

The decoupling disc is stationary and not attached to either element. Its function is to eliminate viscous coupling between the impeller and turbine.

Torque on the turbine shaft is in accordance with

$$T = \frac{dH}{dt} \tag{7-2}$$

where: T = torque on turbine shaft

H = angular momentum of fluid stream

t = time.

Examining a differential fluid particle whose mass is dm and which passes a reference point, a, in the time interval dt, the angular momentum of this small mass can be expressed as

$$dH = \omega dI \tag{7-3}$$

where: ω = angular velocity of the stream at the entrance of the turbine

dI = mass moment inertia of dm about the axis of the impeller.

The mass moment of inertia, dI can be expressed as

$$dI = K^2 dm \tag{7-4}$$

where: K = radius of gyration of dm about the axis of rotation.

By substitution, and dividing by dt:

$$\frac{dH}{dt} = \omega K^2 \frac{dm}{dt} \tag{7-5}$$

Note that dm/dt is the mass flow rate, $\dot{M}$.

But $dH/dt = T$, so that

$$T = \omega K^2 \dot{M} \tag{7-6}$$

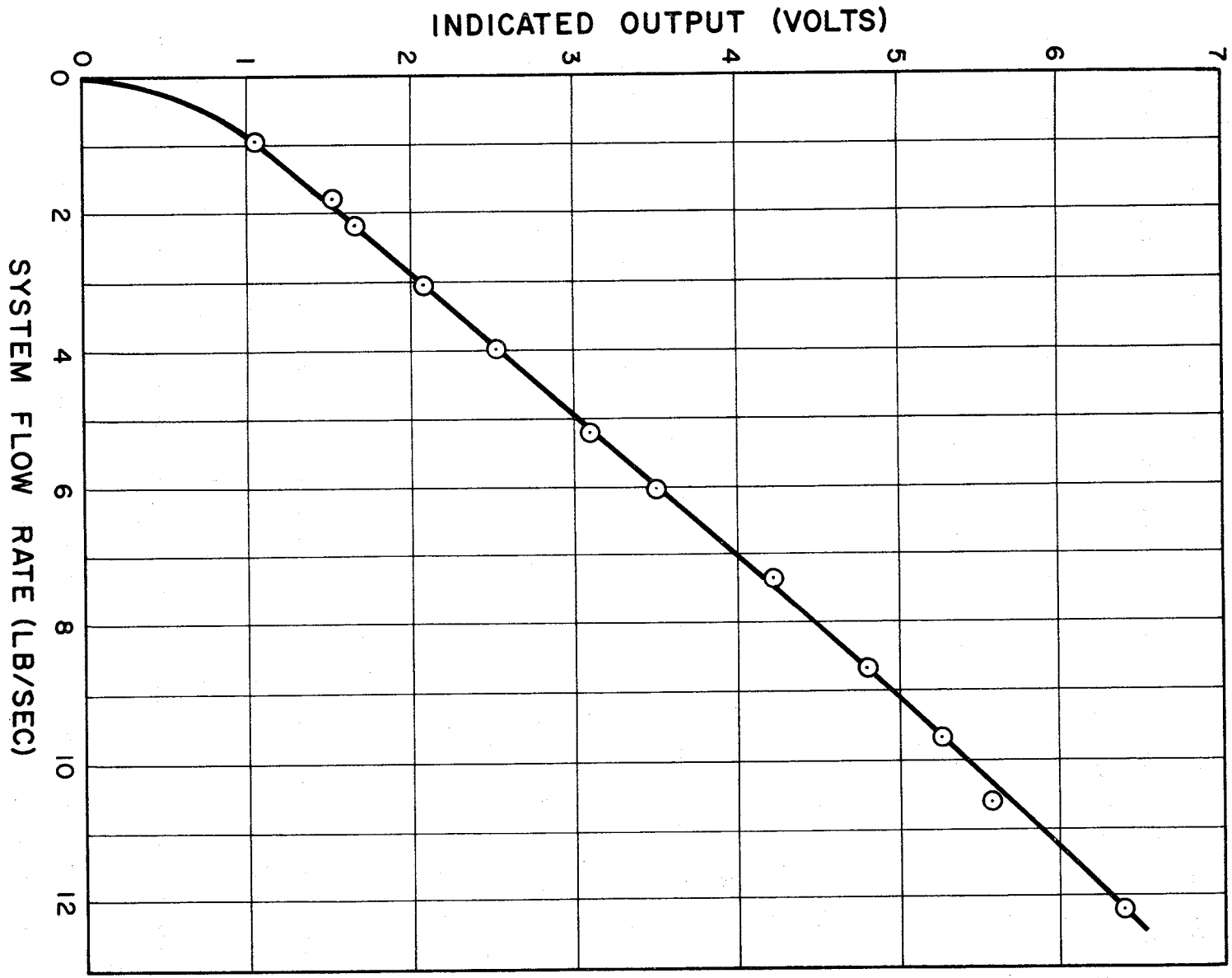

Figure 35. Liquid Hydrogen Calibration of Axial Flow Transverse Momentum Mass Flowmeter

If the speed ω is constant and K is a geometrical constant,

$$T = C_1 \dot{M} \tag{7-7}$$

This equation shows that turbine shaft torque is directly proportional to mass flow rate. Detection of this torque in the General Electric flowmeter is by means of a calibrated spring which is attached to an electro-mechanical angle detector.

For slush hydrogen service, this flowmeter offers the following advantages:

(a) Direct mass flow measurement

(b) Applicable to two-phase fluids

(c) Requires no flow straighteners

(d) Good rangeability

(e) Linear calibration.

Disadvantages include:

(a) Moving parts in the fluid stream

(b) Torque measuring spring requires low temperature calibration

(c) Slow response time.

Figure 35 shows a liquid hydrogen calibration curve for a mass flowmeter of this type.

If equation (7-6) is rewritten as

$$\omega = \frac{T}{K^2 \dot{M}}, \tag{7-8}$$

an alternate scheme may be used to determine mass flow. This equation illustrates that if torque is maintained constant, then impeller speed must vary inversely as the mass flow rate. This scheme is used by Waugh-Foxboro in their mass flowmeter. Figure 36 is a schematic of this flowmeter.

In this technique, motor speed must be detected, which is simple; however, the output is an inverse function of mass flow rate. This has the advantage of high resolution at low flow rates but as the flow rate increases the resolution decreases.

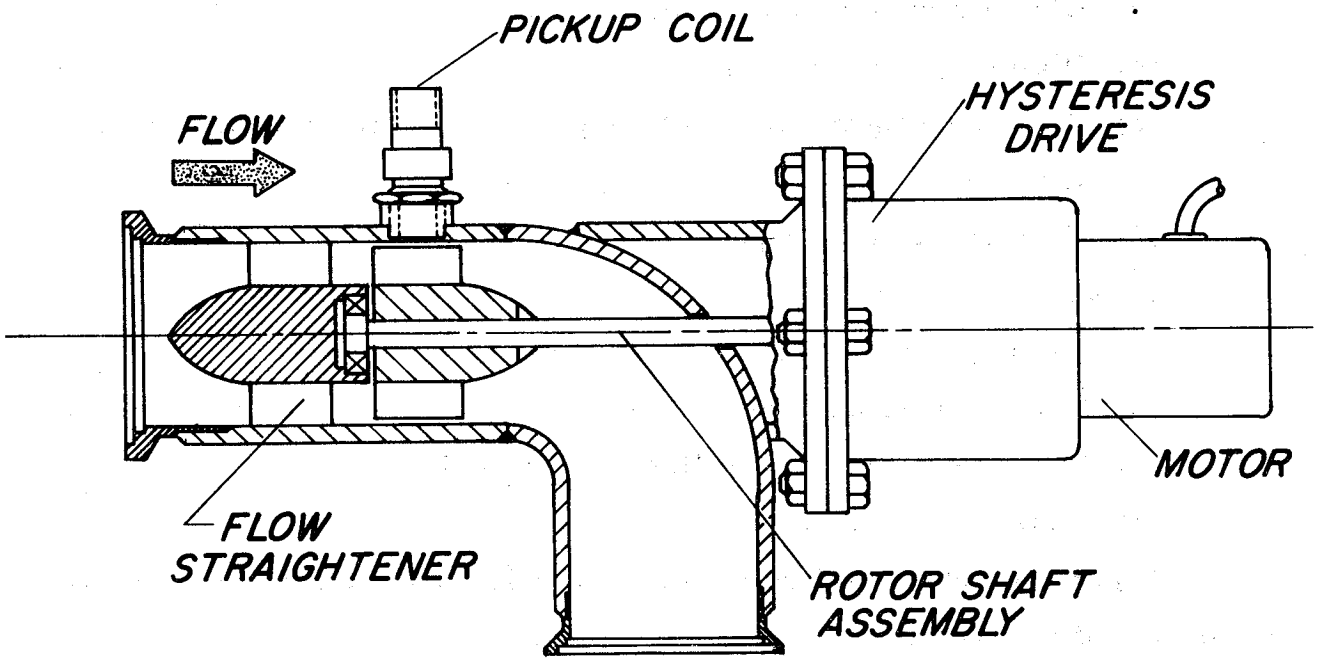

AXIAL FLOW TRANSVERSE MOMENTUM
MASS FLOWMETER

Figure 36

The rotor portion of the flowmeter has a zero pitch angle impeller that is driven so as to impart a constant torque to the fluid. The constant torque is provided by means of a hysteresis drive and an electric motor. The electric motor is driven at essentially a constant speed. The hysteresis drive transfers the torque developed by the motor to the impeller. The hysteresis drive has the characteristic of transmitting a constant torque, regardless of the operating slip speed. As a consequence, torque measurements are not required, thereby leaving only the measurement of impeller speed.

For slush hydrogen service, this flowmeter offers the following advantages:

(a) Direct measurement of mass flow

(b) Digital type output signal

(c) Does not require calibrated springs or other torque sensing devices

(d) Two-phase fluid capability.

Disadvantages include:

(a) Moving parts in the fluid stream

(b) Will not measure zero flow

(c) Non linear calibration (frequency vs flow)

(d) Slow response time.

Figure 37 shows a liquid hydrogen calibration curve for a mass flowmeter of this type.

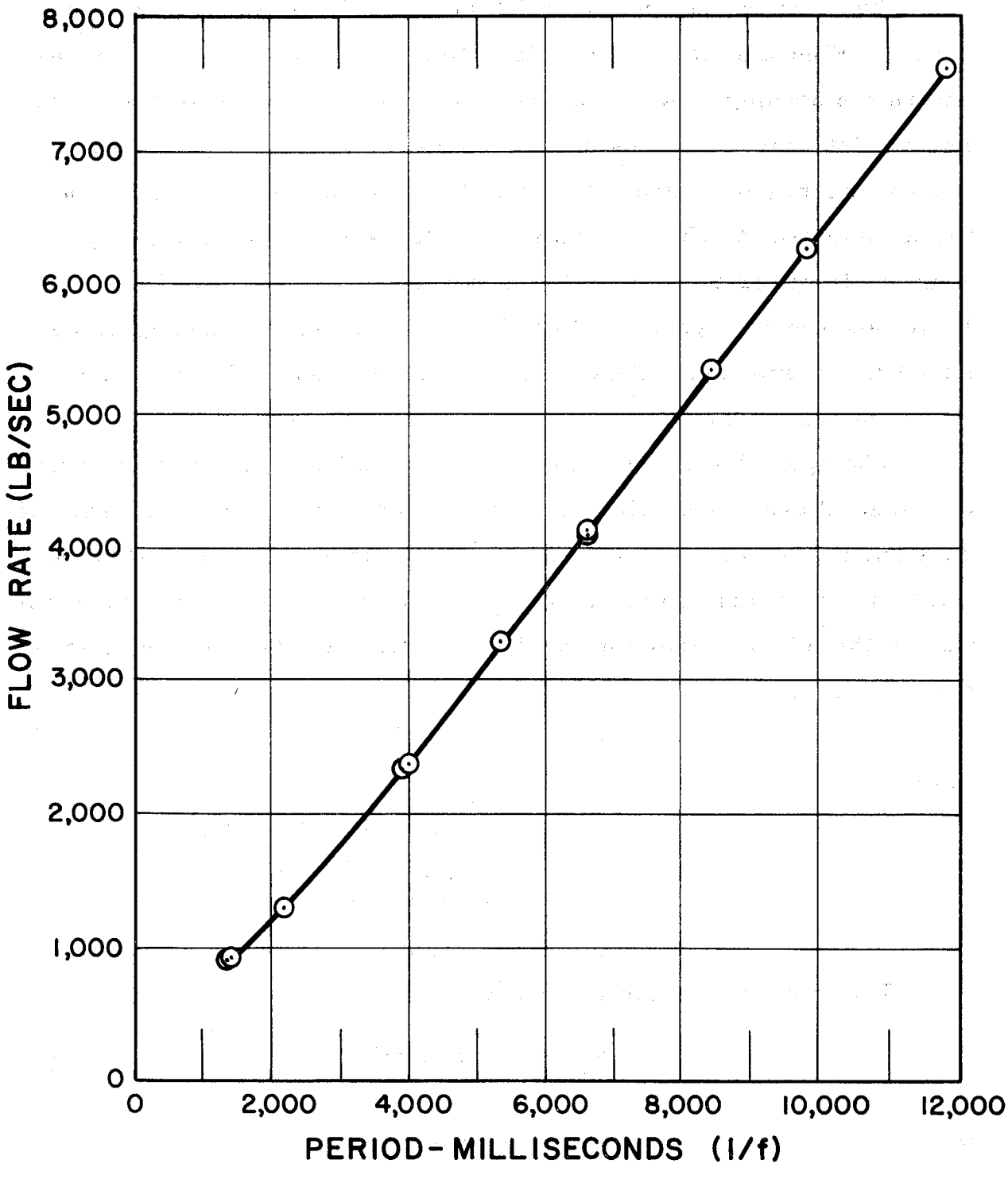

Figure 37. Liquid Hydrogen Calibration of Axial Flow Transverse Momentum Mass Flowmeter

7.3.2.2 Radial Flow Transverse Momentum Mass Flowmeter

This flowmeter commonly is called the "Coriolis" mass flowmeter. Figure 38 is a schematic of this flowmeter. The fluid stream enters the housing which is driven at a constant angular velocity. The housing interior is composed of a flow sensing element (impeller), and a downstream guide vane. Note that the housing, the impeller, and the turbine are attached and rotating at the same angular velocity. Both the impeller and the guide vanes are radial, and of sufficient length and closely spaced so that the stream is set to rotating at the speed of the impeller. This causes the flow to leave the impeller and enter the guide vanes with zero tangential velocity.

The operation of this flowmeter is explained most simply by use of a special case where flow is confined to a straight radial channel of constant cross-sectional area as shown in Figure 39. Note that the fluid stream flowing down the tube is subjected to a Coriolis acceleration as the tube is rotated about the point O. This Coriolis acceleration is equal to:

$$a = 2V\omega \qquad (7\text{-}9)$$

where:

a = Coriolis acceleration

V = Velocity of fluid mass down the tube

ω = Angular velocity

The moment created about O is

$$M_o = \int r(a\,dm) \qquad (7\text{-}10)$$

But, $dm = \rho A dr$

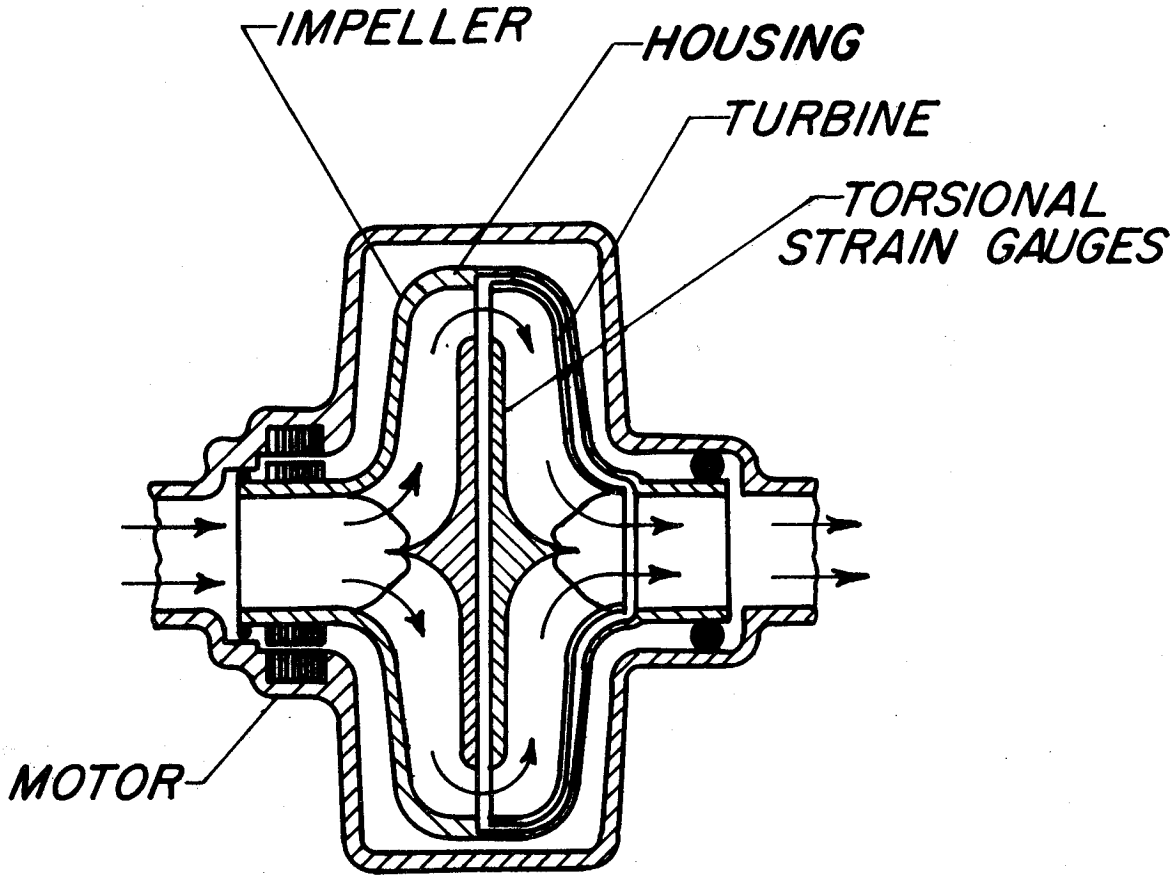

RADIAL FLOW TRANSVERSE MOMENTUM
MASS FLOWMETER

Figure 38

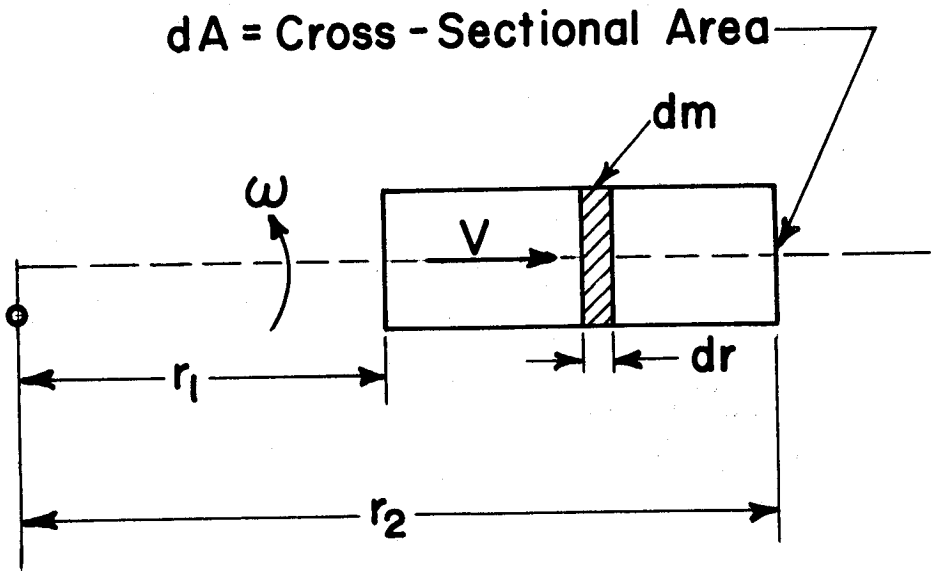

RADIAL FLOW MASS FLOWMETER

Figure 39

$$M_o = \int_{r_1}^{r_2} 2V\omega\rho A dr = V\rho A\omega (r_2^2 - r_1^2) \tag{7-11}$$

Note that $$V\rho A = \dot{M} \tag{7-12}$$

therefore $$M_o = \dot{M}\omega(r_2^2 - r_1^2) \tag{7-13}$$

Thus, the moment on the sensing element is proportional to the mass flow rate, the speed of the impeller, and geometry. If impeller speed and the geometry are constant, then

$$M_o = C_2 \dot{M} \tag{7-14}$$

This shows that the impeller moment is directly proportional to mass flow rate through the flowmeter. It is characteristic of this flowmeter that if the flow through the meter is reversed, the torque on the impeller is reversed. Therefore this flowmeter is inherently bidirectional, if the torque sensing element is capable of negative measurement as well as positive measurement.

A particular advantage of this radial flow transverse momentum flowmeter is that the angular momentum supplied to the stream by the impeller is recovered by the guide vanes. Consequently, the power supplied to the flowmeter must be sufficient only to overcome bearing friction, seal friction, windage losses and viscous losses at the meter entrance and exit.

A flowmeter of this type is being considered for cryogenic fluid applications by Space Sciences, Incorporated. Space Sciences proposes improved mounting or suspension of the impeller-turbine assembly and an improved method of torque measurement.

For slush hydrogen service, this flowmeter offers the following advantages:

(a) Direct measurement of mass flow

(b) Two-phase fluid capability

(c) Bi-directional flow (For loading and unloading of a storage vessel)

(d) Good rangeability

(e) Linear output signal

(f) Low power requirement

(g) No flow straighteners.

Disadvantages include:

(a) Moving parts in the flow stream

(b) Complex mechanical design

(c) No experience or evaluation in cryogenic fluid applications.

7.3.2.3 Gyroscopic Transverse Momentum Mass Flowmeter

The gyroscopic mass flowmeter is shown schematically in Figure 40 and Figure 41. The mechanical analog to the flowmeter, Figure 42 , shows how it resembles a conventional gyroscope mounted on two gimbal rings. The gyroscopic flowmeter consists of a closed loop through which the fluid flows freely. Suitable bearings and seals at points 1 and 2 permit the closed loop to be rotated about the x-axis.

For any general gyroscope, the moment about the y-axis can be expressed by:

$$M_y = I_z \Omega\omega \tag{7-15}$$

where:

ω = precessional velocity of gryoscope

Ω = angular velocity of gyroscope rotor

I_z = polar moment of inertia of fluid in conduit about z-axis

as $$I_z = \rho(2\pi rA)r^2 \tag{7-16}$$

and $$V = \omega r \tag{7-17}$$

Then $$M_y = (\rho VA)\, 2\pi\omega r^2 \tag{7-18}$$

Thus, equation (7-18) now fits the familiar pattern of a moment proportional to the mass flow rate times the product of a constant speed and a geometrical constant so that

$$M_y = C_3\dot{M} \tag{7-19}$$

In an actual flowmeter, therefore, it is obvious that the moment about the y-axis must be measured or, more realistically, the reaction R, at the bearings 1 and 2 must be measured. Note that the

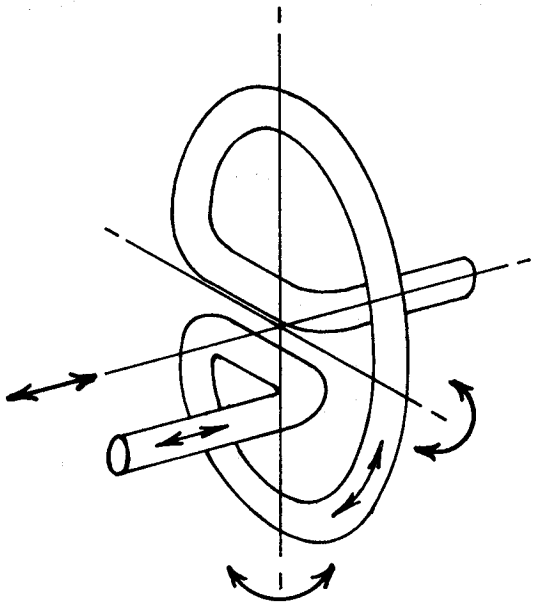

VIBRATING GYROSCOPIC MASS FLOMETER

Figure 40

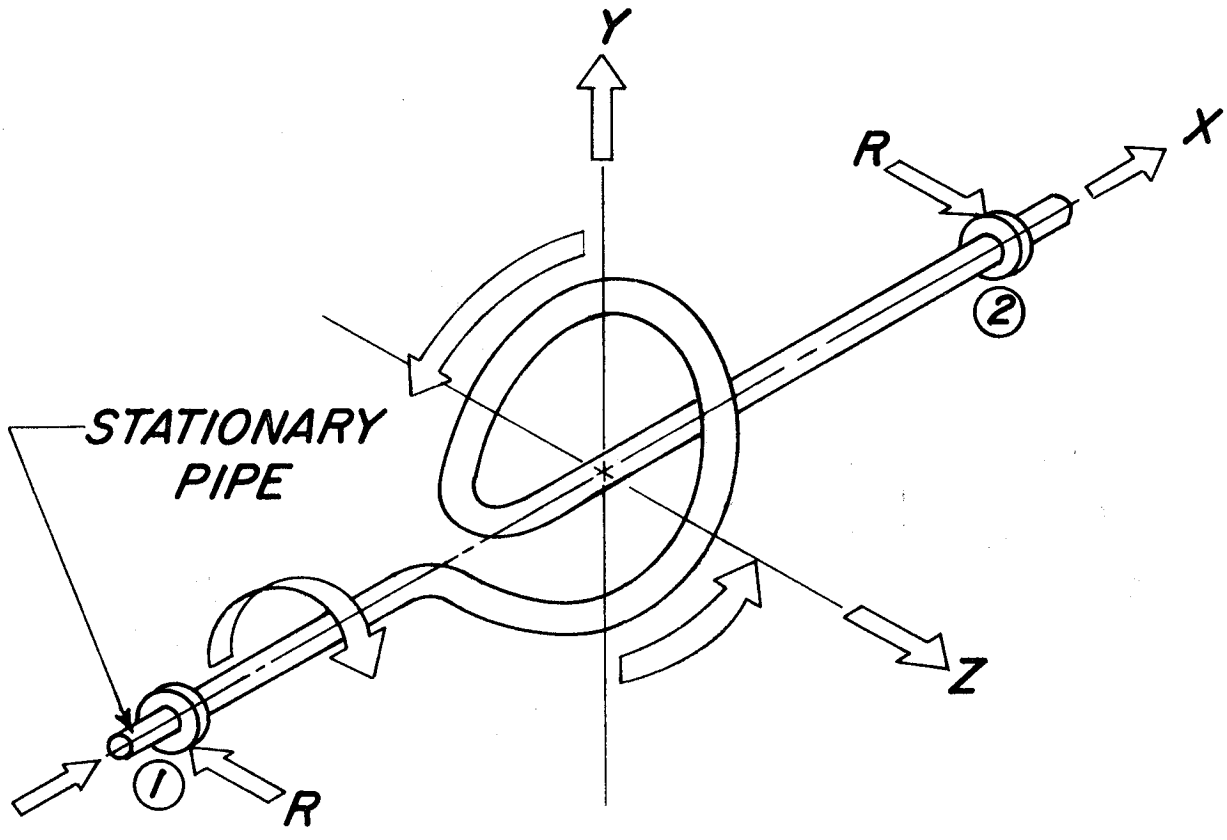

GYROSCOPIC TRANSVERSE-MOMENTUM
MASS FLOWMETER

Figure 41

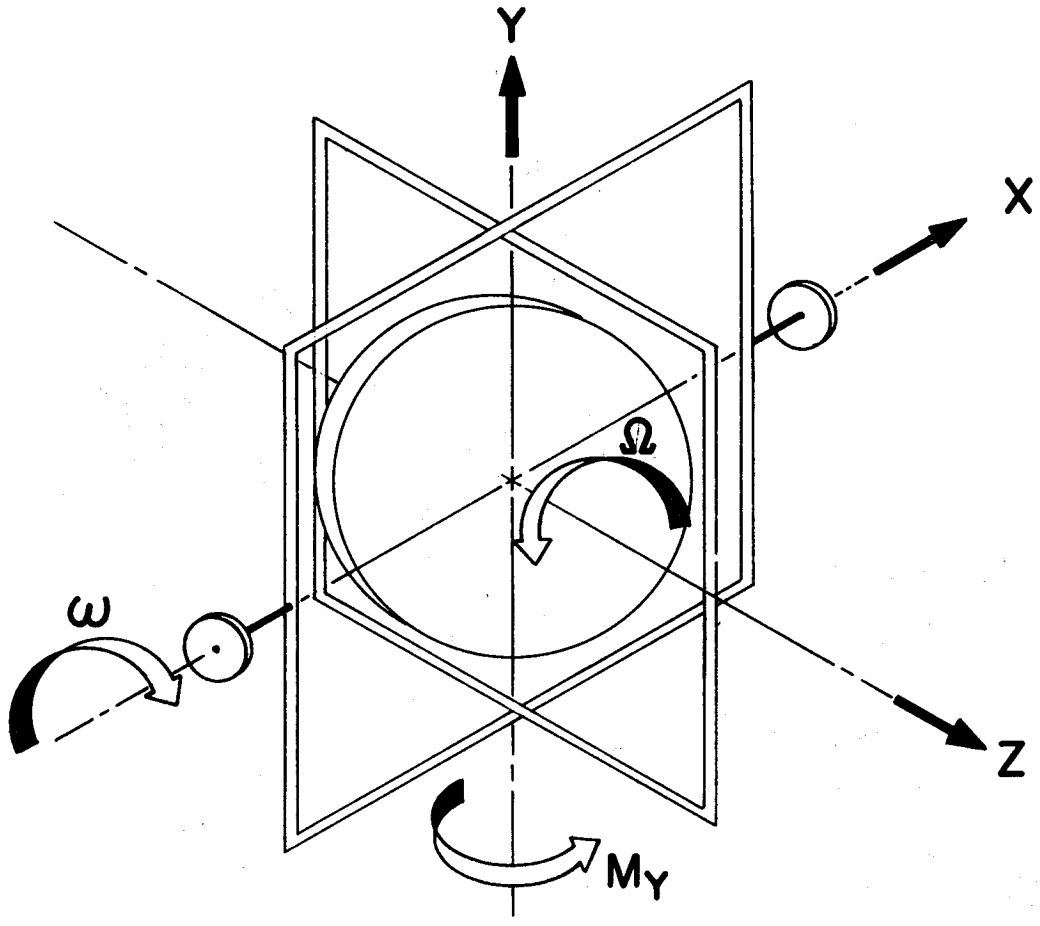

This mechanical analog to the gyroscopic meter helps to understand its operating principle.

Figure 42

magnitude of the reaction vector R is directly proportional to mass flow rate M, and that vector R rotates at an angular speed equal to ω.

This flowmeter is capable of measuring bidirectional flow. The flowmeter must be provided with rotating seals and suitable bearings.

The Decker Corporation, in a variation of this gyroscopic flowmeter, has the angular precessional velocity applied about the x-axis as a small oscillatory angular velocity instead of a constant angular velocity. As a result, reaction R is an oscillating value that can be measured. An advantage of this scheme is that rotating seals are not required. Instead, a flexible length of conduit or bellows can be attached upstream and downstream of the flowmeter.

In the Decker design, the loop is vibrated through a small angle of constant amplitude about an axis in the plane of the loop. This vibration results in an alternating gyro-coupled torque about the mutually orthogonal axis. The peak amplitude of this torque is directly proportional to mass flow rate. The torque acts against elastic restraints (torsion bars) to produce an alternating angular displacement about the torque axis. Velocity pickups, appropriately mounted, convert the alternating displacement to a proportional alternating electric signal. The peak amplitude signal is directly proportional to mass flow rate. This signal is then conditioned to provide a dc signal output linearly related to mass flow rate.

For slush hydrogen service, this flowmeter offers the following advantages:

(a) Direct mass flow measurement

(b) Two-phase fluid capability

(c) No moving parts in the flow stream

(d) Requires no flow straighteners

(e) Linear calibration

(f) Bidirectional flow (For loading and unloading storage vessel).

Disadvantages include:

(a) Large size

(b) Difficult to vacuum jacket

(c) Complex mechanical design

(d) Vibration sensitive.

Figure 43 shows a liquid hydrogen calibration curve for this type of mass flowmeter.

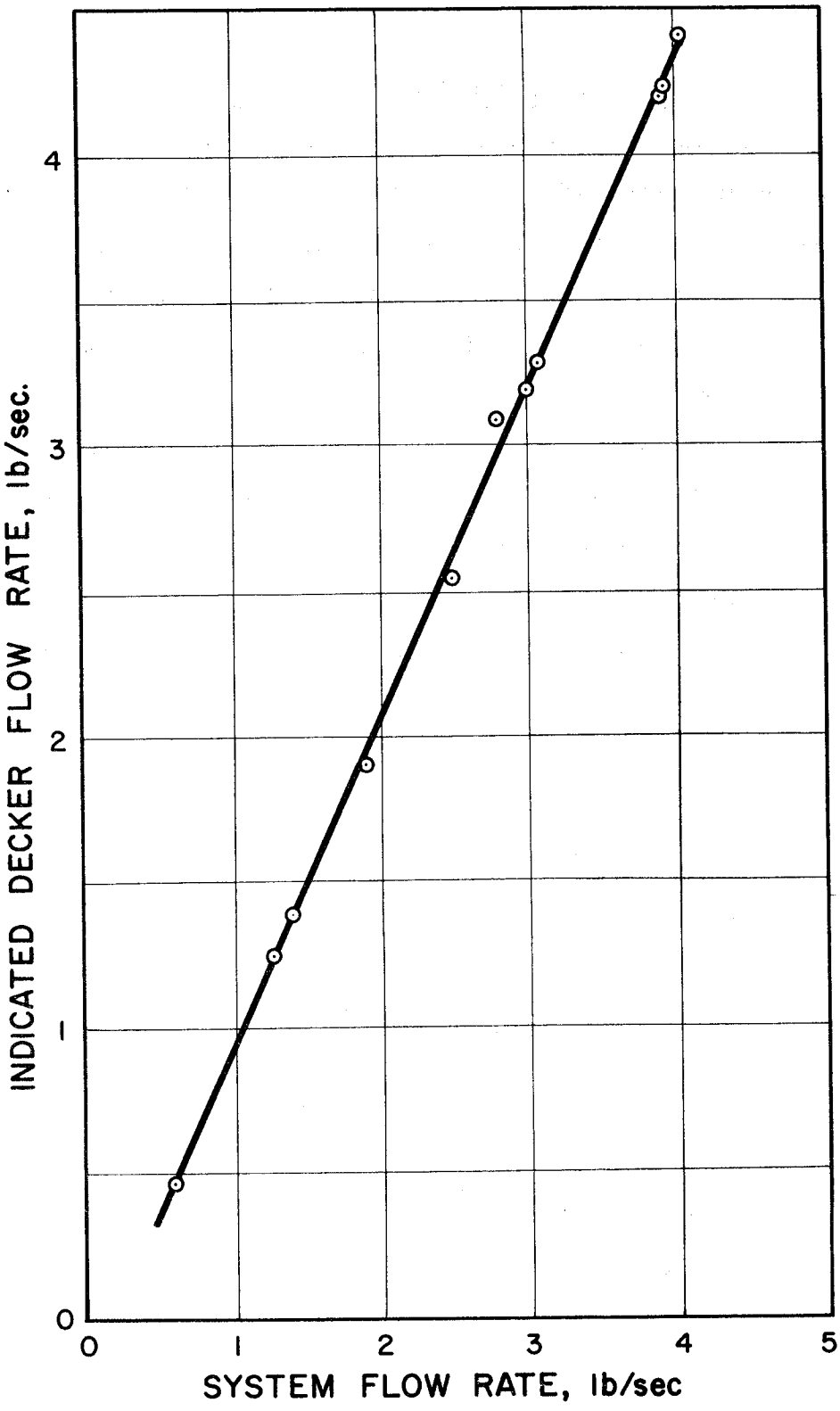

Liquid Hydrogen Calibration of a One and One-Half Inch Decker Gyro Mass Flowmeter, Model 600-1

Figure 43

7.3.3 Momentum-Capacitance Mass Flowmeter

The momentum-capacitance mass flowmeter is shown schematically in Figure 44. The Bendix Corporation employs this design in their cryogenic fluid mass flowmeter.

This flowmeter has two sensing elements located in the fluid stream. One element is a fluid sampling densitometer while the other element senses fluid momentum. Both elements are open mesh configurations offering a small impedance to flow. The densitometer element employs "honeycomb" plates in a parallel plate configuration while the momentum sensor employs round wire screens in a parallel plate configuration.

The pressure drop across a wire screen is expressed by:

$$\Delta P \equiv K_1 \rho V^2 \qquad (7\text{-}20)$$

where:

ΔP = Pressure drop

ρ = Fluid density

V = Fluid velocity

K_1 = Constant when Reynolds Number ≥ 1000 and a fixed solidity ratio for the screen.

The force exerted on a wire screen is:

$$F_F = A\Delta P \qquad (7\text{-}21)$$

where

F_F = Force on screen

A = Screen cross-sectional area

ΔP = Pressure drop.

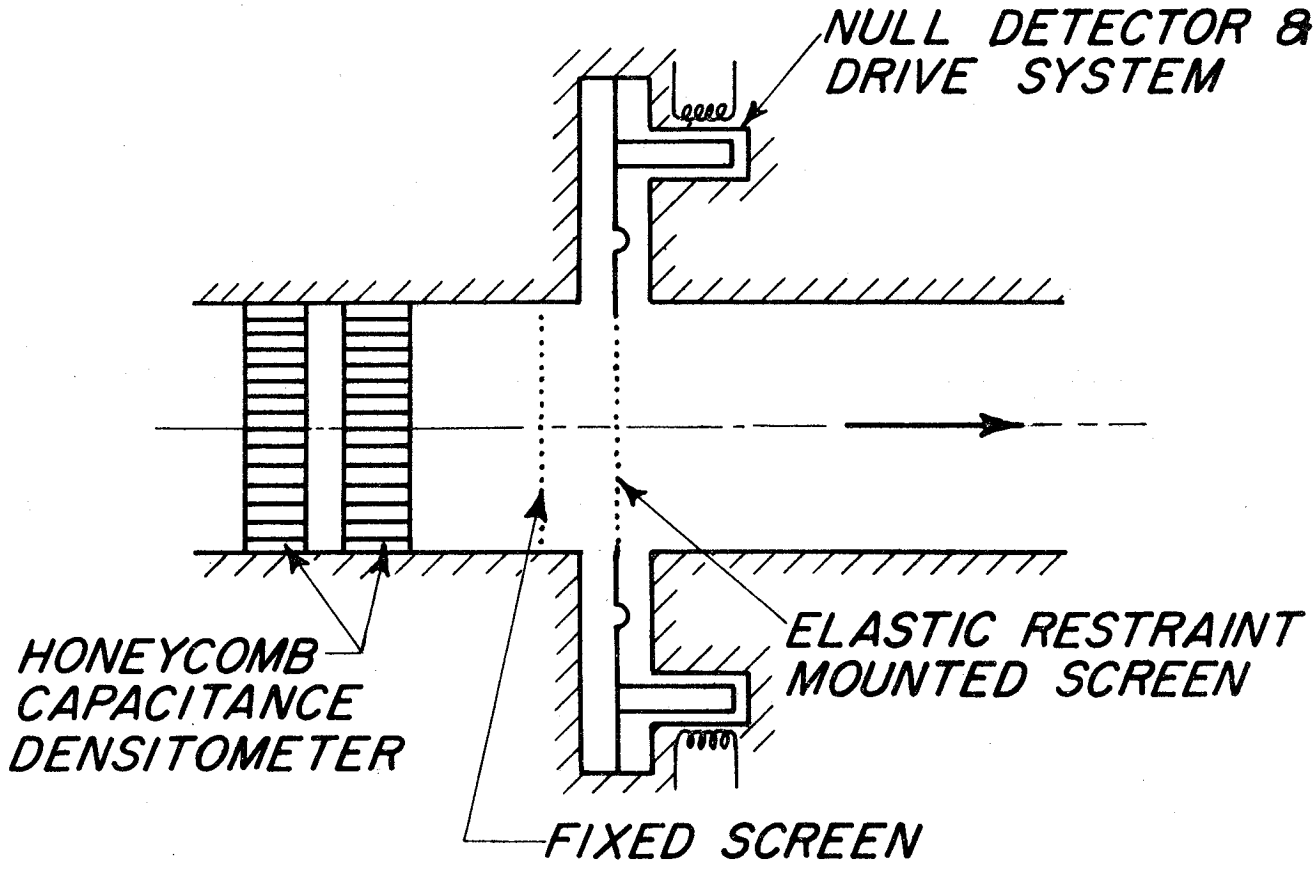

Figure 44. Momentum-Capacitance Mass Flowmeter

The balancing force of end attracting electromagnets required to return the screen to the no-flow (null) position is:

$$F_E = K_2 I^2 \tag{7-22}$$

where

F_E = Balancing force

I = Electromagnet current to hold screen at null position

K_2 = Proportionality constant.

Therefore, with the screen held at the null position under fluid flow conditions

$$F_E = F_F \tag{7-23}$$

$$K_2 I^2 = A\Delta P$$

$$K_2 I^2 = AK_1 \rho V^2$$

Solving for I,

$$I_1 = K_3 V \sqrt{\rho} \tag{7-24}$$

where K_3 = a proportionality constant.

Using the Clausius-Mosotti relation of fluid density to fluid dielectric constant

$$\epsilon = K_5 + K_6 \rho \tag{7-25}$$

The capacitance of the densitometer element can be expressed by

$$C = \epsilon C_o \tag{7-26}$$

where:

C = Measured capacitance of the densitometer element

ϵ = Dielectric constant

C_o = Vacuum-capacitance of the densitometer element.

By substitution:

$$C = \left[K_5 + K_6 \rho\right] C_o$$

$$C = K_5 C_o + K_6 \rho C_o$$

$$\rho = \frac{C - K_5 C_o}{K_6 C_o} \qquad (7\text{-}27)$$

Taking the square root of equation (7-27) by electronic means and then combining with equation (7-24), the following results:

$$I_2 = K_3 V \rho \qquad (7\text{-}28)$$

$$I_2 = K_4 \rho Q$$

or

$$I_2 = K_3 \dot{M} \qquad (7\text{-}29)$$

For slush hydrogen service, this mass flowmeter offers the following advantages:

(a) Applicable to two-phase flow

(b) Requires no flow straighteners

(c) No moving parts in fluid stream.

Disadvantages include:

(a) Inferential mass flow measurement

(b) Slow response time

(c) Screen and "honeycomb" open area may be insufficient to allow free passage of solid particles.

7.3.4 Electromagnetic Flowmeter

Faraday's law of induction, $E = uB$, where E is the induced electric field, u is the velocity of motion, and B is the intensity of magnetic induction, is the basis for the electromagnetic flowmeter. In such a flowmeter, a uniform magnetic induction is established transverse to a flow pipe; and flow of the metered fluid generates a potential difference at suitable detecting electrodes.

Figure 45 is a schematic of the magnetoelectric flowmeter method showing the relative directions of the transverse electric field E, the flow velocity u, and the induced magnetic field H.

Engineering Physics Company has under development an electromagnetic flowmeter that is based on the fact that a moving, polarized dielectric generates an effective magnetic moment according to:

$$M = Pu \qquad (7\text{-}30)$$

where:

M = induced magnetic moment per unit volume

P = polarization in the dielectric

u = velocity of the moving dielectric.

This equation (7-30) is analogous to the equation describing Faraday induction. For a linear dielectric, equation (7-30) can be written as:

$$M = K_o (K-1) Eu \qquad (7\text{-}31)$$

where:

K_o = permittivity of free space

K = dielectric constant of flowing fluid

E = electric field which polarizes the dielectric.

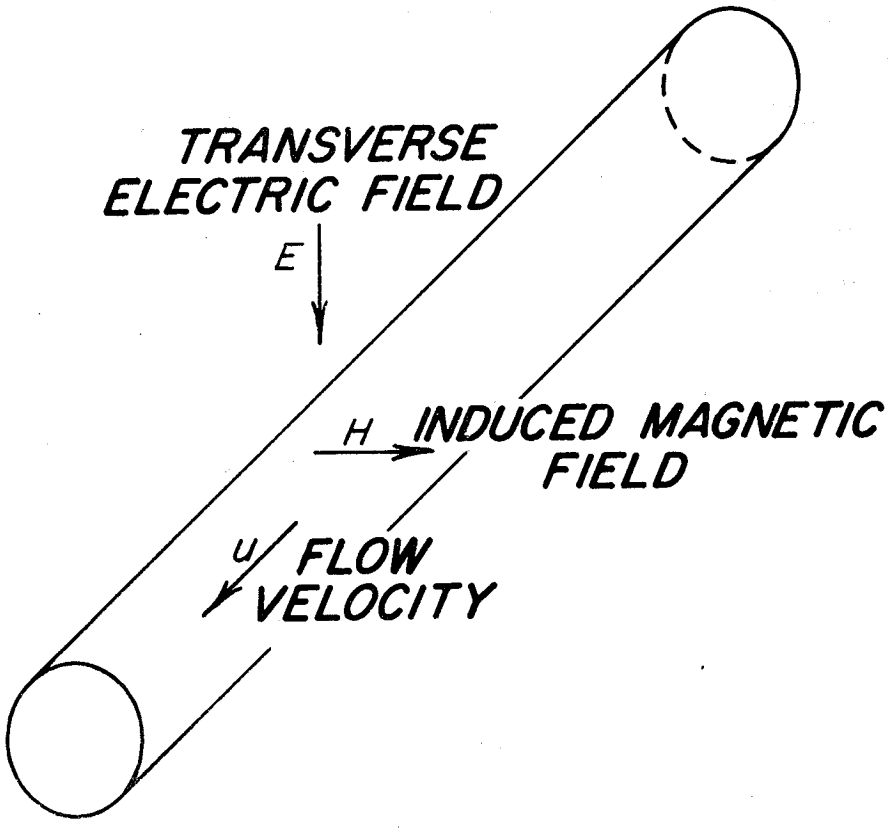

ELECTROMAGNETIC FLOWMETER

Figure 45.

This flowmeter is dependent upon the fact the flowmeter is operating in dielectric regime--i.e., where conduction currents are negligible. The criterion that the flowmeter be operating in the dielectric regime is simply that the liquid's relaxation time must be large compared with the period alternation of the magnetic induction--a requirement that

$$\omega t > 1 \tag{7-32}$$

where

$$t \equiv K K_o / \sigma \tag{7-33}$$

where: ω = angular frequency of magnetic induction

σ = electrical conductivity of the liquid.

Many cryogenic liquids, including hydrogen, are made up of homonuclear molecules, which have no permanent dipole moment and so typically the dielectric constant is low, as is the electrical conductivity.

For mass flowmeter applications, Engineering Physics design is based upon the expression:

$$V_M = \left(\frac{BMF_M}{a} \right) \left(\frac{\sin \beta}{E(\beta, 1)} \right) \tag{7-34}$$

where:

V_M = output voltage

B = magnetic induction

M = Clausius-Mosotti constant for the molecular species which makes up the metered fluid

F_M = mass flow rate

a = interior radius of transducer tube

β = semiangle subtended by the curvelinear detection electrodes

$E(\beta, 1)$ = tabulated elliptic integral.

Equation (7-34) shows that the output signal is proportional to the mass flow rate, provided the Clausius-Mosotti constant is indeed constant for the fluid being measured and that the flow tube maintains structural integrity.

For slush hydrogen service, this mass flowmeter offers the following advantages:

(a) No moving parts in the flow stream

(b) Possible two-phase fluid capability

(c) Direct mass flow measurement

(d) Good time response

(e) Linear calibration.

Disadvantages include:

(a) Zero point drift with temperature

(b) Difficulty in maintaining a hydrogen leak proof flow tube

(c) Complex electronics

(d) Still in development stage

(e) Flow velocity profile must be symmetric with respect to the axis of the pipe.

Figure 46 shows a liquid hydrogen calibration curve for a mass flowmeter of this type.

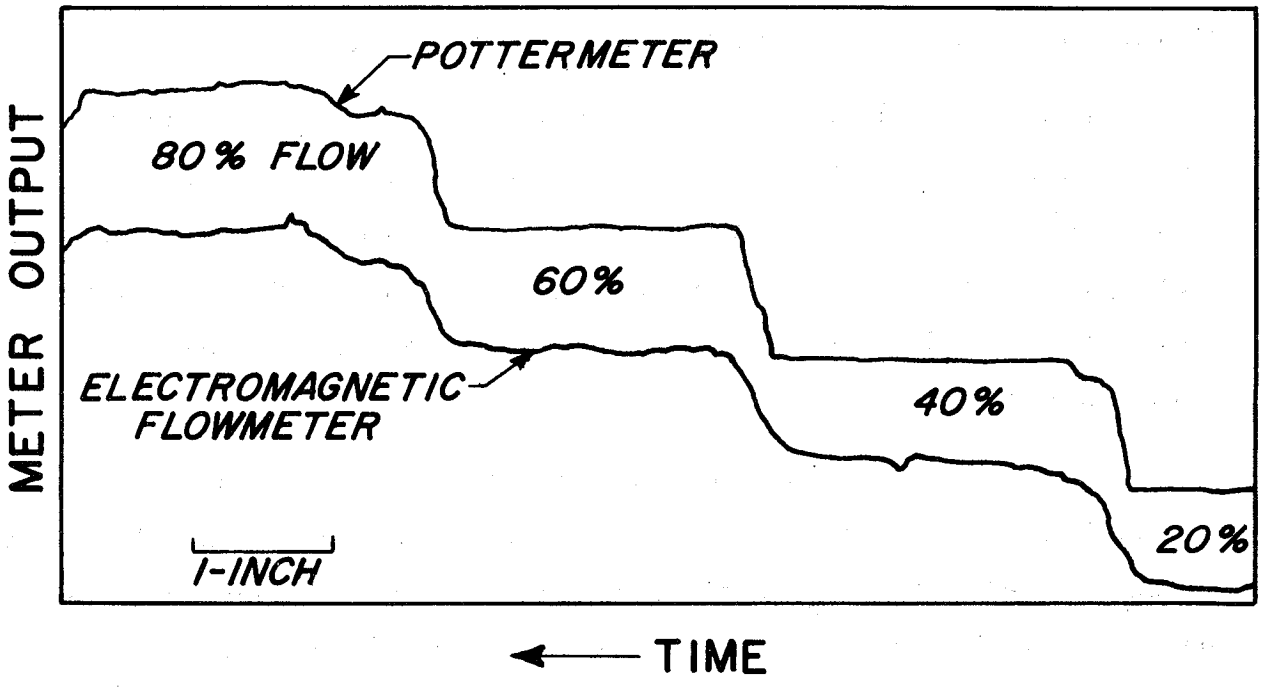

Figure 46. Liquid Hydrogen Calibration of Electromagnetic Flowmeter

7.4 Summary

This investigation of the feasibility of a slush hydrogen flowmeter program has revealed that flow measurement for a slush hydrogen application is, indeed, a needed measurement, and that direct mass rate measurement is preferred. Mass flow measurements will be required in research efforts directed towards fluid transfer characteristics and performance. Also, mass flow measurements will be required in future commercial and aero-space vehicle custody transfer applications. A side benefit to such a development of a mass flowmeter is the possibility of improved aero-space vehicle propellant management.

Because of the nature of the slush hydrogen fluid, mass flow measurement is a difficult task using conventional flow measuring techniques. Particularly, the present inferential mass flow measuring techniques may be unsuitable. Slush hydrogen applications demand measurement techniques that are adaptable to the special characteristics of the slush mixture.

Several direct mass flow measuring techniques appear feasible for slush hydrogen applications. These techniques, however, do require further research and development to approach an idealized mass flowmeter design that includes (a) accuracy, (b) good rangeability, (c) minimum heat input to the fluid, (d) reliability, and (e) solid-liquid mixture fluid capability.

Because of the limited number of cryogenic fluid flow calibration facilities, and their limitation of liquid flow calibration only, no adequate means is presently available for slush hydrogen flowmeter calibration and testing. Any slush hydrogen mass flowmeter development program is absolutely contingent upon the availability of an appropriate calibration and test facility.

7.5 Recommendations

The foregoing has shown that flow measurement (preferably direct mass rate) is necessary to the proper utilization and investigation of slush hydrogen. It has also shown that a number of candidate techniques are available, or under development, which could possibly be adapted for slush hydrogen use. The basic fact remains however, that no development, test, or evaluation of a slush hydrogen flowmeter can be performed without a flow facility; and that further, no such facility exists.

Thus it is impossible to suggest a flowmeter development program without a concurrent flow facility development. If such an effort were deemed appropriate, then a program along the following lines would have to be implemented:

(1) As a slush hydrogen mass flowmeter appears feasible, a development program should be initiated using one or more of the candidate techniques discussed in this report. The following schedule is suggested to implement a development program:

A. Establish design and performance requirements
   1. Applicability to two-phase slush hydrogen
   2. Accuracy
   3. Flow range
   4. Heat input
   5. Pressure drop

B. Conduct industry briefing
   1. The need for a slush hydrogen mass flowmeter
   2. The characteristics of slush hydrogen
   3. Mass flow measurement performance goals

C. Solicit development programs proposals

D. Evaluation of proposals

E. Award of contract(s)

F. Test and evaluation of developed mass flowmeter(s)

G. Reporting of test and evaluation

H. Recommendations.

(2) Concurrent with Item (1), a development program should be inititated to provide a slush hydrogen calibration and testing flow facility. The following schedule is suggested to implement such a development program:

A. Establish design and performance requirements

1. Slush hydrogen to be made and stored according to procedures determined in other study contracts
2. Establish calibration techniques
3. Establish accuracy of calibration goals
4. Establish required flow range
5. Establish plumbing requirements
6. Establish fluid drive system
7. Establish run time

B. In the light of the design and performance requirements of (A.) above:

1. Conduct a review of all present known cryogenic fluid flow facilities
2. Determine feasibility of modification of an existing cryogenic fluid flow facility by seeking proposals from facility operators.

C. Concurrent with Item B. 2 above, study the feasibility of building a small "pilot plant" cryogenic flow facility specifically for slush hydrogen service.

D. Evaluation of feasibility studies of Item B. 2 and C, above

E. Award of contract to provide a slush hydrogen flow facility.

7.6 Flow References

1. L. N. Mortenson, "Design and Operation of a High-Accuracy Calibration Stand for Cryogenic Flowmeters," Advances in Cryogenic Engineering, 6, 379-87 (1961)

2. R. L. Bucknell, "Calibration Systems for Turbine-Type Flow Transducers for Cryogenic Flow Measurement," Advances in Cryogenic Engineering, 8, 360-69, (1963)

3. G. R. Deppe and R. H. Dow, "The Design, Construction and Operation of a Cryogenic Flow Calibration Facility," Advances in Cryogenic Engineering, 8, 371-77, (1963)

4. H. L. Minkin, H. F. Hobart, and I. Warshawsky, "Liquid Hydrogen Flowmeter Calibration Facility," Advances in Cryogenic Engineering, 7, 189-197 (1962)

5. "A Review of Mass Flowmetering," I. S. A. Journal, 7, No. 6 June 1960

6. Thompson, "Evaluation of Fluid Mass Flowmeters," NASA TMX-53065, June 19, 1964

7. Private Communication, The Foxboro Company, January 4, 1965

8. Private Communication, Space Sciences Incorporated

9. Bulletin 600-1, The Decker Corporation

10. Private Communication, The Bendix Corporation, January 1964

11. Cushing, "Magnetoelectric Flowmeter," Review of Scientific Instruments, 35, No. 4 April 1964

12. Cushing, Reily, and Edmunds, "Development of an Electromagnetic Induction Flowmeter for Cryogenic Fluids," Final Report to NASA under contract NASw-381, May 15, 1964

13. Private communication, Engineering Physics Company

8. The Performance of Point Level Sensor in Slush Hydrogen

Level sensing in slush hydrogen applications is useful in determining (a) total fluid volume, (b) settled slush volume, and (c) bulk density of the fluid when the fluid mass is known. Accordingly, a part of the slush hydrogen instrumentation program was concerned with the test and evaluation of commercial liquid hydrogen point liquid level sensors. These sensors represent typical commercially available products.

8.1 Objectives of Test Program

Objectives of this test program were to determine the performance of commercially available liquid hydrogen point liquid level sensors in:

(a) Detecting a near triple point hydrogen liquid-vapor interface

(b) Detecting a settled slush hydrogen-clear liquid interface

(c) Detecting a stirred slush hydrogen-vapor interface.

Sensor accuracy, repeatability, or hysteresis were not included in the test program. The principal objective was simply to determine whether or not these readily available products would function or not.

8.2 Test Apparatus

The liquid level sensors were tested in a 6-inch diameter by 30-inch deep clear glass dewar to permit a visual observation of the sensors.

The glass dewar was mounted on a 2-foot long section of 6-inch diameter copper pipe. This glass dewar-copper pipe assembly was located adjacent to a 6-inch diameter vacuum pumping stack. A 1-inch diameter copper tubing served as the vacuum pumping connection between the assembly and the vacuum pumping stack.

One end (top end) of the copper pipe section was blanked off by a brass plate which then served as a mounting base for a gas driven mixer motor, a sensor lift mechanism, and a vent line. Stand-offs were used to minimize heat conduction to these components. A hydrogen fill line

valve was located at the side of the copper pipe section. Electrical leads entered the side of the copper pipe section through Kovar-cap seals.

Veeco fittings were used at the top end of the stand-offs to permit vertical movement of the mixer shaft and the sensor lift mechanism when raising and lowering the sensors. To prevent ambient air leakage into the slush hydrogen via the Veeco fittings, plastic bags were placed so as to surround the fittings. These bags were pressurized with helium gas.

A liquid nitrogen shielding glass dewar and a clear plastic shield surrounded the test dewar. The liquid nitrogen served to reduce heat input to the slush hydrogen while the plastic shield served as a safety measure in case of a glass dewar failure.

An electrical heater was located in the bottom of the test dewar. This heater provided for controlled melting of the solid hydrogen. Electrical leads to the heater were contained in helium gas filled tubing while the heater was contained in a helium gas filled chamber. Heat capacity of the heater was variable from 0 to 100 watts.

Liquid hydrogen flow into the apparatus was controlled by manually operated valves located at the slush generator and at the hydrogen supply dewar. Between 10 and 12 liters of liquid hydrogen were used for the generation of slush hydrogen. Slush was generated by the "freeze-thaw" technique using a large capacity vacuum pump and appropriate control valves and bias gas. Figure 47 shows the slush hydrogen generator.

8.3 Liquid Level Sensors

The liquid level sensors used in this test program represented commercial, "off-the-shelf," liquid hydrogen point level sensors. These sensors are nominally used to determine a liquid-vapor interface. Three different types of sensors were tested, each type using a different principle of operation.

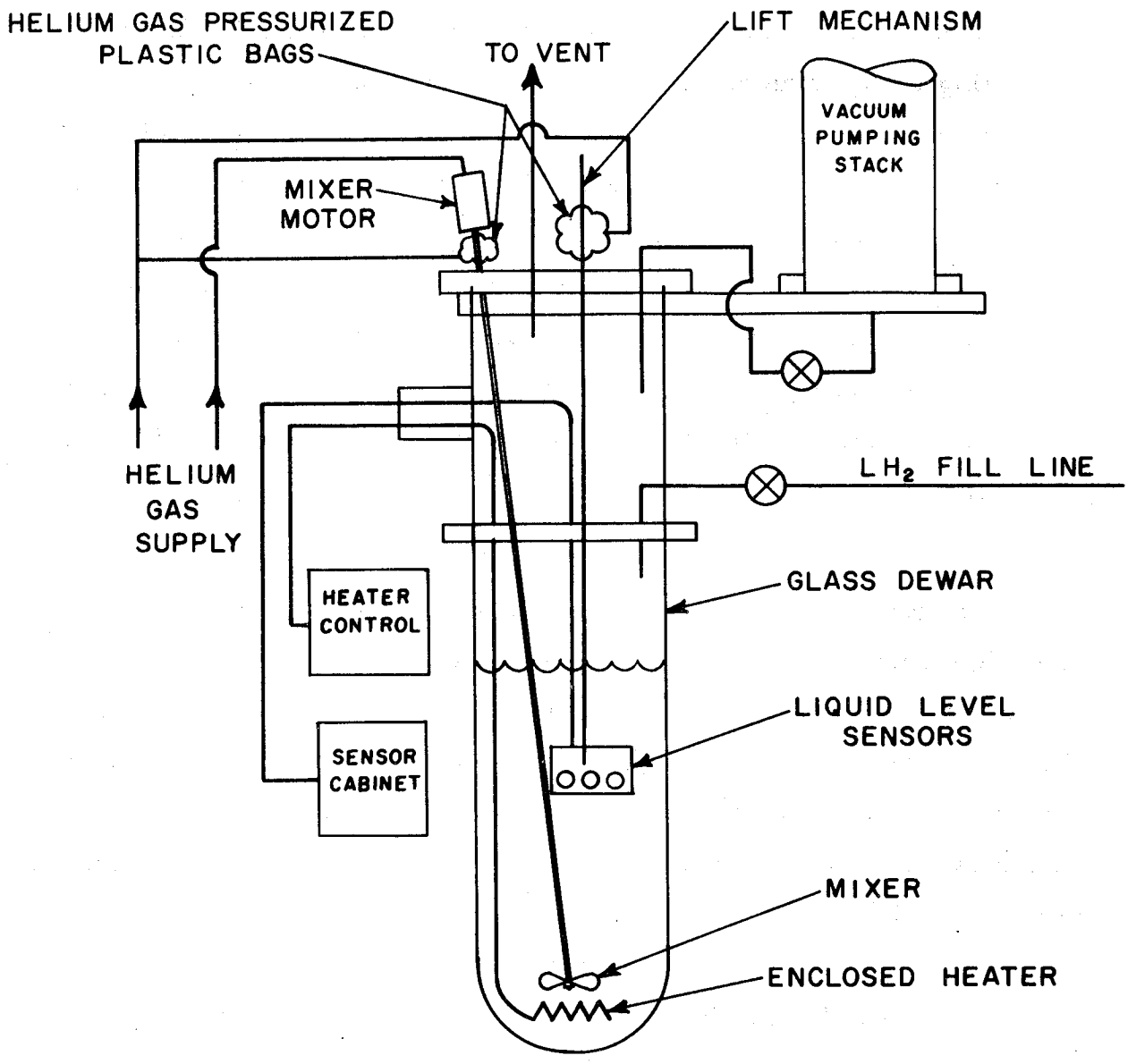

Figure 47. Slush Hydrogen Apparatus for Testing Liquid Level Sensor

8.3.1 Magnetostrictive Type Level Sensor

This type of liquid level sensor employs the acoustic damping difference between a liquid and a vapor to detect a liquid-vapor interface. A driving coil produces an oscillatory magnetic field around a tubular magnetostrictive element causing the element to elongate and contract at ultrasonic frequencies. Another coil senses the element motion and provides a positive feedback signal to sustain circuit oscillation. When the element is restrained, such as when immersed in liquid hydrogen, the feedback signal is lost and oscillation ceases. A detection circuit is employed to rectify the oscillations to drive an output device. This detection circuit is adjustable. Figure 48 shows this type of liquid level sensor.

8.3.2 Optical Type Level Sensor

Figure 49 contains both a schematic representation of an optical type liquid level transducer, and a commercially available version. In the latter, note the prism and means for centering this device on a stillwell. This transducer contains a light source and a light sensitive cell which are isolated from one another but which do communicate down a prism. The prism is cut in such a way as to have total internal reflection when in gas, and yet let the light escape when in liquid. This is possible since there is a difference in the index of refraction of the liquid and the vapor, and since the critical angle depends upon the index refraction.

8.3.3 Capacitance Type Level Sensor

This type of liquid level sensor uses the difference in dielectric constant between a liquid and a vapor to detect a liquid-vapor interface. A change in dielectric constant produces a change in capacitance which is sensed by a series of concentric wire rings which serve as capacitor plates. The concentric rings have a spacing of approximately 1/4 inch between the rings. The resultant capacitance is detected and amplified by electronic

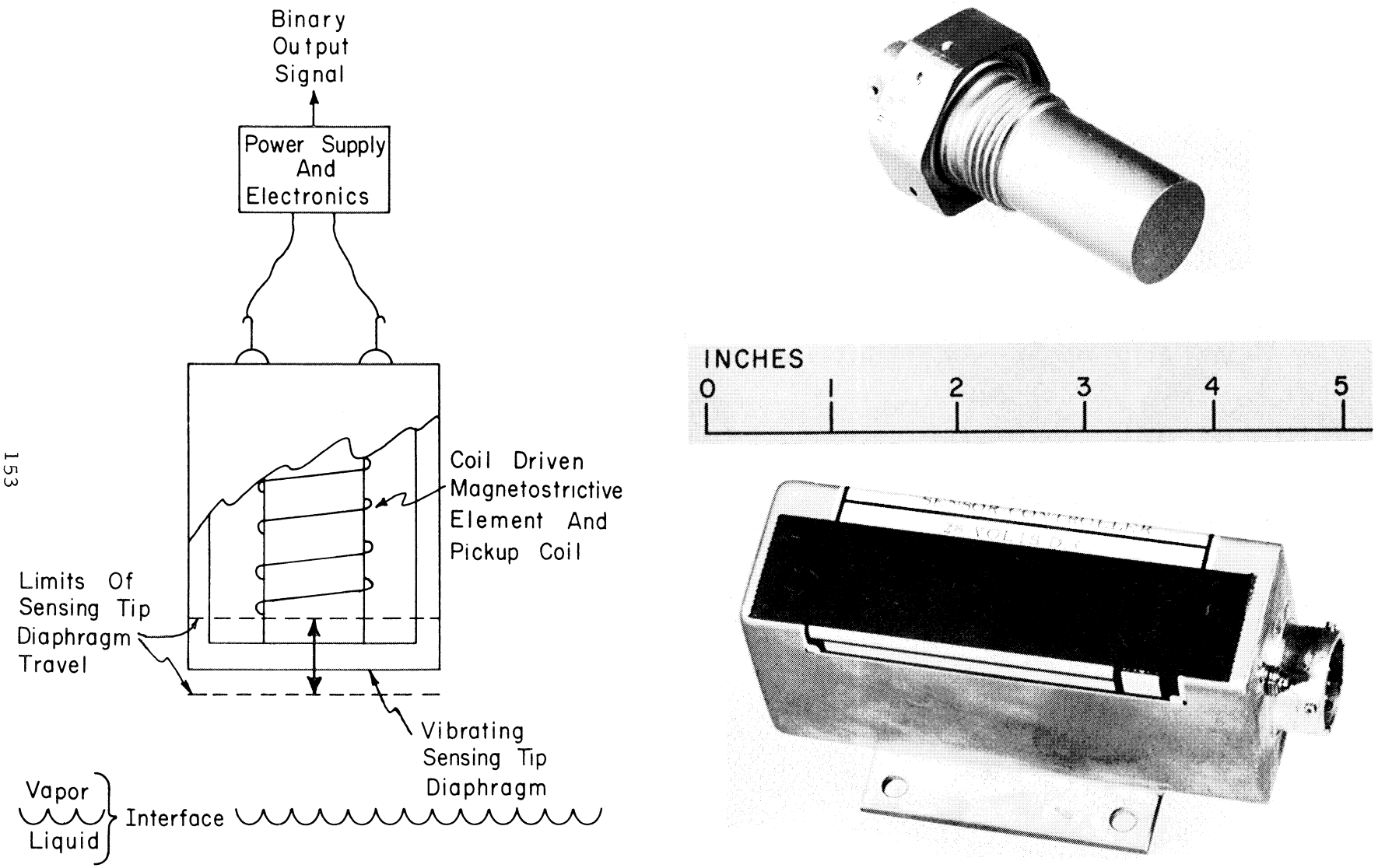

Figure 48. Magnetostrictive Liquid Level Sensor

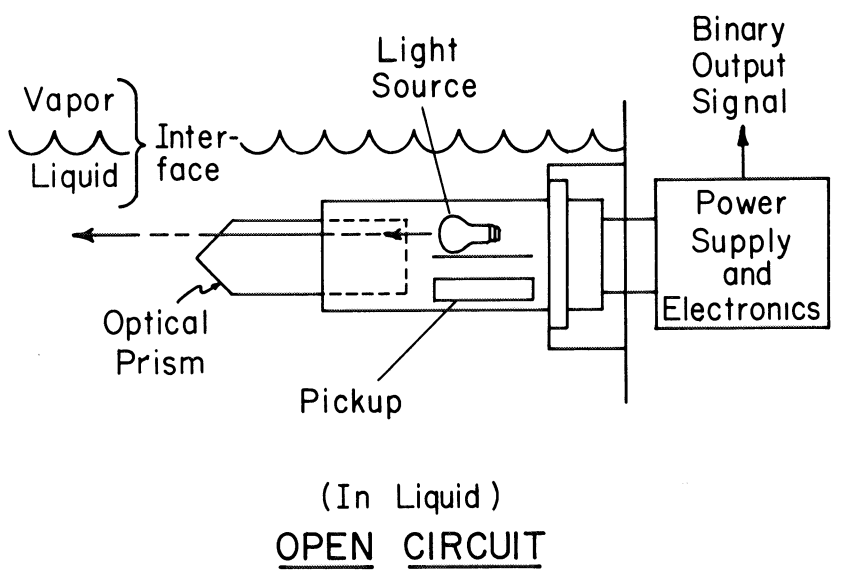

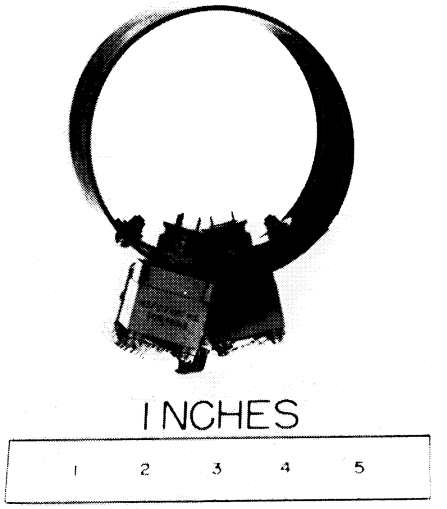

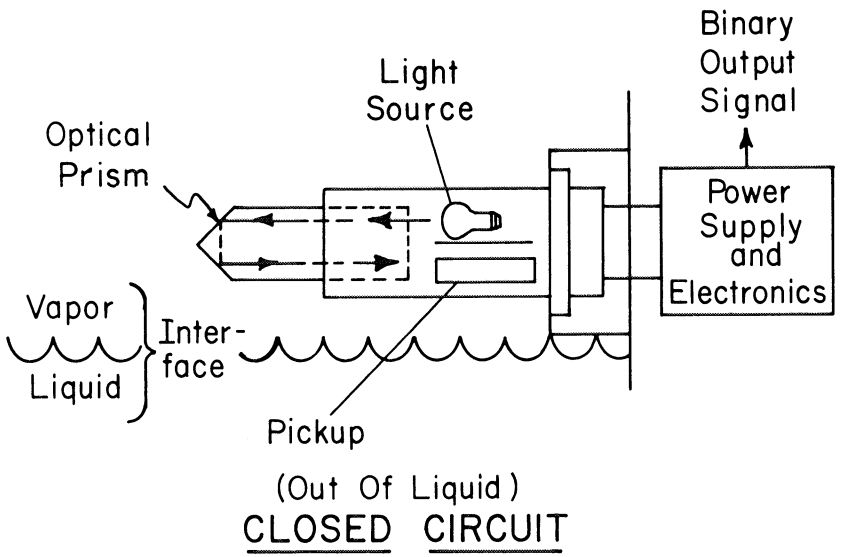

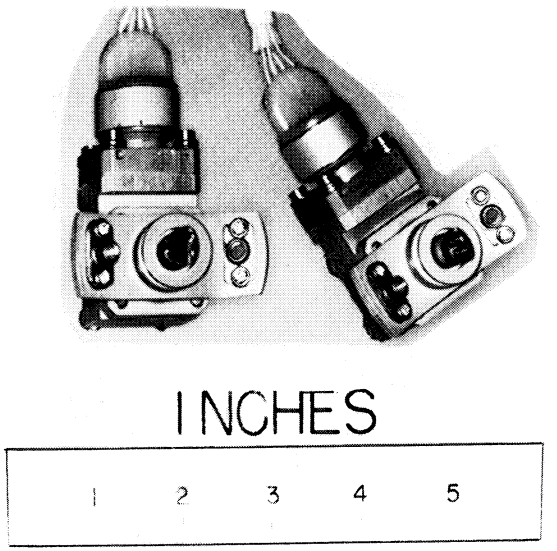

Figure 49. Optical Type Liquid Level Sensor

circuitry which is adjustable. Figure 50 shows schematically and pictorially the capacitance type of point liquid level sensor. These sensors are installed so that the plane of the rings is parallel to the liquid vapor interface.

8.4 Liquid Level Sensor Mounting

As it was desired to simultaneously test the three selected liquid level sensors, a common mounting was used. Each level sensor was mounted in its normal operating position. The common mounting provided for movement of the sensors into and out of the slush hydrogen fluid. Movement of the mounting was by a manually operated gear mechanism, located at the top of the copper pipe section. A fluid mixer was located near the bottom of the test dewar. See Figure 47. Electrical leads for the sensors entered the slush generator by Kovar-cap seals. Sufficient slack was allowed in the electrical leads to permit vertical movement of the level sensors. The position of the sensors was determined by visual observation through the glass dewar. Figure 51 shows the mounting of the liquid level sensors.

8.5 Liquid Level Sensor Read-Out

The individual electronic controls (bridges, relays, etc.) for each liquid level sensor were contained in individual modules which, in turn, were contained in a metal cabinet located 15 feet from the slush generator. Electrical power for the sensors was provided by a common power supply, also located in the cabinet. The metal cabinet was well ventilated as a safety precaution. Figure 52 shows this control cabinet.

8.6 Test Procedure and Results

Normal operational performance of the selected liquid level sensors was first verified using liquid hydrogen at ambient atmospheric pressure. The sensors were moved vertically, into and out of the liquid, across the liquid-vapor interface. All sensors performed satisfactorily in detecting this liquid-vapor interface.

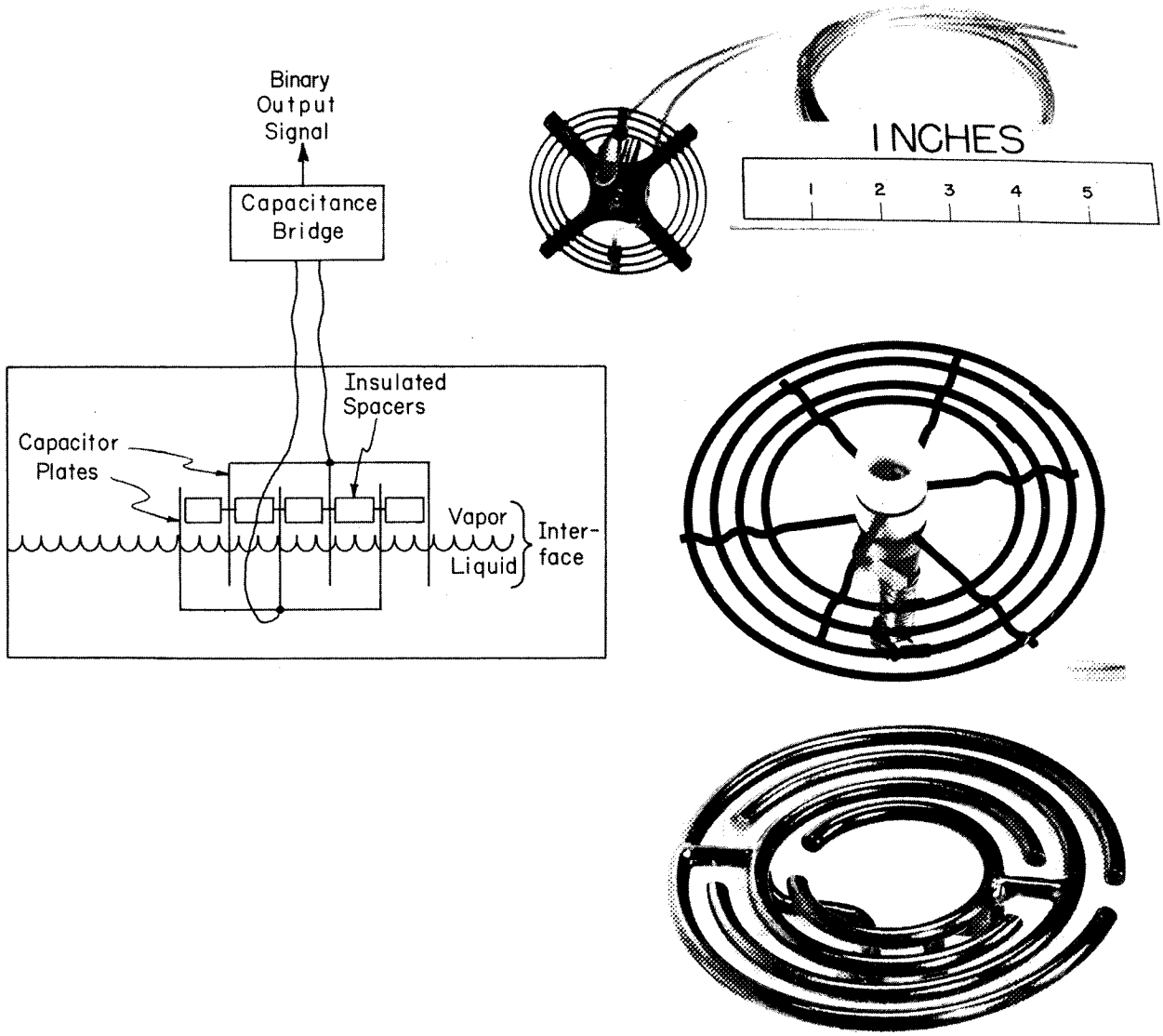

Figure 50. Capacitance Type Liquid Level Sensor

Figure 51. Mounting Arrangement of Liquid Level Sensor

B-56728

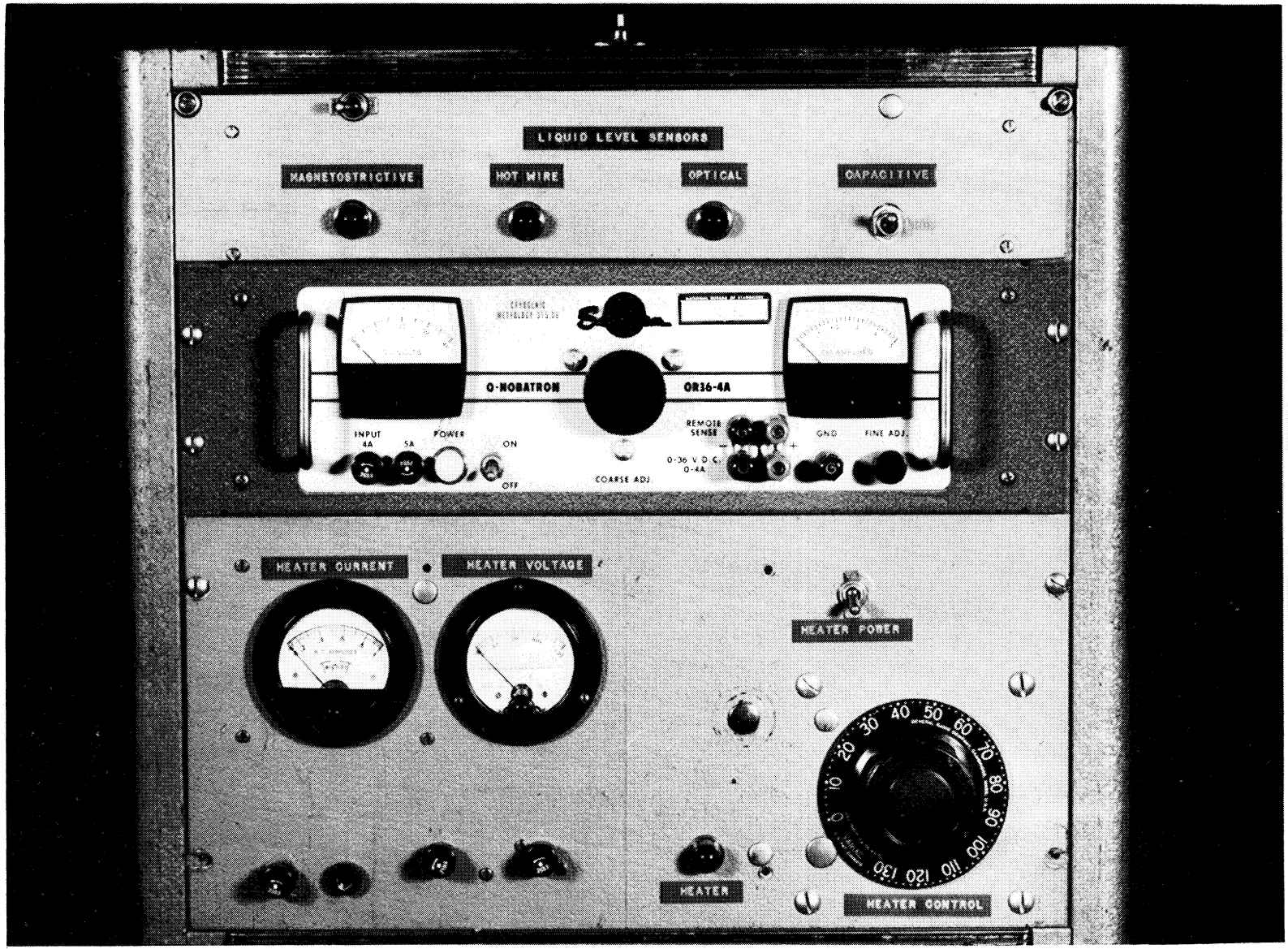

Figure 52. Liquid Level Sensors Control Cabinet

Next, vacuum pumping on the liquid hydrogen was maintained until a point just above the hydrogen triple point was reached. The hydrogen in this case existed as a supercooled liquid. The sensors were moved into and out of the liquid, thus across a supercooled liquid-vapor interface. All sensors performed satisfactorily in detecting this liquid-vapor interface.

Furthur vacuum pumping on the liquid hydrogen generated slush hydrogen. Slush generation was by the "freeze-thaw" technique, previously described. The solid hydrogen thus produced was allowed to settle to the bottom of the test dewar. With settled slush in the test dewar, adjustments were made, where possible, in the individual adjustable controls for each sensor. In the case of the capacitance type sensor, adjustments were made in the electronic circuitry so that the sensor would indicate "dry" in the triple point liquid and "wet" in the settled slush. "Dry" and "wet" refer to the normal liquid level sensor terminology used to indicate if the sensor is in vapor (dry) or liquid (wet). Similar adjustments were made with the optical type level sensor. Adjustments were also attempted with the magnetostrictive type level sensor. With such adjustments, the sensors were moved into and out of the settled slush hydrogen, thus across the settled slush-triple point liquid interface. Both the capacitance type and the optical type level sensor detected the settled slush-triple point liquid interface. The magnetostrictive type level sensor did not detect this particular interface, either because of insufficient adjustment or of inherent inability to detect such an interface.

The final test procedure concerned stirred slush hydrogen. As before, the slush hydrogen was generated by the "freeze-thaw" technique, but, instead of allowing the solid hydrogen to settle out, the total fluid volume was stirred by the mixer, a four-bladed propeller located near the bottom of the test dewar. With readjustment of the capacitance type and of the optical type level sensors from the previous test, all three sensors

were moved into and out of the stirred slush hydrogen, thus across a stirred slush hydrogen-vapor interface. All sensors detected this stirred slush vapor-interface. No attempts were made to detemine level sensor interface detection accuracy or repeatability. Table VI summarizes the results.

Table VI.

Performance of Point Level Sensors in Slush Hydrogen

	Near Triple Point Mixture		
Type	Liquid-Vapor	Stirred Slush-Vapor	Settled Slush-Liquid
Capacitance	yes	yes	yes
Optical	yes	yes	yes
Magnetostrictive	yes	yes	no

8.7 Conclusions

Commercial, "off-the shelf," liquid hydrogen point liquid level sensors, as represented by the selected capacitance type, magnetostrictive type, and optical type, without an adjustment or changes and mounted in their normal operating position, were capable of:

(a) Detecting a near triple point liquid-vapor hydrogen interface.

(b) Detecting a stirred slush-vapor hydrogen interface.

With adjustment of the electronics circuitry, the capacitance type and the optical type liquid level sensors would detect a settled slush-clear triple point liquid hydrogen interface.

These liquid level sensors were provided by:

1. Capacitance type - Minneapolis-Honeywell.
2. Optical type - Bendix Corporation.
3. Magnetostrictive type - Delavan Company.

8.8 Recommendations

Level sensing instrumentation can be a valuable tool in the research and development of slush hydrogen technology. Some possible applications for such instrumentation are: (1) the determination of the level of settled slush in a production or storage vessel and (2) when used in conjuction with tank weighing, the determination of the bulk fluid density, hence the bulk solid content of slush hydrogen.

Although the results of this test program revealed that "off-the-shelf" liquid level sensors are capable of detecting slush hydrogen interfaces, the full potential of level sensing instrumentation will be realized only if a continued program of investigation and development is pursued. Such a program can lead to more refined level sensing which, in turn, can lead to improved accuracy and repeatability. Therefore, it is recommended that a continued program of investigation and development be established. It is further recommended that this program consider the following:

A. Development of improved level sensor electronics. Such improvements can provide for more stable operation and for more sensitive operation. This will, thus, improve sensor repeatability and accuracy.

B. Investigation of sensor position mounting. As slush hydrogen exists as a two phase solid-liquid fluid there undoubtedly exists some preferred mounting position for each type of sensor. For instance, in the case of the concentric wire ring configuration of the capacitance sensor, a horizontal plane of mounting can cause a build up of solid particles on the wire rings which can affect the accuracy and repeatability of level sensing whereas if the sensor is mounted in a vertical plane there can be no such particle build up.

C. Investigation of the percent solid content of slush hydrogen necessary to activate each type of sensor. It is obvious that there exists a minimum percent solid content necessary to "trigger" each type of

sensor. To date, there exists no knowledge of the amount of solid content necessary for sensor activation.

D. Investigation of other principles of level sensing. Other principles may offer even further advantages than the principles already evaluated; therefore, these other principles, in particular nuclear radiation attenuation, merit investigation.

E. Investigation of a combination of level sensing with fluid weighing to determine bulk fluid density, hence, bulk fluid solid content. Such a system would offer the advantage of indicating the fluid mass content in a slush hydrogen production or storage vessel.

9. A Superconducting Liquid Level Sensor for Use in Slush Hydrogen

9.1 Introduction

Slush exists at the triple point temperature of hydrogen, and since this temperature is below the transition temperature of several superconducting compounds, it should be possible to construct a superconducting liquid level sensor (point or continuous) for use in slush hydrogen.

A system of three superconducting niobium stannide liquid level sensors was constructed and tested in triple point liquid hydrogen. Tests indicated that the sensors were capable of detecting, in a linear fashion, the liquid level of the system over a range of about 60% of the total sensor length. One of the sensors was shown to be capable of detecting a liquid level change on the order of 0.2 mm. Sensitivity of the sensors was investigated and was shown to be a function of the current applied to the sensors as well as a function of several physical characteristics of the sensors themselves. A heat balance was used to obtain an approximation to the measurement error of the sensors.

9.2 Principle of Operation

Since the triple point temperature of hydrogen (13.81°K) [1] is below the transition temperature of niobium stannide (18.05°K) [2], it is possible to utilize the temperature of the system being studied to obtain knowledge of its liquid level. A continuous liquid level sensor consists of a length of superconducting wire strung vertically over the length of a tank. Due to the high rate of heat transfer in the slush phase as compared to the vapor phase, the portion of the wire in the vapor phase may be easily heated to above the transition temperature by passing a small current through it. The portion of the wire in the slush phase will remain superconducting and will make no contribution to the resistance of the element. Hence the resistance of the wire should be a linear function of the system.

Superconducting liquid level sensors have been operated successfully in helium systems [3, 4], but this is the first reported application of the principle to a hydrogen system.

9.3 Apparatus

9.3.1 Sensor Assembly

The sensor assembly consists of four sensor elements mounted on plastic supports around a hollow brass rod fitted with setscrews (Figure 53). The elements are soldered to hermetic glass to metal seals; in each case one end of the element is fixed while the other is spring loaded. The supports are approximately 1/8 inch in thickness and are fashioned from disks about 4 inches in diameter. The brass rod is of sufficient inside diameter to enclose the 1/4-inch elevating rod to which it is fixed during operation. The rod itself is held in place by setscrews.

Three of the sensors contained superconducting niobium stannide (Nb_3Sn); the fourth was a 24-gage high purity copper thermocouple wire element, and was originally intended to serve as a "dummy" for purposes of performance comparison. It could operate as a conventional hot wire sensor. Sensor A is 4.455 inches in length, 0.090 ± 0.003 inches wide, 0.0020 ± 0.0002 inches in overall thickness, and consists of a ribbon of stainless steel substrate surrounded by successive layers of niobium stannide and silver. Sensor B is 4.508 inches in length, 0.125 ± 0.003 inches wide, 0.0017 ± 0.0002 inches in overall thickness, and has a niobium core with successive layers of niobium stannide and copper. Sensor C is 4.518 inches in length, 0.250 ± 0.003 inches wide, 0.0017 ± 0.0002 inches in overall thickness, and has a niobium core with a niobium stannide exterior. Separate current and potential leads were provided for each sensor while tempering was used to minimize heat leak via conduction to the assembly.

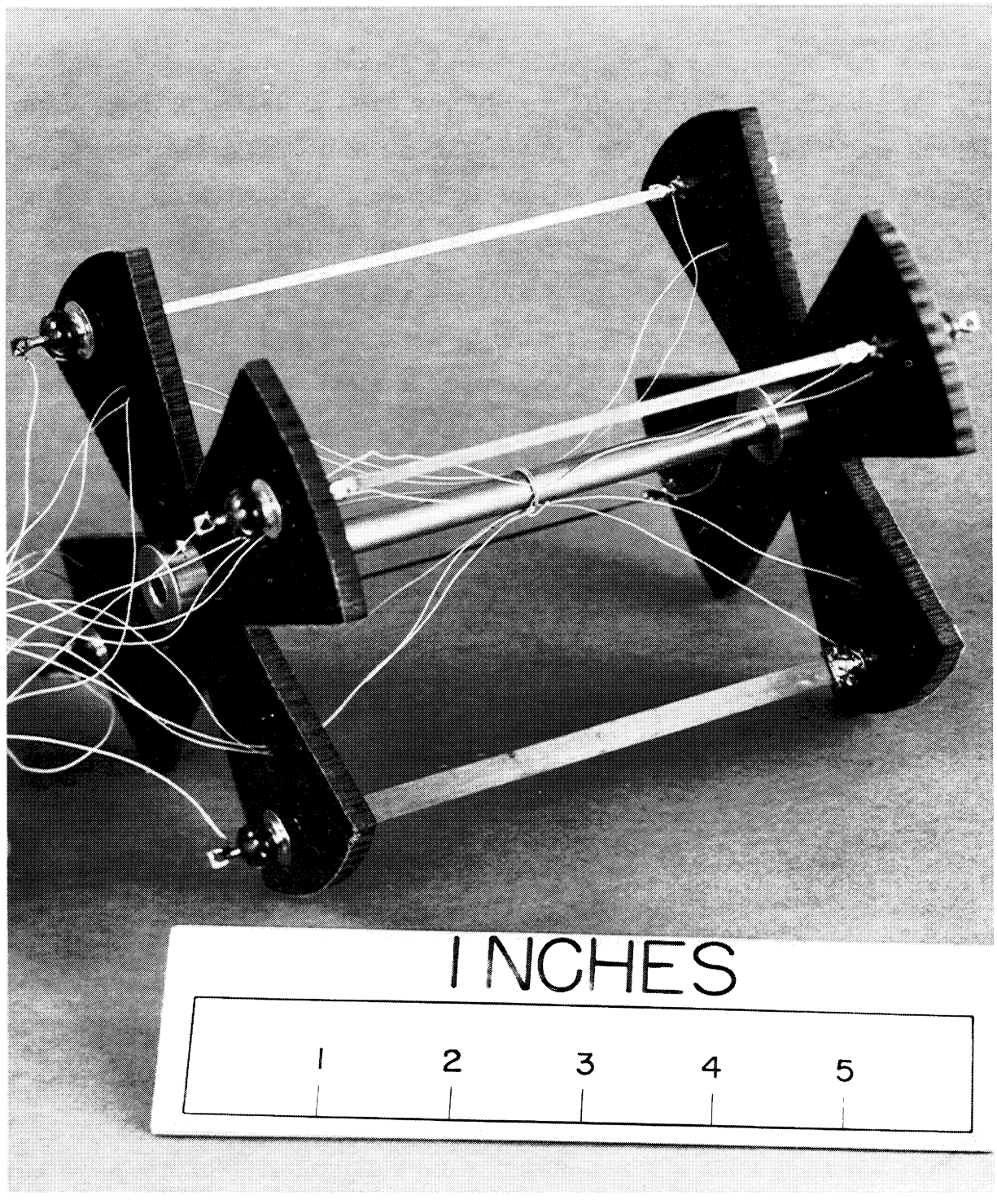

Figure 53. Superconductor Level Sensor Assembly

B- 51686

9.3.2 Electrical Circuitry

A constant current power supply was used in series with an ammeter and the sensor assembly. By holding the current constant, voltage readings could have been taken as the liquid level of the system changed; in actual operation, the sensors were raised and lowered in the dewar, causing an effective change in the liquid level of the system and resulting changes in the sensor resistance and in the measured voltage. The Fluke power supply is capable of supplying currents greater than 1 A with a constancy of ± 0.02%. Readings from the Rubicon potentiometer are known to within ± 1μV.

9.3.3 Slush Generator

The apparatus used in this study consisted of a copper spacer section and a glass dewar (Figure 54). Liquid injection occurs in the spacer section while the triple point hydrogen liquid is contained in the dewar. The spacer is a 2-foot section of 6-inch copper pipe with appropriate 150 psi brass flanges. The lower flange connects to the glass dewar while the upper flange is blanked off by a brass plate. This brass plate serves as the base for the mixer motor, lift rod, and vent line. Stand-offs are used to minimize heat conduction to these items. The liquid hydrogen fill line enters at the side of the copper spacer. The electrical leads for the test sensors also enter the apparatus at the side of the spacer section. Hermetic seals prevent the entry of air into the hydrogen system.

Since the mixer shaft and elevating rod must be capable of vertical movement to raise and lower the sensor assembly in the dewar, compressed O-ring seals are used at the top end of the stand-offs. Plastic bags surround these seals to prevent air leakage into the system; the bags are purged with helium gas during operation.

Liquid hydrogen was supplied from an 800-liter dewar located outside the test building by a cryogenic transfer line. Liquid hydrogen flow into the apparatus was controlled by manually operated valves located at

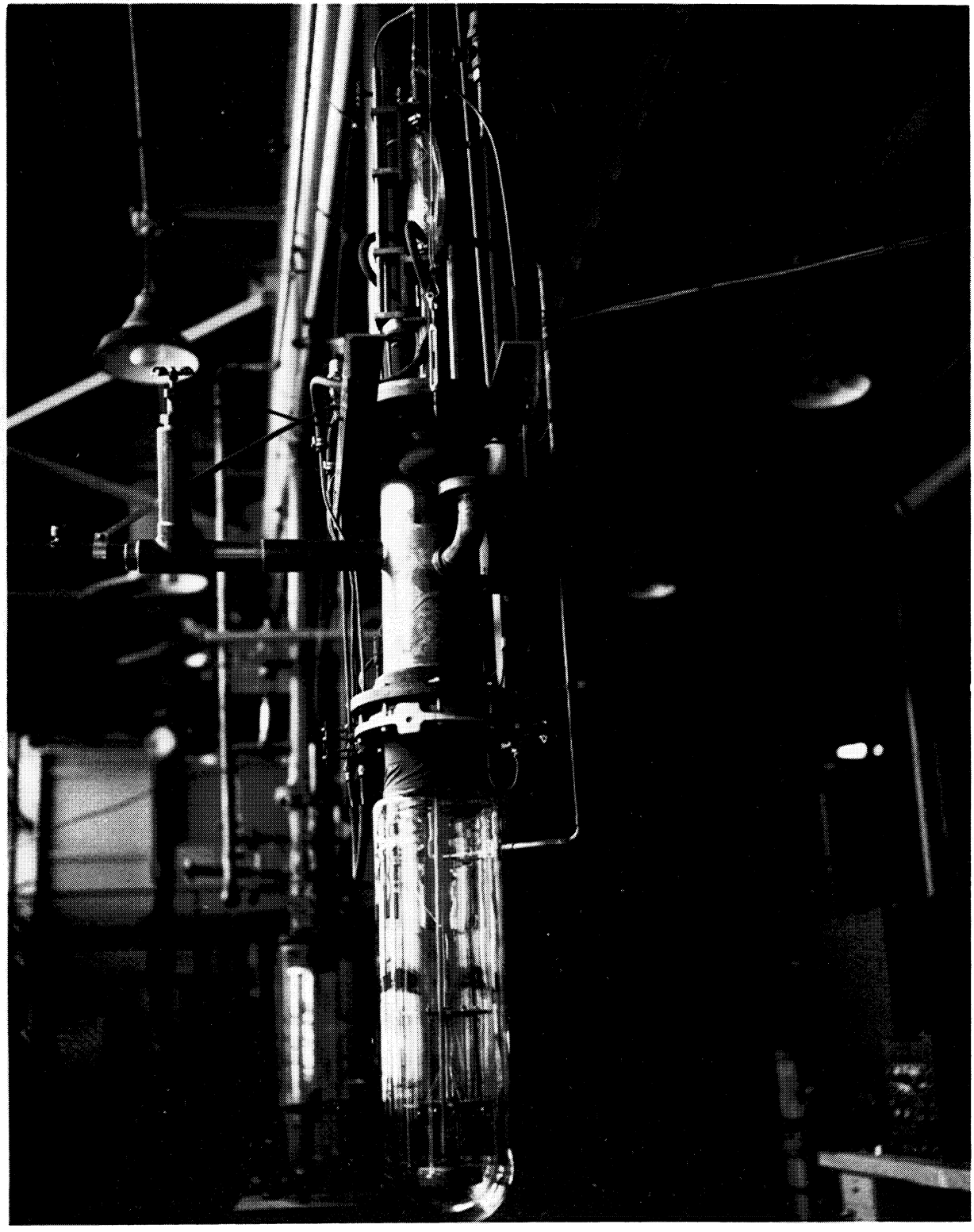

Figure 54. Slush Generator with Super-Conducting Level Sensor Assembly in Place

B- 52772

the side of the spacer section and the side of the supply dewar. Flanges using PTFE* O-rings connect to the base plate and the glass dewar.

The use of a glass dewar for the evaluation of the sensors was not ideal from a safety standpoint, but it enabled the sensors to be calibrated optically, with a precision cathetometer. The dewar itself is 30 inches in depth and 6 inches in diameter, with the hydrogen section being surrounded by a liquid nitrogen shielding dewar. The quantity of triple point liquid in the dewar did not exceed 12 liters during operation, and a small heater was located in the bottom of the dewar to facilitate removal of the liquid prior to shut-down.

9.4 Results

Tests were completed using operating currents of 10 and 50 mA. A calibration curve for sensor A (10 mA) is presented in Figure 55. In all cases, the sensor resistance, and hence the readout voltage, is a linear function of the liquid level of the system until approximately 60% of the sensor surface is exposed to the vapor. Calculations indicate that the temperature of the vapor exposed portion of the sensor under these conditions is about 18.5°K. Output voltages deviate appreciably from the expected linear values when more than 60% of the sensor surface is exposed to the vapor in each case. These deviations are caused by two factors: (1) The temperature gradient in the hydrogen gas in the region of non-linear readout voltages is great enough to establish a temperature gradient in the sensors in this region; and (2) in this same region, their conduction paths are increased, with the net result that the temperature gradients in the sensors in the non-linear output region are maintained. In the region of non-linear readout voltages, the sensor resistance is affected by both the change in liquid level (a linear response) and the change in sensor temperature. Since the sensors are constructed of composite layers of materials whose individual resistivities are very temperature-sensitive in the range of operating temperatures [5], the temperature

* Polytetrafluroethylene

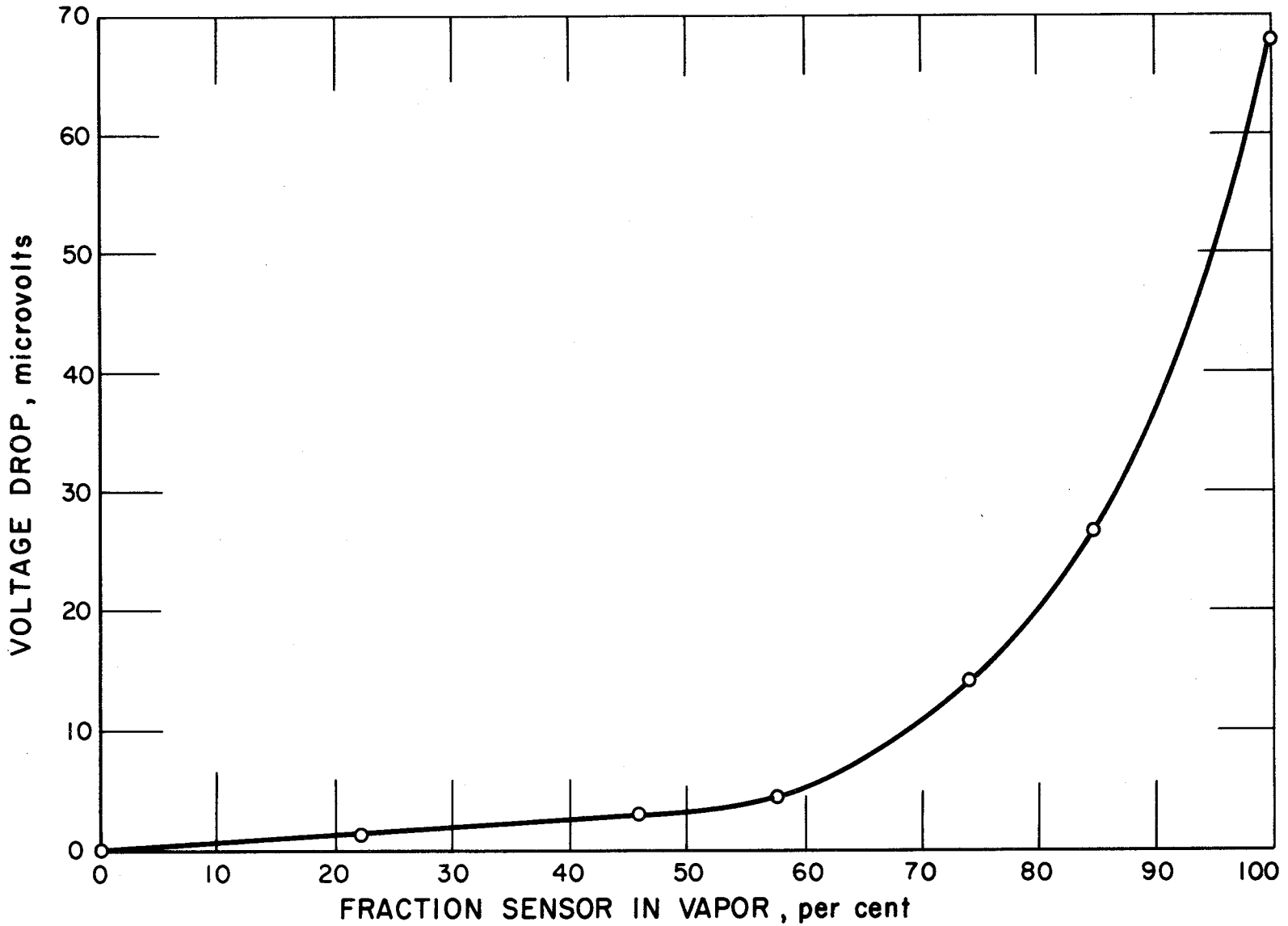

Figure 55. Calibration Curve for a Superconducting Level Gage

gradient in the sensors in the non-linear region causes the non-linearity in the calibration curves.

The sensitivity of the sensors was determined for each operating current. Defining sensitivity as the change in voltage per unit change in length, dV/dL, the appropriate values were determined in the linear output region and are presented in Table VII.

Table VII.

Sensor Sensitivity as a Function of Current

Sensor	Current, mA	Sensitivity, μV/mm
A	10	0.05
	50	0.34
B	10	0.14
	50	0.78
C	10	0.95
	50	0.25

Under the existing experimental conditions, a direct calculation of the measurement error of the sensors was not possible. A trial and error calculational procedure indicated that the sensors possessed a measurement error on the order of 1 mm. This means that the transition from the superconducting to the normal state in the sensor does not occur exactly at the liquid interface, but approximately 1 mm above it. It is interesting to note that in the region of linear output voltages the operating current did not supply sufficient heat to drive the elements normal; the bulk of this heat deficiency was made up by convective heat transfer from the hydrogen gas to the sensor near the liquid interface. Thus the sensors may be operated successfully at currents less than 10 mA.

9.5 Conclusions

Experimental tests confirmed that all three sensors were capable of detecting the liquid-vapor interface in a system of slush or liquid hydrogen at the triple point. Sensor C proved to be the most sensitive of the three sensors; based on its high resistance, it was found

to be capable of detecting a liquid level change on the order of 0.2 mm with an operating current of 50 mA using the apparatus described.

It is evident from the preceeding results that, in general, the most effective superconducting liquid level sensors are those which possess: (1) a high value of electrical resistivity in the normal region and (2) an electrical resistivity essentially independent of temperature in the range of operating temperatures. It is essential that the transition temperature of the superconductor be greater than the temperature of the system.

The resistance of the sensors was shown to be a linear function of the liquid level of the system except in regions where a temperature gradient existed in the sensors themselves. In this region, due to the high temperature dependence of resistivity of the sensors, the relationship was extremely non-linear. When operating under the conditions described, the measurement error of these sensors was found to be approximately 1 mm.

9.6 References

[1.] R. B. Scott, Cryogenic Engineering, D. Van Nostrand Co., Inc., Princeton, N. J. (1959), p. 338.

[2.] B. W. Roberts, General Electric Research Laboratory Report No. 63-RL-3252M, Schenectady, N. Y. (March 1963), p. 92.

[3.] J. R. Feldmeier and B. Serin, Rev. Sci. Instr. 19, 916, (1948).

[4.] B. F. Figgins, T. A. Shepherd, and J. W. Snowman, J. Sci. Instr. 41, 520, (1964).

[5.] R. B. Stewart and V. J. Johnson, A Compendium of the Properties of Materials at Low Temperatures, Phase II, National Bureau of Standards, Cryogenic Engineering Laboratories, Boulder, Colo., WADD Tech. Report 60-56, Part IV, p. 225, (1961) ASD Contr. No. D. O. 33(616)59-6, DDC AD 272 769.

10. Distribution List for Final Report

COPIES	RECIPIENT
	NASA Headquarters, Washington, D. C. 20546
1	Contracting Officer, BCA
1	Patent Office, AGP
	NASA Lewis Research Center 21000 Brookpark Road, Cleveland, Ohio 44135
1	Office of Technical Information
1	Contracting Officer
1	Patent Office
	NASA Marshall Space Flight Center Huntsville, Alabama 35812
1	Office of Technical Information, M-MS-IPC
1	Purchasing Office, PR-CH
1	Patent Office, M-PAT
1	Keith Chandler, R-P&VE-PA
	NASA Western Operations Office 150 Pico Boulevard, Santa Monica, California 90406
1	Office of Technical Information
1	Contracts Management Division
1	General Counsel for Patent Matters
4	Chief, Liquid Propulsion Technology, RPL Office of Advanced Research and Technology NASA Headquarters Washington, D. C. 20546
25	NASA Scientific and Technical Information Facility P. O. Box 33 College Park, Maryland 20740
1	Mr. Vincent L. Johnson Director, Launch Vehicles and Propulsion, SV Office of Space Science and Applications NASA Headquarters, Washington, D. C. 20546
1	Mr. Edward L. Gray Director, Advanced Manned Missions, MT Office of Manned Space Flight NASA Headquarters, Washington, D. C. 20546

COPIES	RECIPIENT
1	Mr. Clarence A. Syvertson Mission Analysis Division NASA Ames Research Center Moffett Field, California 24035
1	(Technical Monitor) Mr. Jean Olivier, K-DF-2 Marshall Space Flight Center Huntsville, Alabama 35812
1	Mr. Frank Gasper, EDV-17 Marshall Space Flight Center Huntsville, Alabama 35812
1	Mr. Jerold L. Vaniman, R-P&VE-PTP NASA Marshall Space Flight Center Huntsville, Alabama 35812

NASA FIELD CENTERS

COPIES	RECIPIENT	DESIGNEE
2	Ames Research Center Moffett Field, California 94035	Harold Hornby Mission Analysis
2	Goddard Space Flight Center Greenbelt, Maryland 20771	Merland L. Moseson Code 620
2	Jet Propulsion Laboratory California Institute of Technology 4800 Oak Grove Drive Pasadena, California 91103	Henry Burlage, Jr. Propulsion Div., 38
2	Langley Research Center Langley Station Hampton, Virginia 23365	Dr. Floyd L. Thompson Director
2	Lewis Research Center 21000 Brookpark Road Cleveland, Ohio 44135	Dr. Abe Silverstein Director
2	Marshall Space Flight Center Huntsville, Alabama 35812	Hans G. Paul Code R-P&VED
2	Manned Spacecraft Center Houston, Texas 77001	Dr. Robert R. Gilruth Director
2	Western Operations Office 150 Pico Boulevard Santa Monica, California 90406	Robert W. Kamm Director
2	John F. Kennedy Space Center, NASA Cocoa Beach, Florida 32931	Dr. Kurt H. Debus

GOVERNMENT INSTALLATIONS

COPIES	RECIPIENT	DESIGNEE
1	Aeronautical Systems Division Air Force Systems Command Wright-Patterson Air Force Base Dayton, Ohio 45433	D. L. Schmidt Code ASRCNC-2
1	Air Force Missile Development Center Holloman Air Force Base, New Mexico	Maj. R. E. Bracken Code MDGRT
1	Air Force Missile Test Center Patrick Air Force Base, Florida	L. J. Ullian
1	Air Force Systems Division Air Force Unit Post Office Los Angeles 45, California	Col. Clark Technical Data Center
1	Arnold Engineering Development Cntr Arnold Air Force Station Tullahoma, Tennessee 37389	Dr. H. K. Doetsch
1	Bureau of Naval Weapons Department of the Navy Washington, D. C.	J. Kay RTMS-41
1	Defense Documentation Center Headquarters Cameron Station, Building 5 5010 Duke Street Alexandria Virginia 22314 ATTN: TISIA	
1	Headquarters, U. S. Air Force Washington, D. C. 20330	Col. C. K. Stambaugh AFRST
1	Picatinny Arsenal Dover, New Jersey 07801	I. Forsten, Chief Liquid Propulsion Laboratory, SMUPA-DL
1	Air Force Rocket Propulsion Laboratory Research and Technology Division Air Force Systems Command Edwards, California 93523	RPRR/Mr. H. Main

GOVERNMENT INSTALLATIONS

COPIES	RECIPIENT	DESIGNEE
1	U. A. Atomic Energy Commission Technical Information Services Box 62 Oak Ridge, Tennessee	A. P. Huber Oak Ridge Gaseous Diffusion Plant (ORGDP) P. O. Box P
1	U. S. Army Missile Command China Lake, California 93557	Dr. Walter Wharton Chief, Missile Propulsion Division.

CPIA

1	Chemical Propulsion Informations Agency Applied Physics Laboratory 8621 Georgia Avenue Silver Spring, Maryland 20910	Neil Safeer

INDUSTRY CONTRACTORS

1	Aerojet-General Corporation P. O. Box 296 Azusa, California 91703	L. F. Kohrs
1	Aerojet-General Corporation P. O. Box 1947 Technical Library, Bldg. 2015, Dept. 2410 Sacramento, California 95809	R. Stiff
1	Aeronautronic Philco Corporation Ford Road Newport Beach, California 92663	D. A. Carrison
1	Aerospace Corporation 2400 East El Segundo Boulevard P. O. Box 95085 Los Angeles, California 90045	John G. Wilder MS-2293 Propulsion Dept.

INDUSTRY CONTRACTORS

COPIES	RECIPIENT	DESIGNEE
1	Arthur D. Little, Inc. 20 Acorn Park Cambridge, Massachusetts 02140	E. Karl Bastress
1	Astropower Laboratory Douglas Aircraft Company 2121 Paularino Newport Beach, California 92663	Dr. George Moc Director, Research
1	Astrosystems International, Inc. 1275 Bloomfield Avenue Fairfield, New Jersey 07007	A. Mendenhall
1	Atlantic Research Corporation Edsall Road and Shirley Highway Alexandria, Virginia 22314	A. Scurlock
1	Beech Aircraft Corporation Boulder Division Box 631 Boulder, Colorado 80302	J. H. Rodgers
1	Bell Aerosystems Company P. O. Box 1 Buffalo, New York 14240	W. M. Smith
1	Bendix Systems Division Bendix Corporation 3300 Plymouth Road Ann Arbor, Michigan	John M. Brueger
1	Boeing Company P. O. Box 3707 Seattle, Washington 98124	J. D. Alexander
1	Missile Division Chrysler Corporation P. O. Box 2628 Detroit, Michigan 48231	John Gates

INDUSTRY CONTRACTORS

COPIES	RECIPIENT	DESIGNEE
1	Wright Aeronautical Division Curtiss-Wright Corporation Wood-Ridge, New Jersey 07075	G. Kelley
1	Missile and Space Systems Division Douglas Aircraft Company, Inc. 3000 Ocean Park Boulevard Santa Monica, California 90406	R. W. Hallet Chief Engineer Advanced Space Tech.
1	Aircraft Missiles Division Fairchild Hiller Corporation Hagerstown, Maryland 21741	J. S. Kerr
1	General Dynamics/Astronautics Library & Information Services (128-00) P. O. Box 1128 San Diego, California 92112	Frank Dore
1	Re-Entry Systems Department General Electric Company 3198 Chestnut Street Philadelphia, Pennsylvania 19101	F. E. Schultz
1	Advanced Engine & Technology Dept. General Electric Company Cincinnati, Ohio 45215	D. Suichu
1	Grumman Aircraft Engineering Corp. Bethpage, Long Island, New York	Joseph Gavin
1	Ling-Temco-Vought Corporation Astronautics P. O. Box 5907 Dallas, Texas 75222	Warren C. Trent
1	Lockheed California Company 2555 North Hollywood Way Burbank, California 91503	G. D. Brewer

INDUSTRY CONTRACTORS

COPIES	RECIPIENT	DESIGNEE
1	Lockheed Missiles and Space Co. ATTN: Technical Information Center P. O. Box 504 Sunnyvale, California 94088	Y. C. Lee
1	Lockheed Propulsion Company P. O. Box 111 Redlands, California 92374	H. L. Thackwell
1	The Marquardt Corporation 16555 Saticoy Street Van Nuys, California 91409	Warren P. Boardman, Jr.
1	Balitmore Division Martin Marietta Corporation Baltimore, Maryland 21203	John Calathes (3214)
1	Denver Division Martin Marietta Corporation P. O. Box 179 Denver, Colorado 80201	J. D. Goodlette (A-241)
1	McDonnell Aircraft Corporation P. O. Box 516 Municipal Airport St. Louis, Missouri 63166	R. A. Herzmark
1	Space & Information Systems Division North American Aviation, Inc. 12214 Lakewood Boulevard Downey, California 90241	H. Storms
1	Rocketdyne (Library 586-306) North American Aviation, Inc. 6633 Canoga Avenue Canoga Park, California 91304	E. B. Monteath
1	Northrop Space Laboratories 3401 West Broadway Hawthorne, California	Dr. William Howard

INDUSTRY CONTRACTORS

COPIES	RECIPIENT	DESIGNEE
1	Astro-Electronics Division Radio Corporation of America Princeton, New Jersey 08540	S. Fairweather
1	Reaction Motors Division Thiokol Chemical Corporation Denville, New Jersey 07832	Arthur Sherman
1	Republic Aviation Corporation Farmingdale, Long Island, New York	Dr. William O'Donnell
1	Space General Corporation 9200 East Flair Avenue El Monte, California 91734	C. E. Roth
1	Stanford Research Institute 333 Ravenswood Avenue Menlo Park, California	Lionel Dickinson
1	Space Technology Laboratories TRW Incorporated One Space Park Redondo Beach, California 90278	G. W. Elverum
1	TAPCO Division TRW, Incorporated 23555 Euclid Avenue Cleveland, Ohio 44117	P. T. Angell
1	Thiokol Chemical Corporation Huntsville Division Huntsville, Alabama	John Goodloe
1	Research Laboratories United Aircraft Corporation 400 Main Street East Hartford, Connecticut 06108	Erle Martin

INDUSTRY CONTRACTORS

COPIES	RECIPIENT	DESIGNEE
1	United Technology Center 587 Methilda Avenue P. O. Box 358 Sunnyvale, California 94088	B. Abelman
1	Aerospace Operations Walter Kidde and Company, Inc. 567 Main Street Belleville, New Jersey 07109	R. J. Hanville Director of Research Engineering
1	Florida Research and Development Pratt and Whitney Aircraft United Aircraft Corporation P. O. Box 2691 West Palm Beach, Florida 33402	R. J. Coar
1	Allied Chemical Corporation General Chemical Division P. O. Box 405 Morristown, New Jersey 07960	Dr. Hans Newmark
1	Technidyne, Inc. 310 East Rosedale Avenue West Chester, Pennsylvania 19380	Dr. Wm. B. Tarpley
1	Air Products and Chemicals, Inc. P. O. Box 538 Allentown, Pennsylvania	Dr. Clyde McKinley
1	New York University College of Engineering University Heights New York, New York 10453	Dr. P. F. Winternitz
1	Union Carbide Corporation Linde Division Research Lab, P. O. Box 44 Tonawanda, New York 14152	Dr. G. A. Cook